Fall 2008

Inter-area oscillation damping in large scale power systems with unified power flow controllers

Mahyar Zarghami

INTER-AREA OSCILLATION DAMPING IN LARGE SCALE POWER SYSTEMS WITH UNIFIED POWER FLOW CONTROLLERS

by

MAHYAR ZARGHAMI

A DISSERTATION

Presented to the Faculty of the Graduate School of the

MISSOURI UNIVERSITY OF SCIENCE AND TECHNOLOGY

In Partial Fulfillment of the Requirements for the Degree

DOCTOR OF PHILOSOPHY

in

ELECTRICAL ENGINEERING

2008

Approved by

Mariesa L. Crow, Advisor
Jagannathan Sarangapani
Badrul H. Chowdhury
Mehdi Ferdowsi
Bruce M. McMillin

PUBLICATION DISSERTATION OPTION

This dissertation has been prepared in the form of ten papers for publication. The first paper consisting from pages 3 to 21 has been published in the conference proceedings of the 38th North American Power Symposium. The second paper consisting from pages 22 to 28 has been published in IEEE Transactions on Power Systems, volume 22, issue 4, Nov. 2007. The third paper consisting from pages 29 to 46 has been published in the conference proceedings of the 39th North American Power Symposium. The fourth paper consisting from pages 47 to 65 is under review for publication in the IEEE Transactions on Power Delivery. The fifth paper consisting from pages 66 to 84 has been submitted for review for publication in the IEEE Transactions on Power Systems. The sixth paper consisting from pages 85 to 99 has been published in the conference proceedings of the IEEE Power and Energy Society 2008 Summer Meeting. The seventh paper consisting from pages 100 to 111 has been published in the conference proceedings of the 40th North American Power Symposium. The eighth paper consisting from pages 112 to 130 is in preparation for submission to the IEEE Transactions on Power Systems. The ninth paper consisting from pages 131 to 146 has been accepted to be published in the conference proceedings of the Power Systems Conference and Exposition 2009. The tenth paper consisting from pages 147 to 163 is in preparation for submission to the IEEE Transactions on Power Systems.

ABSTRACT

Power system oscillations occur in power networks as a result of contingencies such as faults or sudden changes in load or generation. They are detrimental to the operation of the system since they affect system stability and the optimal power flow through it. These oscillations do not usually damp out in tie-lines unless certain controls are applied to the system. Local and inter-area oscillations have traditionally been controlled by Power System Stabilizers (PSS). However, Flexible Alternating Current Transmission Controllers (FACTS) have significant potential as alternatives to PSS.

The main goal of this research is to damp inter-area oscillations by Unified Power Flow Controllers (UPFC). UPFC is a series-shunt FACTS device which is used for purposes such as the control of active and reactive power flow through the corridors of the system. However, using supplementary controls and proper coordination of UPFCs, they can be used for fast damping of inter-area oscillations in multi-area power systems.

The research consists of ten papers. There are several issues associated with dynamic control of FACTS devices which need to be taken into consideration. In the first two papers the role of pre-fault UPFC operating points on the stability and dynamic behavior of power systems is discussed. Linear approaches for the control of inter-area oscillations have been discussed in the third and fourth papers. Since the discussed algorithms for damping oscillations need global feedback data for control implementation, decentralized and wide-area methods for dynamic state estimation have been presented in the fifth and sixth papers. Seventh paper shows that using similar methodologies to UPFCs, multiple coordinated Static Synchronous Compensators (STATCOM) can also be used for controlling power system oscillations. A nonlinear method for controlling oscillations has been presented in the eighth paper. Finally, since FACTS placement plays an important role in the dynamic behavior of the system, the last two papers propose two different methods for optimal dynamic placement of UPFCs.

ACKNOWLEDGMENTS

The author would like to express his deepest appreciation to his advisor, Dr. Mariesa L. Crow for her continuous guidance, advice and help during this research.

My appreciation is extended to the members of advisory committee, Dr. Jagannathan Sarangapani, Dr. Badrul H. Chowdhury, Dr. Mehdi Ferdowsi and Dr. Bruce M. McMillin for their time and effort for reviewing this dissertation. Special thanks to Dr. Sarangapani for his advices during my work.

Financial support of the National Science Foundation is gratefully acknowledged.

Last but not least, my work would have not been fulfilled without blessings of my dear parents, brothers and my lovely wife Atousa.

TABLE OF CONTENTS

LIST OF ILLUSTRATIONS

PAPER 3

PAPER 4

PAPER 5

PAPER 6

PAPER 7

PAPER 8

PAPER 9

PAPER 10

LIST OF TABLES

PAPER 8

PAPER 9

PAPER 10

1. INTRODUCTION

Today, FACTS controllers have become less expensive and because of their fast response to system disturbances they will be used even more extensively in the future. However, there are still problems associated with their application especially in the dynamic control area. Phenomena such as inter-area oscillations impact power systems in wide area distances. For the same reason, controlling such phenomena needs proper coordination between the controlling devices. The main goal of this research is to damp inter-area oscillations in multi-area power systems using multiple FACTS devices. The UPFC is the most versatile FACTS device and the focus of this research has been based on the application of multiple UPFCs for damping oscillations. In the literature, there have been several methods proposed for the control of UPFCs based on linear and nonlinear methods. However, the application of most of these methods is limited to the control of an individual UPFC without its coordination with other devices. Considering that multi-area power systems have several oscillation modes, more than one FACTS device is needed in order to affect all those modes. Thus, coordination of the devices becomes an important issue.

In this research which consists of ten papers, several contributions have been made in the area of dynamic control of the UPFC for the purpose of damping inter-area oscillations. In the initial work, it has been shown that the pre-fault operating status of UPFC plays an important role in its dynamic behavior. This has been discussed in the first two papers. Then, a novel method has been proposed for the control of inter-area oscillations using UPFCs based on controlling their bus voltages. Papers three and four describe this method and show its comparison with other methods. The proposed methods for oscillation damping generally need global feedback data for implementation. However in practice, global feedback is not available and dynamic feedback estimation is usually needed. A decentralized method based on Linear Matrix Inequality (LMI) approach has been discussed in the fifth paper. Decentralized methods usually use local measurements for data estimation. As these local measurements might not always be adequate for proper feedback estimation, a centralized wide-area method for feedback estimation based on selected global measurements using reduced order observers has been discussed in the sixth paper. Although the focus of the research is on the UPFC, in the seventh paper it has been shown that using similar methodologies for system modeling and control, it is also possible to use multiple STATCOMs for damping power system oscillations. The next contribution of this research is to propose a new nonlinear method for oscillation damping which has been described in the eighth paper. Since dynamic placement of FACTS controllers plays an important role on

the dynamic behavior of the power system, the other contribution of this research has been devoted to two different methods for dynamic placement of UPFCs which have been discussed in the ninth and tenth papers.

1. The Effect of Various UPFC Operating Points on Transient Stability

Mahyar Zarghami Mariesa L. Crow
Department of Electrical and Computer Engineering
Missouri University of Science and Technology, MO, 65409, USA

ABSTRACT: In this paper, it is shown that using the power injection model for a UPFC, there exist sets of operating points for which the same amount of ac bus voltage and active/reactive series power injections can be evaluated. These various operating points are designated by different dc bus voltages (V_{dc}) and modulation amplitudes (k_1, k_2) and phases (α_1, α_2). Simulations show that the dynamic behavior of a UPFC could be related to its pre-fault operating situations. The question to be answered is to verify which operating point would be the best candidate from a network stability point of view. A linear approach based on the eigenvalue problem has been used to answer the question and satisfactory results have been outlined.

Index Terms: UPFC, Transient Stability

I. INTRODUCTION

The power injection model has so far been widely used for power system simulations where FACTS devices such as UPFCs exist in a network. In this approach, UPFCs are modeled by converting their phasor variables into the $dq0$ domain, which has the advantage that in steady-state, the UPFC variables are constant. In addition, it is possible to directly incorporate the differential-algebraic equations of the UPFC into the power network. Using the power injection model, the action of a UPFC in the network is represented by its series and shunt current injections where these currents are controlled by the variations of the dc bus (V_{dc}) and modulation amplitudes (k_1, k_2) and phases (α_1, α_2) [1]. In this paper, it will be shown that for the same ac bus voltage and active/reactive series power injection in a UPFC, there exists a set of operating points designated by different sets of $V_{dc}, k_1, \alpha_1, k_2, \alpha_2$ values.

Although each of these sets of control parameters result in the same power injection model,

the different control parameter sets have different impacts on transient stability. Therefore, the choice of a proper operating point is of vital importance. Some work already exists in the literature related to the choice of optimal set of operating points for the FACTS devices in steady-state conditions. These approaches mostly focus on the operation of the system from aspects such as optimal power flow and UPFC internal constraints [2, 3]. Despite the work done so far, there is still considerable work to be done in the area of the system dynamics to analyze the effect of various operating points on the stability and control of the power system.

In the following sections, the power injection model will be described along with an algorithm for finding sets of operating points of UPFCs. These operating points are visualized using corresponding operating plots. In the plots, the stable/unstable regions are designated based on determining the eigenvalues of the linearized power system state space matrix evaluated at steady-state. Power system simulations have been accomplished to find a probable relation between the stable/unstable pre-fault operating areas and the likelihood of the power system to go unstable after a fault. Observations are reported and further work is proposed.

II. THE POWER INJECTION MODEL OF THE UPFC

The equations of the power injection model for the UPFC are taken from [4]. It is assumed that the power system is balanced and therefore no zero sequence voltages and currents exist in the network. There are basically nine equations governing a UPFC and its interface to the power network. Each of the series and shunt parts has two differential equations and there is one differential equation relating the series and shunt parts through the dc link. The four remaining algebraic equations interface the UPFC with the power network through the two buses of the UPFC. The two buses of the UPFC are denoted as Bus1 and Bus2, where Bus1 is the bus connected to the shunt transformer of the UPFC.

The equations that describe the shunt part of the UPFC are:

$$\frac{1}{\omega_B}\dot{i}_{d_1} = -\frac{R_1}{X_1} i_{d_1} + i_{q_1} + \frac{k_1}{X_1}\cos(\theta_1 + \alpha_1)V_{dc} - \frac{V_1}{X_1}\cos\theta_1 \tag{1}$$

$$\frac{1}{\omega_B}\dot{i}_{q_1} = -\frac{R_1}{X_1} i_{q_1} - i_{d_1} + \frac{k_1}{X_1}\sin(\theta_1 + \alpha_1)V_{dc} - \frac{V_1}{X_1}\sin\theta_1 \tag{2}$$

Similarly, the series equations are:

$$\frac{1}{\omega_B}\dot{i}_{d_2} = -\frac{R_2}{X_2} i_{d_2} + i_{q_2} + \frac{k_2}{X_2}\cos(\theta_1 + \alpha_2)V_{dc} - \frac{V_2}{X_2}\cos\theta_2 + \frac{V_1}{X_2}\cos\theta_1 \tag{3}$$

$$\frac{1}{\omega_B}\dot{i}_{q_2} = -\frac{R_2}{X_2} i_{q_2} - i_{d_2} + \frac{k_2}{X_2}\sin(\theta_1 + \alpha_2)V_{dc} - \frac{V_2}{X_2}\sin\theta_2 + \frac{V_1}{X_2}\sin\theta_1 \tag{4}$$

The equation for the dc capacitor that links the shunt and series parts is:

$$\begin{aligned}\frac{C}{\omega_B}\dot{V}_{dc} &= -k_1\cos(\theta_1 + \alpha_1)i_{d_1} - k_1\sin(\theta_1 + \alpha_1)i_{q_1} \\ &-k_2\cos(\theta_1 + \alpha_2)i_{d_2} - k_2\sin(\theta_1 + \alpha_2)i_{q_2} - \frac{V_{dc}}{R_p}\end{aligned} \tag{5}$$

The power balance equations at Bus1 are:

$$V_1(\cos(\theta_1)(i_{d_1} - i_{d_2}) + \sin(\theta_1)(i_{q_1} - i_{q_2})) - V_1\sum_{j=1}^{n} V_j Y_{1j}\cos(\theta_1 - \theta_j - \Phi_{1j}) = 0 \tag{6}$$

$$V_1(\sin(\theta_1)(i_{d_1} - i_{d_2}) - \cos(\theta_1)(i_{q_1} - i_{q_2})) - V_1\sum_{j=1}^{n} V_j Y_{1j}\sin(\theta_1 - \theta_j - \Phi_{1j}) = 0 \tag{7}$$

Finally the power balance equations at Bus2 are:

$$V_2(\cos(\theta_2)i_{d_2} + \sin(\theta_2)i_{q_2}) - V_2\sum_{j=1}^{n} V_j Y_{2j}\cos(\theta_2 - \theta_j - \Phi_{2j}) = 0 \tag{8}$$

$$V_2(\sin(\theta_2)i_{d_2} - \cos(\theta_2)i_{q_2}) - V_2\sum_{j=1}^{n} V_j Y_{2j}\cos(\theta_2 - \theta_j - \Phi_{2j}) = 0 \tag{9}$$

where the following variables are defined:

ω_B : Base frequency of the network (rad/S)

R_1, X_1 : Equivalent Resistance & Reactance of the shunt transformer (pu)

R_2, X_2 : Equivalent Resistance & Reactance of the series transformer (pu)

i_{d_1}, i_{q_1} : The shunt currents of the UPFC in the direct and quadrature axes, respectively (pu)

i_{d_2}, i_{q_2} : The series currents of the UPFC in the direct and quadrature axes, respectively (pu)

k_1, k_2 : Amplitude modulation indices of the shunt and series parts, respectively

α_1, α_2 : Phase modulation indices of the shunt and series parts, respectively

V_{dc} : dc link capacitor voltage (pu)

C : Capacitance of the dc link (pu)

R_p : Equivalent resistance parallel with the capacitor of the dc link, representing the dc losses (pu)

III. MULTIPLE OPERATING POINTS OF THE UPFC

In this section, we verify the existence of multiple operating points of a UPFC in steady-state conditions. Fig. 1 shows a UPFC embedded into a line between buses 1 and 2. We mean to regulate the active/reactive power flow through the line as P_{sc} / Q_{sc} and the voltage magnitude at the ac bus of the UPFC as V_{sc}.

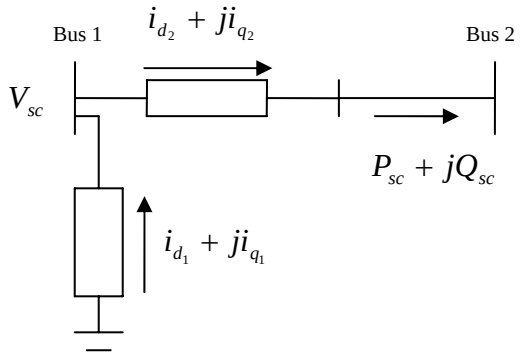

Fig. 1. Power injection model of the UPFC embedded into the line from Bus1 to Bus2

In a conventional power system with no FACTS device, two active/reactive power flow equations can be written at every PQ bus. With the introduction of a UPFC into the power system, the four power flow equations at buses 1 and 2 cannot be written in their conventional form anymore. These four equations are vital for the evaluation of two voltage magnitudes and two voltage phases. Instead of the four powerflow equations to determine the bus voltages magnitude and angle, equations (6)-(9) are used. But equations (6)-(9) introduce four additional

unknowns of $i_{d_1}, i_{q_1} i_{d_2}, i_{q_2}$ into the system. However, because $V_1 = V_{sc}$ is known, there are actually only three additional unknowns. Using equations (1)-(5) also adds the additional unknowns of $V_{dc}, k_1, \alpha_1, k_2, \alpha_2$. So up to this point, the UPFC has 9 additional equations and 12 additional unknowns. In order for the system to be solvable, 3 more equations are needed for every UPFC. From the power injection model, two of the equations can be written as:

$$V_2(\cos(\theta_2) i_{d_2} + \sin(\theta_2) i_{q_2}) = P_{UPFC} \tag{10}$$

$$V_2(\sin(\theta_2) i_{d_2} - \cos(\theta_2) i_{q_2}) = Q_{UPFC} \tag{11}$$

To develop the last equation, consider Fig. 2. Here, active power balance at the dc link in steady-state can be written as:

$$P_{shunt} + P_{series} = -\frac{V_{dc}^{\ 2}}{R_p} \tag{12}$$

where P_{shunt} and P_{series} are the active powers injected from the shunt and series parts of the UPFC, respectively. More specifically, these two powers can be written as:

$$P_{shunt} = -k_1 V_{dc} \cos(\theta_1 + \alpha_1) i_{d_1} + k_1 V_{dc} \sin(\theta_1 + \alpha_1) i_{q_1} \tag{13}$$

$$P_{series} = +k_2 V_{dc} \cos(\theta_1 + \alpha_2) i_{d_2} + k_2 V_{dc} \sin(\theta_1 + \alpha_2) i_{q_2} \tag{14}$$

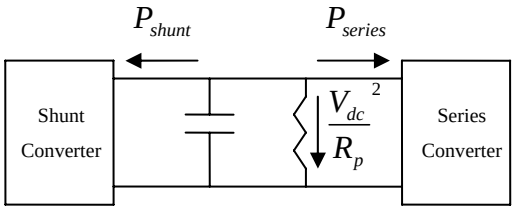

Fig. 2. Active Power Balance in Steady-State Conditions

Considering P_{shunt} to be specified, equation (13) is the last equation needed to determine the UPFC parameters. Since P_{shunt} is a specified value, each value of P_{shunt} determines a possible UPFC operating point.

Figs. 3 show sets of operating k_1, k_2 and V_{dc} plots for a UPFC installed between buses 1 and

2 in the IEEE 118 bus test system. The parameters of the UPFC have been given in Section V. As can be seen in Fig. 3a, there is a large variation in the value of k_1 with changes of P_{shunt}. However, the value of $k_1 V_{dc}$ remains around 1 pu to regulate the voltage of the ac bus of the UPFC to be equal to V_{sc}. The dotted lines in Fig. 3 represent the unstable regions determined by the eigenvalues of the linearized system explained in section IV.

IV. EFFECT OF PRE-FAULT OPERATING CONDITIONS ON TRANSIENT STABILITY

In this section, the effect of the initial operating point on the transient stability of the system will be considered. One basic approach to determining stability is to linearize the system equations around its equilibrium point. Although power systems are nonlinear, this approach is able to roughly predict the relative likelihood of the system to go unstable.

Consider the following nonlinear differential/algebraic equations of the system [5]:

$$\dot{X} = f(X,Y) \tag{15}$$

$$0 = g(X,Y) \tag{16}$$

where X is the state vector and Y is the vector of voltage magnitude/angles of the power system.

The linearized equations are of the form:

$$\Delta\dot{X} = AX + BY \tag{17}$$

$$0 = CX + DY \tag{18}$$

where Δ shows the linearized variable around its equilibrium point.

Using equations (17) and (18), it is possible to get the state space matrix of the linearized system as:

$$A_{sys} = A - BD^{-1}C \tag{19}$$

The eigenvalues of A_{sys} determine the relative stability of the system after a fault. If the eigenvalues have positive real parts, then the relative stability of the system is poor.

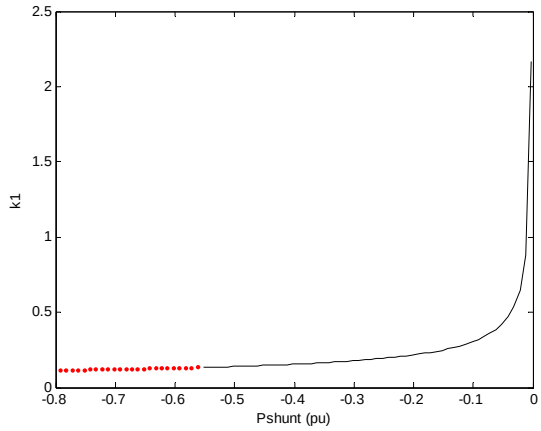

(a) k_1 vs. P_{shunt}

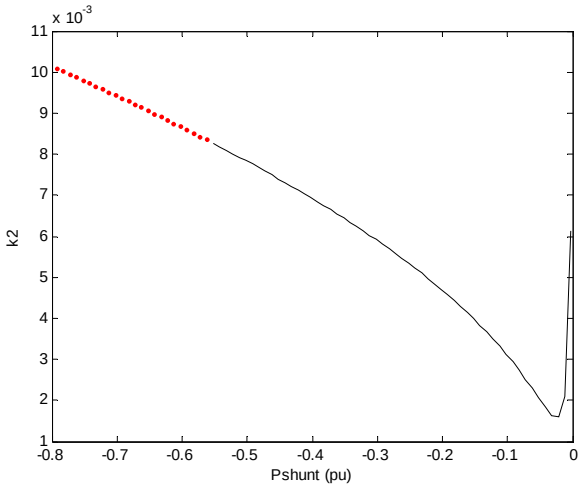

(b) k_2 vs. P_{shunt}

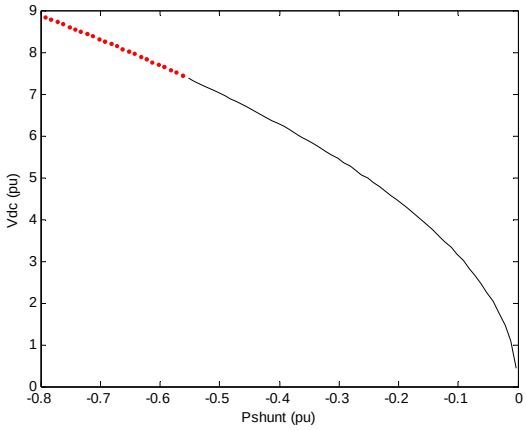

(c) V_{dc} vs. P_{shunt}

Fig. 3. Operating Plots of the UPFC

V. SIMULATIONS AND RESULTS

To verify the assumption made in the previous section, we show two examples using the IEEE 118 bus test system [6]. This system has 20 machines, where the order of each machine is 10, containing the two-axis generator model, Type I Exciter/AVR model and turbine and governor models. As we discussed in the above sections, every UPFC would add 5 state variables into the system. So the order of the linearized power system with one UPFC would be 205. Two different UPFC placements have been considered in the following examples and their results are explained. The parameters of the UPFC are:

$R_1 = 0.01 pu$, $X_1 = 0.15 pu$

$R_2 = 0.001 pu$, $X_2 = 0.015 pu$

$R_p = 100 pu$, $C = 1.1364 pu$

Example 1

As the first example, a UPFC placement between buses 1 and 2 has been considered with $P_{sc} = -0.1178 pu$, $Q_{sc} = -0.1353 pu$ and $V_{sc} = 0.9528 pu$. These are basically the line power and voltage values before the UPFC installation.

(a) When $P_{shunt} = -0.01 pu$ **,** we get an operating point where:

$k_1 = 0.9626$, $k_2 = 0.0024$

$\alpha_1 = 6.2815 rad$, $\alpha_2 = 3.4029 rad$

$k_1 V_{dc} = 0.9533 pu$

$i_{d_1} = -0.0110 pu$, $i_{q_1} = 0.0015 pu$

$i_{d_2} = -0.0452 pu$, $i_{q_2} = 0.1827 pu$

With the above conditions, all eigenvalues of A_{sys} have negative real values. To observe the transient stability of the system, a fault is applied to bus 30 at 1 s and is cleared after 0.1 s. Figs. 4-7 show the behavior of the system with and without PI controllers. Four simple PI controllers have been applied to control the series active power, series reactive power and voltages of the dc and ac buses of the UPFC [4]. The controller parameters are shown in Table I.

TABLE I

PI Controller Parameters for Examples 1 and 2

	Series Controller	
	k_P	k_I
Active Power	1e-3	1e-3
Reactive Power	1e-3	1e-3
	Shunt Controller	
	k_P	k_I
dc voltage	5e-2	5e-2
ac voltage	5e-3	5e-3

Figs. 4a and 4b show the series injected power (P_{series}) of the UPFC before and after the fault for the uncontrolled and controlled cases, respectively. Figs. 5, 6 and 7 depict the variations of the series injected reactive power (Q_{series}), $k_1.V_{dc}$ and ac voltage of the UPFC (V_1) for the uncontrolled and controlled cases. In this example, it is obvious that the system is stable and easily controlled.

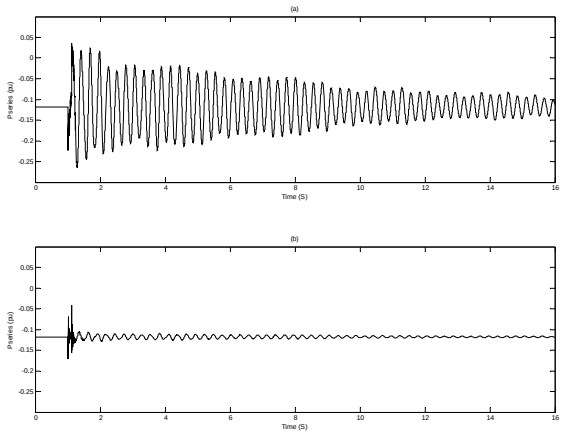

Fig. 4. UPFC Injected Series Active Power in Example 1a
(without control – top, with control – bottom)

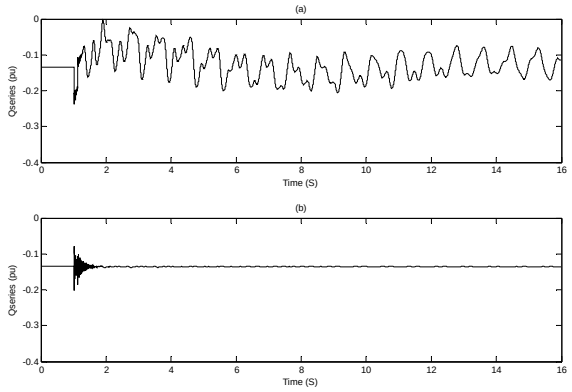

Fig. 5. UPFC Injected Series Reactive Power in Example 1a
(without control – top, with control – bottom)

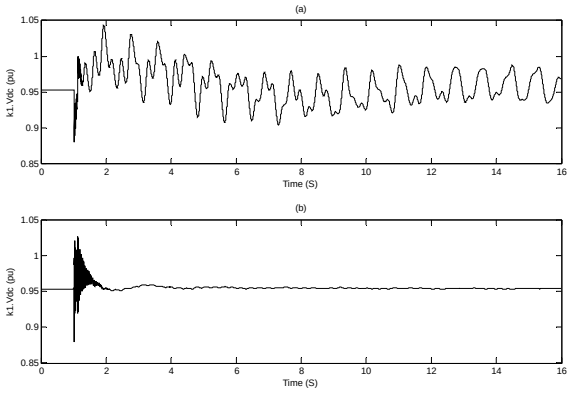

Fig. 6. ac voltage of the shunt converter of the UPFC in Example 1a
(without control – top, with control – bottom)

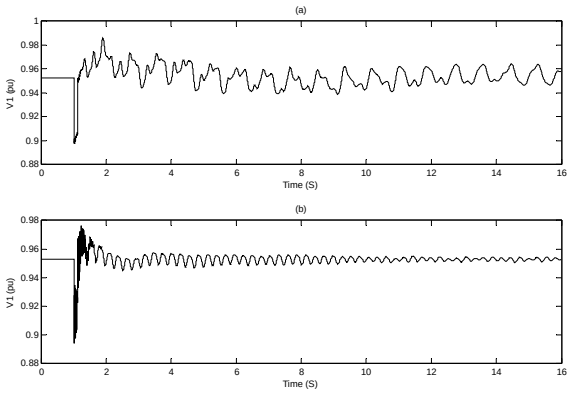

Fig. 7. ac bus voltage of the UPFC in Example 1a
(without control – top, with control – bottom)

(b) Next, an alternate operating point is chosen with the **same** values of P_{sc}, Q_{sc} and V_{sc}, but where $P_{shunt} = -0.6\,pu$. Note that for the power injection model, these two operating points are identical because they have the same series active and reactive power and bus voltage. For this situation, two complex conjugate eigenvalues have positive real parts, thus this operating point is locally unstable. From the participation factors, it is determined that these unstable eigenvalues are associated mostly with the angular frequency of the generators connected to buses 100 and 112. This means that the UPFC itself is not contributing directly to the instability. The control parameters of the UPFC at this point are:

$$k_1 = 0.1287 \quad k_2 = 0.0086$$

$$\alpha_1 = 6.1842 rad \quad \alpha_2 = 1.6396 rad$$

$$k_1 V_{dc} = 0.9891 pu$$

$$i_{d_1} = -0.6641 pu \quad i_{q_1} = 0.1577\, pu$$

$$i_{d_2} = -0.0332\, pu \quad i_{q_2} = 0.1853 pu$$

The same fault is applied to the system as in the previous example. The same PI controller is used to stabilize the system. As can be seen in Figs. 8-11, the controlled network becomes unstable rapidly. This shows how important the choice of initial operating condition is to the controllability and stability of the system, regardless of the choice of initial series active and reactive power flows and system bus voltage.

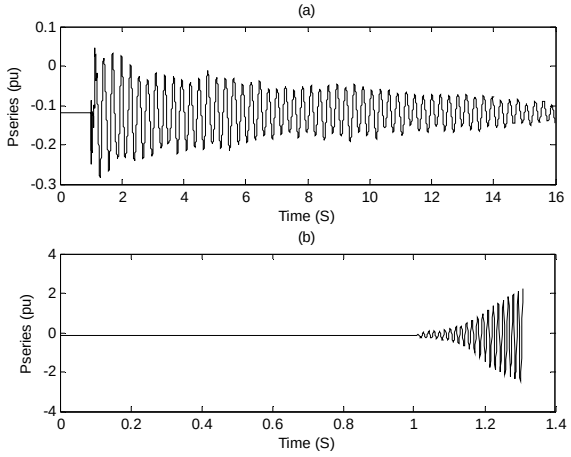

Fig. 8. UPFC Injected Series Active Power in Example 1b
(without control – top, with control – bottom)

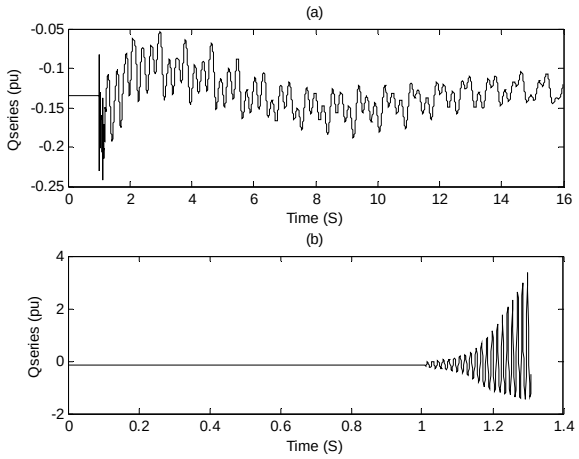

Fig. 9. UPFC Injected Series Reactive Power in Example 1b
(without control – top, with control – bottom)

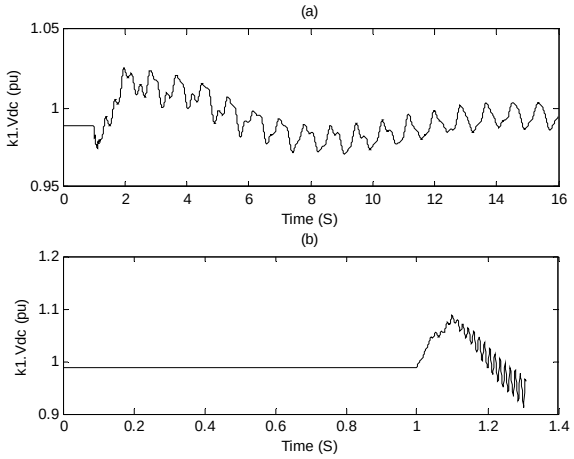

Fig. 10. ac voltage of the shunt converter of the UPFC in Example 1b
(without control – top, with control – bottom)

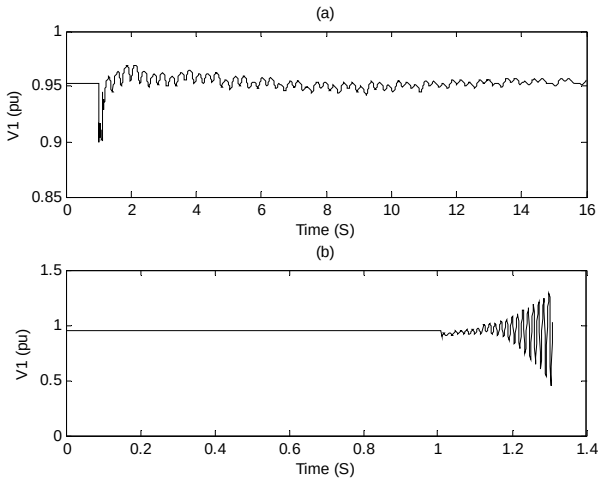

Fig. 11. ac bus voltage of the UPFC in Example 1b
(without control – top, with control – bottom)

Example 2

In the second example, a UPFC placement is changed and it is now placed between buses 102 and 101 in the 118 bus network. The initial injection model settings are $P_{sc} = 0.3966\,pu$, $Q_{sc} = -0.1063\,pu$, and $V_{sc} = 0.9866\,pu$. These are basically the line power and voltage values before UPFC installation.

(a) When $P_{shunt} = -0.01\,pu$, the initial parameters are:

$k_1 = 1.0018 \quad k_2 = 0.0075$

$\alpha_1 = 6.2816 rad \quad \alpha_2 = 1.7371 rad$

$k_1 V_{dc} = 0.9867\,pu$

$i_{d_1} = -0.0103\,pu \quad i_{q_1} = -8.9314e-4\,pu$

$i_{d_2} = 0.4113\,pu \quad i_{q_2} = 0.0638\,pu$

With the above conditions, all eigenvalues of A_{sys} have negative real parts. Similar to example 1, a fault is applied to bus 30 of the network at 1 s and cleared after 0.1 s. Figs. 12-15 show the behavior of the system with and without PI controllers. In figures denoted by (a), no control has been applied until 14.25 s. On the other hand, in the figures distinguished by (b), the PI controller has been applied from the very beginning. The same control parameters as in Table I have been

used in this example. As it might be viewed in Figs. 14a and 15a, after about 14.25 s, the PI controllers do a good job for stabilizing the system.

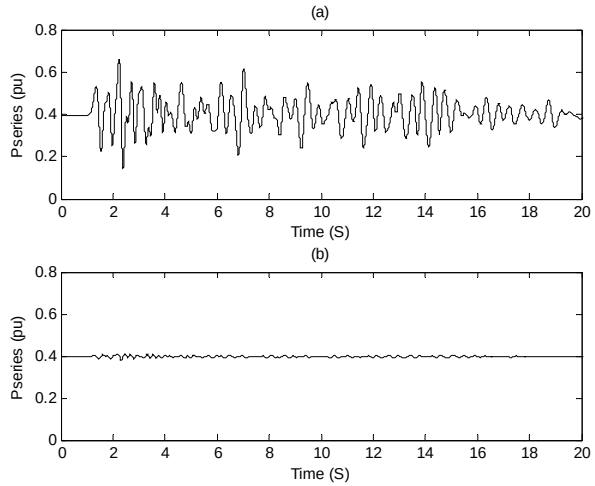

Fig. 12. UPFC Injected Series Active Power in Example 2a
(without control until 14.25s – top, with control – bottom)

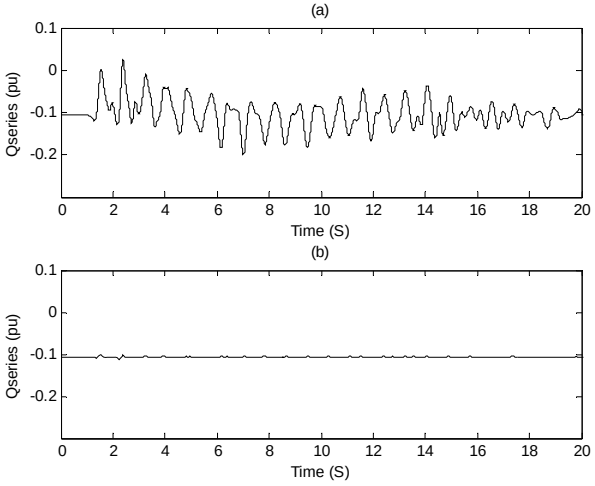

Fig. 13. UPFC Injected Series Reactive Power in Example 2a
(without control until 14.25 – top, with control – bottom)

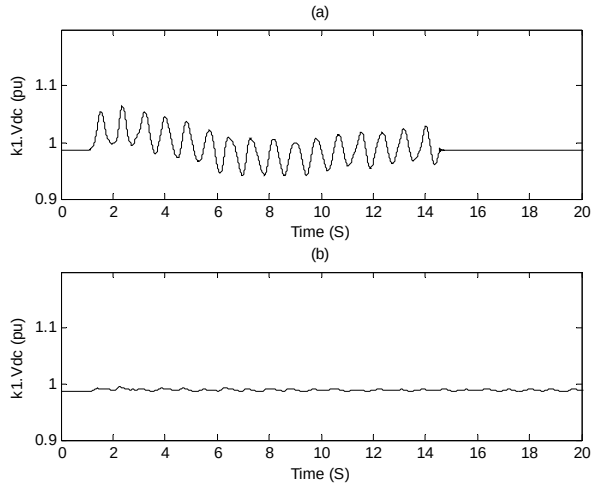

Fig. 14. ac voltage of the shunt converter of the UPFC in Example 2a
(without control until 14.25 – top, with control – bottom)

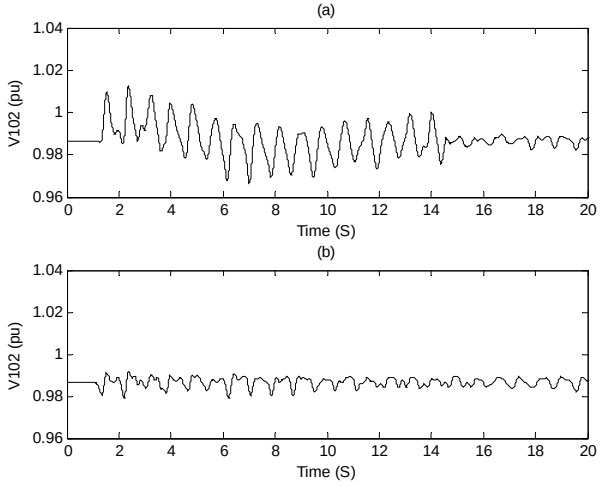

Fig. 15. ac bus voltage of the UPFC in Example 2a
(without control until 14.25 – top, with control – bottom)

(b) Next, an alternate operating point is chosen with the same values of P_{sc}, Q_{sc} and V_{sc} where $P_{shunt} = -0.7\,pu$. For this situation, two complex conjugate eigenvalues have positive real parts, thus this operating point is locally unstable. From the participation factors, it is determined that these unstable eigenvalues are associated mostly with the angular frequency of the generators connected to buses 40 and 112. Here again we conclude that the power system inter-area modes

are corresponding to unstable equilibrium points and not the UPFC modes. The operating conditions of the UPFC in these situations are:

$$k_1 = 0.1216 \quad k_2 = 0.0105$$

$$\alpha_1 = 6.1752 rad \quad \alpha_2 = 1.6288 rad$$

$$k_1 V_{dc} = 1.010 pu$$

$$i_{d_1} = -0.7252 pu \quad i_{q_1} = 0.1139 pu$$

$$i_{d_2} = 0.4158 pu \quad i_{q_2} = -0.0168 pu$$

The control is applied at 12.8s. As it is seen in Figs. 16a, 17a, 18a and 19a, the controller is not able to stabilize the system. Actually the control action makes the situation worse. However, in Figs. 16b, 17b, 18b and 19b it is seen that when the controllers come into action from the very beginning, they could stabilize the system. This again shows that picking an inappropriate operating point could lead the power system into undesirable behavior after a fault.

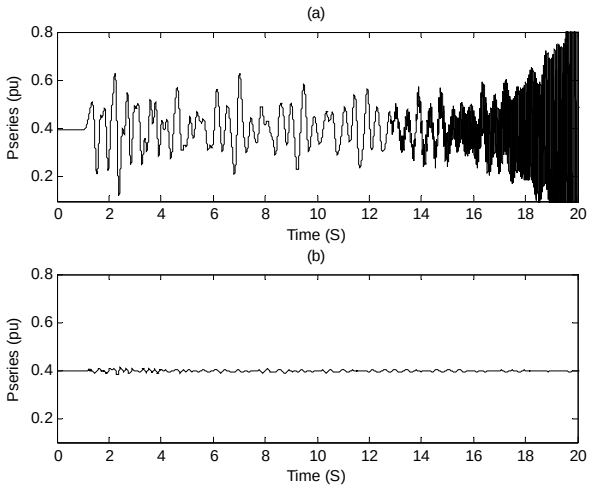

Fig. 16. UPFC Injected Series Reactive Power in Example 2b
(without control until 12.8s – top, with control – bottom)

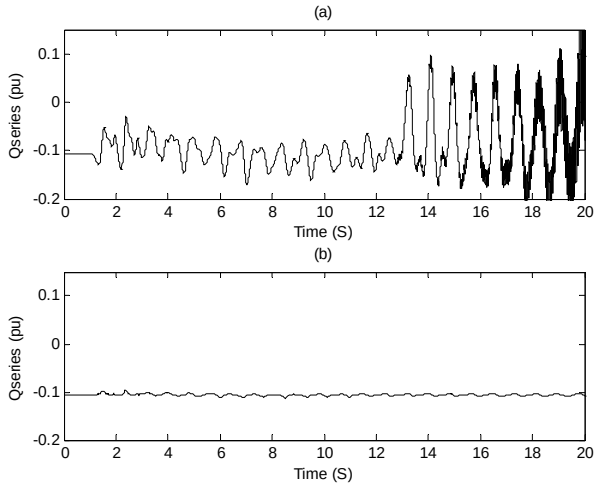

Fig. 17. UPFC Injected Series Reactive Power in Example 2b
(without control until 12.8s – top, with control – bottom)

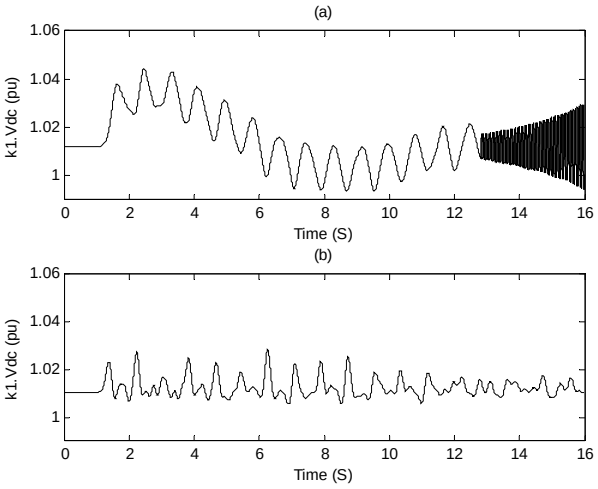

Fig. 18. ac voltage of the shunt converter of the UPFC in Example 2b
(without control until 12.8s – top, with control – bottom)

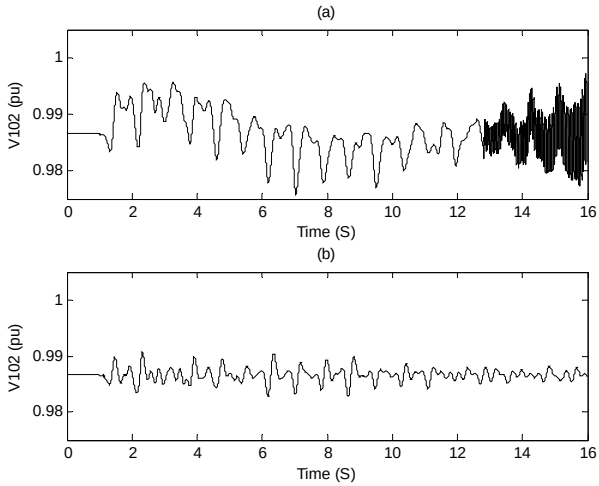

Fig. 19. ac bus voltage of the UPFC in Example 2b
(without control until 12.8s – top, with control – bottom)

VI. CONCLUSIONS

This work shows that the steady-state power injection model of the UPFC is insufficient for transient stability analysis. In the steady-state power injection model, only the series reactive and active powers and the shunt bus voltage magnitude are specified. Even with these values specified, there are many operating states that can be achieved from the dynamic equations. This may lead to unstable initial operating conditions. In addition, even if the initial operating conditions are stable, the stability margin may be sufficiently decreased so as to adversely affect the controllability of the system during transients.

Future work would be to apply nonlinear control theory for the evaluation of an optimal operating condition from the system's stability point of view. Other approaches such as application of the energy function methods might also be able to explain and predict system behavior after a contingency happens to the power system.

REFERENCES

[1] Timothy L. Skvarenina, *The Power Electronics Handbook* CRC Press 2002.

[2] Ying Xiao; Song, Y.H.; Sun, Y.Z., "Power Flow Control Approach to Power Systems with Embedded FACTS devices," *IEEE Transactions on Power Systems*, Vol. 17, No. 4, *Nov. 2002, pp. 943-950*.

[3] Jun-Yong Liu; Yong-Hua Song; Mehta, P.A., "Strategies for Handling UPFC Constraints in Steady-State Power Flow and Voltage Control," *IEEE Transactions on Power Systems*, Vol. 15, No. 2, *May 2000, pp. 566-571*.

[4] L. Dong, M.L. Crow, Z. Yang, C. Shen, L. Zhang, S. Atcitty, "A Reconfigurable FACTS System for University Laboratories," *IEEE Transactions on Power Systems*, Vol. 19, No. 1, *Feb. 2004, pp. 120-128*.

[5] Peter W. Sauer, M.A. Pai, *Power System Dynamics and Stability*, Prentice Hall 1998.

[6] http://www.ee.washington.edu/research/pstca/pf118/pg_tca118bus.htm

2. The Existence of Multiple Equilibria in the UPFC Power Injection Model

M. Zarghami, Student Member, IEEE, M. L. Crow, Senior Member, IEEE

ABSTRACT: This letter shows the existence of multiple equilibria that arise from the use of the state model of the UPFC. These multiple equilibria can arise from a common power injection model for the same terminal conditions of shunt bus voltage and series active and reactive power injections. The multiple equilibria result in two or more sets of eigenvalues, some of which may indicate an unstable operating condition. Therefore, the use of the UPFC power injection model must be used with caution to ensure stable operation of the UPFC.

Index Terms–UPFC, oscillation damping, power system stability

I. INTRODUCTION

The UPFC power injection model is widely used for power system simulations (recent examples include [1]-[3]). In the power injection model, the impact of the UPFC in the network is represented by its series and shunt current injections, or similarly, its series and shunt active and reactive power injections. A common approach to incorporating the UPFC power injection model into the system is to represent the UPFC as two buses: a ‘PQ’ bus at the receiving end in which both active and reactive power are specified, and a ‘PV’ bus at the sending end in which voltage and active power are specified [4]. In this letter, it will be shown that if the power injection model is used instead of the dynamic model **for the same operating conditions**, then multiple equilibria (with possibly different stability properties) can exist.

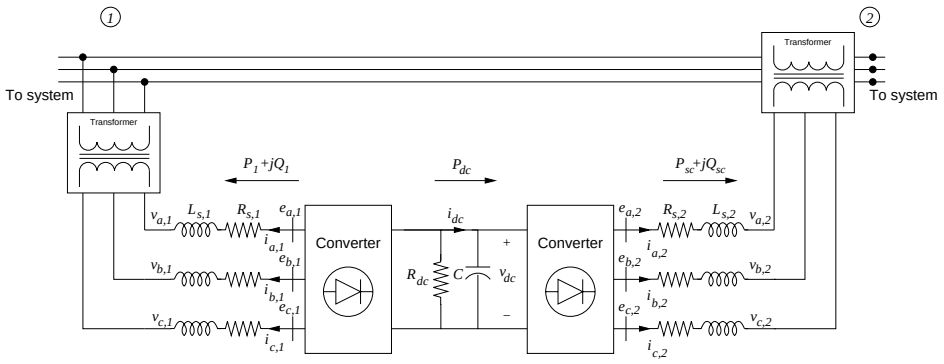

Fig. 1. Unified Power Flow Controller Diagram

II. THE UPFC STATE MODEL

The UPFC is a combination of the STATCOM (static synchronous compensator) and SSSC (static series synchronous compensator) as shown in Figure 1. The series connected inverter injects a voltage with controllable magnitude and phase angle in series with the transmission line, thereby providing active and reactive power to the transmission line. The shunt-connected inverter provides the active power drawn by the series branch and the losses and can independently provide reactive compensation to the system. The UPFC state model is:

$$\frac{1}{\omega_s}\frac{d}{dt}i_{d_1} = \frac{k_1 V_{dc}}{L_{s_1}}\cos\left(\alpha_1+\theta_1\right) + \frac{\omega}{\omega_s}i_{q_1} - \frac{R_{s_1}}{L_{s_1}}i_{d_1} - \frac{V_1}{L_{s_1}}\cos\theta_1 \tag{1}$$

$$\frac{1}{\omega_s}\frac{d}{dt}i_{q_1} = \frac{k_1 V_{dc}}{L_{s_1}}\sin\left(\alpha_1+\theta_1\right) - \frac{R_{s_1}}{L_{s_1}}i_{q_1} - \frac{\omega}{\omega_s}i_{d_1} - \frac{V_1}{L_{s_1}}\sin\theta_1 \tag{2}$$

$$\begin{aligned}\frac{1}{\omega_s}\frac{d}{dt}i_{d_2} &= -\frac{R_{s_2}}{L_{s_2}}i_{d_2} + \frac{\omega}{\omega_s}i_{q_2} + \frac{k_2}{L_{s_2}}\cos\left(\alpha_2+\theta_1\right)V_{dc} \\ &\quad -\frac{1}{L_{s_2}}\left(V_2\cos\theta_2 - V_1\cos\theta_1\right)\end{aligned} \tag{3}$$

$$\begin{aligned}\frac{1}{\omega_s}\frac{d}{dt}i_{q_2} &= -\frac{R_{s_2}}{L_{s_2}}i_{q_2} - \frac{\omega}{\omega_s}i_{d_2} + \frac{k_2}{L_{s_2}}\sin\left(\alpha_2+\theta_1\right)V_{dc} \\ &\quad -\frac{1}{L_{s_2}}\left(V_2\sin\theta_2 - V_1\sin\theta_2\right)\end{aligned} \tag{4}$$

$$\begin{aligned}\frac{C}{\omega_s}\frac{d}{dt}V_{dc} &= -k_1\cos\left(\alpha_1+\theta_1\right)i_{d_1} - k_1\sin\left(\alpha_1+\theta_1\right)i_{q_1} \\ &\quad -k_2\cos\left(\alpha_2+\theta_1\right)i_{d_2} - k_2\sin\left(\alpha_2+\theta_1\right)i_{q_2} - \frac{V_{dc}}{R_{dc}}\end{aligned} \tag{5}$$

where the parameters are as in [5]. The currents i_{d1} and i_{q1} are the dq components of the shunt current. The currents i_{d2} and i_{q2} are the dq components of the series current. The voltages $V_1\angle\theta_1$ and $V_2\angle\theta_2$ are the shunt and series voltage magnitudes and angles respectively. V_{dc} is the voltage across the DC capacitor, R_{dc} represents the switching losses, R_{s_1} and L_{s_1} are the shunt transformer resistance and inductance respectively and R_{s_2} and L_{s_2} are the series transformer resistance and inductance respectively. The control parameters k_1 (k_2) and α_1 (α_2) are respectively the modulation gain and voltage phase angle of the shunt (series) injected voltage.

The power balance equations at bus 1 (sending) are:

$$0 = V_1\left((i_{d_1}-i_{d_2})\cos\theta_1+(i_{q_1}-i_{q_2})\sin\theta_1\right)-V_1\sum_{j=1}^{n}V_jY_{1j}\cos\left(\theta_1-\theta_j-\phi_{1j}\right) \quad (6)$$

$$0 = V_1\left((i_{d_1}-i_{d_2})\sin\theta_1-(i_{q_1}-i_{q_2})\cos\theta_1\right)-V_1\sum_{j=1}^{n}V_jY_{1j}\sin\left(\theta_1-\theta_j-\phi_{1j}\right) \quad (7)$$

and at bus 2 (receiving):

$$0 = V_2\left(i_{d_2}\cos\theta_2+i_{q_2}\sin\theta_2\right)-V_2\sum_{j=1}^{n}V_jY_{2j}\cos\left(\theta_2-\theta_j-\phi_{2j}\right) \quad (8)$$

$$0 = V_2\left(i_{d_2}\sin\theta_2-i_{q_2}\cos\theta_2\right)-V_2\sum_{j=1}^{n}V_jY_{2j}\sin\left(\theta_2-\theta_j-\phi_{2j}\right) \quad (9)$$

Figure 2 shows a power injection model of the UPFC. The series branch shows the series injected voltage (controllable by varying k_2 and α_2) and the shunt branch with voltage controlled by k_1 and α_1.

Combining equations (1)-(9) yields nine equations with thirteen unknowns, therefore additional constraints are necessary to fully determine the operating equilibrium.

In the power injection model, three parameters may be arbitrarily set: the shunt bus voltage magnitude and the series active and reactive powers such that:

$$V_{sc} = V_1 \quad (10)$$

$$P_{sc} = V_{d_2}i_{d_2}+V_{q_2}i_{q_2} \quad (11)$$

$$Q_{sc} = V_{q_2}i_{d_2}-V_{d_2}i_{q_2} \quad (12)$$

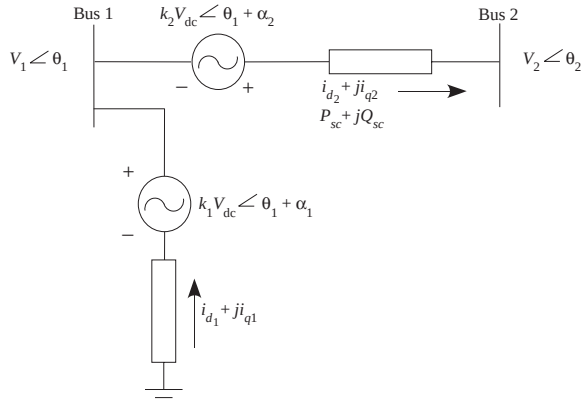

Fig. 2. UPFC Equivalent Model

where V_{sc}, P_{sc} and Q_{sc} are the specified desired values.

Since the power injection model is lossless, the shunt power P_1 is typically set to P_{sc} as well (being a 'PV' bus). However, in the state model the shunt power must account for losses in the converter such that

$$\begin{aligned} -P_1 &= P_{sc} + P_{loss} \\ &= P_{sc} + R_{s_1}\left(i_{d_1}^2 + i_{q_1}^2\right) + R_{s_2}\left(i_{d_2}^2 + i_{q_2}^2\right) + \frac{1}{R_{dc}}V_{dc}^2 \end{aligned} \tag{13}$$

thus providing the thirteenth equation. Therefore, for the same specified values of V_{sc}, P_{sc}, and Q_{sc}, multiple solutions for the remaining variables may exist depending on the choice of P_1. The power injection model in which $P_1 = P_{sc}$ is just one of many solutions that exist to the model of equations (1)-(12).

In applications in which a dynamic model is used, typically the dc link voltage (V_{dc}) is controlled. By controlling V_{dc}, the user is indirectly specifying the value of P_1 since the shunt active power is used to maintain V_{dc}. However, the power injection model is independent of the value of V_{dc}, therefore the value of P_1 can be arbitrarily chosen, which may lead to inconclusive results concerning stability.

III. ILLUSTRATIVE EXAMPLE

In this example, a UPFC is placed in the IEEE 118 bus system with the following parameters (in per unit):

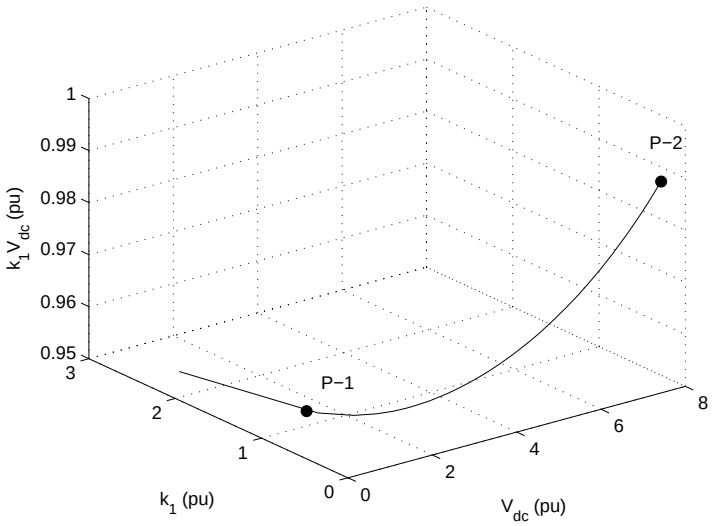

Fig. 3. UPFC parameters for variations in P_1

$$R_{s_1} = 0.01 \quad \omega_s L_{s_1} = 0.15 \quad R_{dc} = 100$$
$$R_{s_2} = 0.001 \quad \omega_s L_{s_2} = 0.015 \quad C = 1.1364$$

Figure 3 shows the variation in k_1 and V_{dc} as P_1 is varied and P_{sc}, Q_{sc} and V_{sc} are held constant. Note that the product $k_1 V_{dc}$ remains nearly constant, thus the magnitude of the injected voltage remains near 1.0 with only a few percent variation to regulate the shunt voltage at the desired V_{sc}.

Consider the two points (P-1 and P-2) indicated in Figure 3. These two points correspond to the same operating conditions where

$$P_{sc} = -0.1178 \text{ pu} \quad Q_{sc} = -0.1353 \text{ pu} \quad V_{sc} = 0.9528 \text{ pu}$$

with

	k_1 (pu)	α_1 (rad)	k_2 (pu)	α_2 (rad)	$k_1 V_{dc}$ (pu)
P-1	0.9626	0.0017	0.0024	-2.8803	0.9533
P-2	0.1287	0.0990	0.0086	1.6396	0.9891

The negative sign in P_{sc} and Q_{sc} indicates that the power flow is from bus 2 to bus 1. Both P-1 and P-2 satisfy **the same injection model constraints**, but with significantly different results. The P-1 system eigenvalues all lie in the left half plane, whereas a pair of P-2 system eigenvalues have migrated to the right half plane. To see the difference in the effect of the operating points, consider a three phase ground fault on bus 30 (of

the IEEE 118 bus test system) cleared after 0.12 seconds (Figure 4). For the system initialized at P-1, the oscillations remain bounded, whereas the system initialized at P-2 results in nonlinear undamped oscillations.

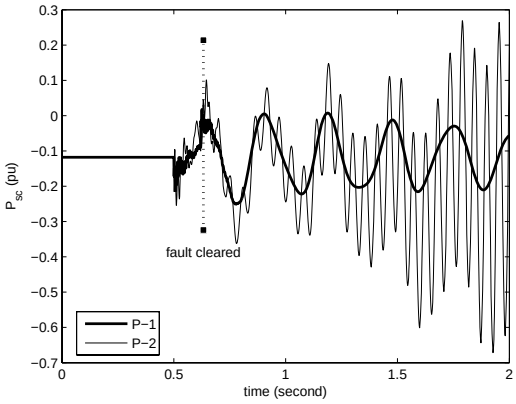

Fig. 4. Dynamic response of UPFC series active power

IV. SUMMARY AND CONCLUSIONS

This letter is intended as a cautionary note for the use of the power injection model. While the power injection model is a useful simplification, it does not represent losses and may therefore lead to inaccurate estimates of the stability and dynamic behavior of the full system.

REFERENCES

[1] B. C. Pal, “Robust damping of interarea oscillations with unified power-flow controller,” *IEE Proc.-Gener. Transm. Distrib.*, vol. 149, no. 6. pp. 733-738, November 2002.

[2] B. Chaudhuri, B. C. Pal, A. Zolotas, I. Jaimoukha, and T. Green, “Mixed-sensitivity approach to H_∞ control of power system oscillations employing multiple FACTS devices,” *IEEE Trans. on Power Systems*, vol. 18, no. 3, pp. 1149-1156, May 2004.

[3] M. M. Farsangi, Y. H. Song, and K. Y. Lee, “Choice of FACTS device control inputs for damping interarea oscillations,” *IEEE Trans. on Power Systems*, vol. 19, no. 2, May 2004.

[4] D. J. Gotham and G. T. Heydt, “Power flow control and power flow studies for systems with FACTS devices,” *IEEE Trans. on Power Systems*, vol. 13, no. 1, pp. 60-65, Feb. 1998.

[5] L. Dong, et.al, “A reconfigurable FACTS system for university laboratories,” *IEEE Trans. Power Systems*, vol. 19, no. 1, Feb. 2004.

3. Discussion on Effective Control of Inter-Area Oscillations by UPFCs

Mahyar Zarghami, *Student Member, IEEE*, and Mariesa. L. Crow, *Senior Member, IEEE*

ABSTRACT: The paper discusses an effective method for damping inter-area oscillations in a power network using UPFCs. This two stage method controls voltage magnitudes/angles of the two sides of the UPFC based on a linearized approach, which in turn will command modulation amplitudes and angles of the UPFC. The method is compared to a one stage linearized approach which directly commands modulation amplitudes and angles of the UPFC. Discussion on the feasibility of the method and its relation to the steady-state operation of the UPFC is also addressed.

Index Terms: UPFC, Inter-Area Oscillations

I. INTRODUCTION

Damping inter-area oscillations in a power network is one of the important applications of a Unified Power Flow Controller [1]-[6]. These oscillations can occur in a system because of contingencies such as sudden load changes or power system faults. Fig. 1 shows a schematic diagram of a UPFC, which is a series-shunt FACTS device. Controlling power oscillations can be done by rapidly changing the power flow through the series part of the UPFC. The needed electrical power to do this action comes from the UPFC's capacitor, which can be discharged temporarily during the control. This in turn brings up the issue of control and maintaining the capacitor dc voltage. There has been numerous work reported in the area of damping inter-area oscillations, some of which are based on linear control analysis of the UPFC and power system [1, 3 and 5], and others are based on nonlinear control systems theory and Lyapunov Energy Functions [2, 4 and 6]. Whichever method is used for the problem, the controller does its action by commanding the modulation amplitudes (k_1, k_2) and angles (α_1, α_2) of the UPFC.

Despite all the work done so far, authors have rarely found thorough work which not only

shows results of the control in a complex multi-machine network with numerous oscillating modes, but also takes into account the dynamics of the UPFC capacitor and its shunt part in the studies.

In the present work, two control schemes for damping inter-area oscillations have been considered. In the first scheme, a one stage controller has been designed which directly commands the modulation amplitudes and angles of the UPFC. In the second scheme a two stage controller is devised. The first stage calculates the needed voltage magnitudes and angles at the two buses of the UPFC and the second stage commands the values of modulation amplitudes and angles of the UPFC based on the calculated values in the first stage. Both methods are based on the linear control theory and linearization of the state space model of the power system and they both take into account the dynamics of the shunt part and capacitor of the UPFC in the design. However, nonlinear simulations have been carried out to show the capability of the controllers in damping multiple inter-area oscillations. Studies show that the two stage controller shows remarkably better results on the IEEE 118 bus test system. In the following sections, modeling of the power system as well as the design of the controllers will be explained in detail. Then simulation results will be shown and comparison between the operations of the mentioned controllers will be presented. In the end, feasibility of the two stage controller as well as its relation to the steady-state operation of the UPFC will be discussed.

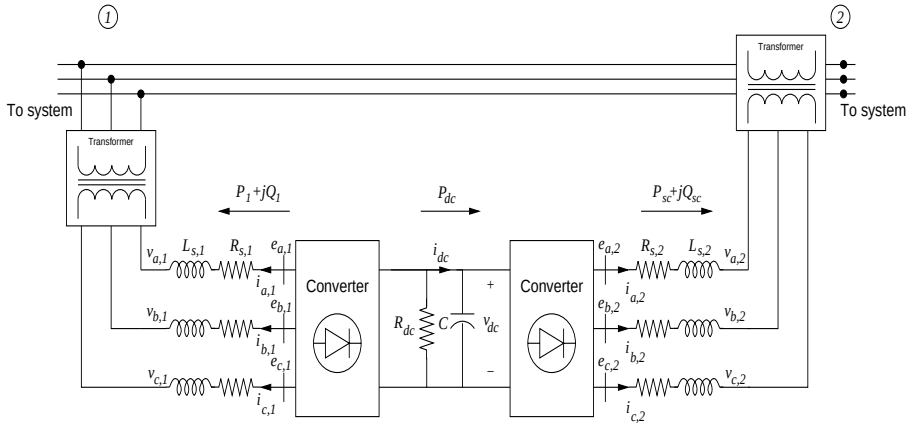

Fig. 1. Unified Power Flow Controller Diagram

II. SYSTEM MODELING FOR CONTROLLER DESIGN

This section describes the process for modeling the power system from the controller's point of view. The goal is to describe the system by a pure nonlinear differential equation set. The resulted state space model can be linearized for the purpose of the present work. In the work, the

system is assumed to have n_g generators, n_l load buses and n_u UPFCs. This results the system admittance matrix to have an order of $n_g + n_l + 2n_u$. If we assume all loads of the system to have constant admittance, and if we consider classical model for the generators, it would be possible to get a reduced admittance matrix of order $n_g + 2n_u$, where n_g internal machine buses are connected to $2n_u$ UPFC buses as shown in Fig. 2. This comes from the fact that there would be no current injection at load buses or generator terminal buses if we assume the loads to be of constant admittance type and hence it would be possible to reduce the order of the system by Cron reduction when the load admittances are taken into the new bus admittance matrix. This method would also take the generators' transient *d* axis reactances into the new admittance matrix so that the equivalent system would be viewed from the injection points of (a) Generator internal buses (b) UPFC sending buses and (c) UPFC receiving buses as shown in Fig. 2.

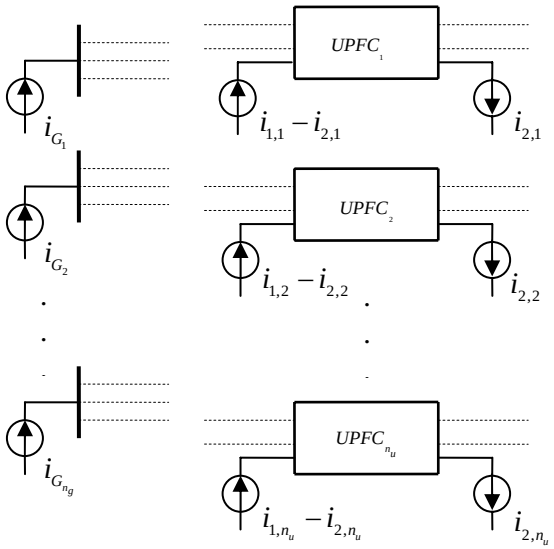

Fig. 2. Equivalent Power System from the Controller's View

The resulted state space system would be of the following format for the generators:

$$\dot{\delta}_j = \omega_j - \omega_s \tag{1}$$

$$\dot{\omega}_j = (1/M_j)(P_{M_j} - E_j \sum_{k=1}^{n_g+2n_u} E_k Y_{jk} \cos(\delta_j - \delta_k - \Phi_{jk})) \tag{2}$$

where:

ω_s : Synchronous speed (rad/s)

ω_j : Speed of machine j (rad/s) $j = 1, ..., n_g$

M_j : Inertia at machine j (pu) $j = 1, ..., n_g$

P_{M_j} : Mechanical input at machine j (pu) $j = 1, ..., n_g$

δ_i : Angle at bus i (Radians) $i = 1, ..., n_g + 2n_u$

E_i : Bus magnitude at bus i (pu) $i = 1, ..., n_g + 2n_u$

$Y_{jk} \angle \Phi_{jk}$: Admittance matrix of the equivalent reduced system for $j, k = 1, ..., n_g + 2n_u$

For UPFCs we use a power injection model schematically shown in Fig.3.

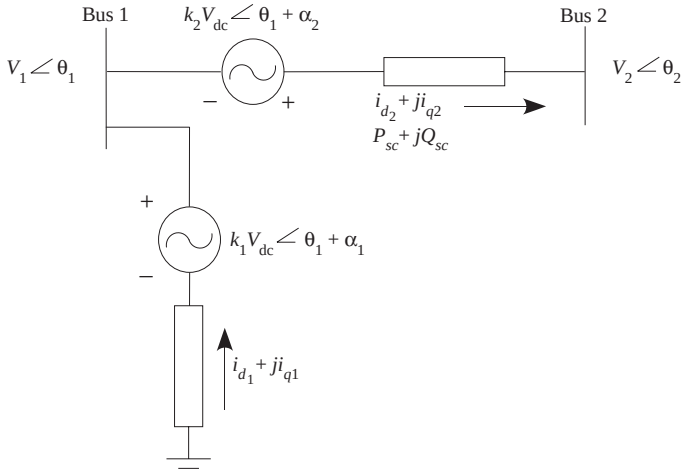

Fig. 3. Power Injection Model for UPFC

According to [7], the dynamical equations for UPFC's power injection model could be written as:

$$\frac{1}{\omega_S} \dot{i}_{d_{1j}} = -\frac{R_{1j}}{L_{1j}} i_{d_{1j}} + i_{q_{1j}} + \frac{k_{1j}}{L_{1j}} \cos(\theta_{1j} + \alpha_{1j}) v_{dc_j} - \frac{V_{1d_j}}{L_{1j}} \tag{3}$$

$$\frac{1}{\omega_S} \dot{i}_{q_{1j}} = -\frac{R_{1j}}{L_{1j}} i_{q_{1j}} - i_{d_{1j}} + \frac{k_{1j}}{L_{1j}} \sin(\theta_{1j} + \alpha_{1j}) v_{dc_j} - \frac{V_{1q_j}}{L_{1j}} \tag{4}$$

$$\frac{1}{\omega_S} \dot{i}_{d_{2j}} = -\frac{R_{2j}}{L_{2j}} i_{d_{2j}} + i_{q_{2j}} + \frac{k_{2j}}{L_{2j}} \cos(\theta_{1j} + \alpha_{2j}) v_{dc_j} - \frac{V_{2d_j}}{L_{2j}} + \frac{V_{1d_j}}{L_{2j}} \tag{5}$$

$$\frac{1}{\omega_S} \dot{i}_{q_{2j}} = -\frac{R_{2j}}{L_{2j}} i_{q_{2j}} - i_{d_{2j}} + \frac{k_{2j}}{L_{2j}} \sin(\theta_{1j} + \alpha_{2j}) v_{dc_j} - \frac{V_{2q_j}}{L_{2j}} + \frac{V_{1q_j}}{L_{2j}} \tag{6}$$

$$\frac{C}{\omega_S}\dot{v}_{dc_j} = -k_{1j}\cos(\theta_{1j}+\alpha_{1j})i_{d_{1j}} - k_{1j}\sin(\theta_{1j}+\alpha_{1j})i_{q_{1j}}$$
$$-k_{2j}\cos(\theta_{1j}+\alpha_{2j})i_{d_{2j}} - k_{2j}\sin(\theta_{1j}+\alpha_{2j})i_{q_{2j}} - \frac{v_{dc_j}}{R_{p_j}} \quad (7)$$

where:

$j = 1, ..., n_u$

$i_{1,j} = i_{d_{1j}} + ji_{q_{1j}}$: Shunt injection current in UPFC j (pu)

$i_{2,j} = i_{d_{2j}} + ji_{q_{2j}}$: Series injection current in UPFC j (pu)

R_{1j} : Equivalent shunt resistance in UPFC j (pu)

L_{1j} : Equivalent shunt inductance in UPFC j (pu)

R_{2j} : Equivalent series resistance in UPFC j (pu)

L_{2j} : Equivalent series inductance in UPFC j (pu)

v_{dc_j} : dc bus voltage in UPFC j (pu)

C_j : Equivalent capacitance in UPFC j (pu)

R_{p_j} : Equivalent dc resistance in UPFC j (pu)

k_{1j}, α_{1j} : Modulation amplitude and angle of the shunt part of UPFC j

k_{2j}, α_{2j} : Modulation amplitude and angle of the series part of UPFC j

$$V_{1d_j} = V_{1j}\cos\theta_{1j} \quad (8)$$

$$V_{1q_j} = V_{1j}\sin\theta_{1j} \quad (9)$$

$$V_{2d_j} = V_{2j}\cos\theta_{2j} \quad (10)$$

$$V_{2q_j} = V_{2j}\sin\theta_{2j} \quad (11)$$

If the buses of the new system are numbered as 1 to n_g for generators, $n_g + 1$ to $n_g + n_u$ for UPFCs' sending buses and $n_g + n_u + 1$ to $n_g + 2n_u$ for UPFCs' receiving buses, then we will have:

$$j = 1, ..., n_u$$

$$V_{1j} = E_{n_g + j} \tag{12}$$

$$\theta_{1j} = \delta_{n_g + j} \tag{13}$$

$$V_{2j} = E_{n_g + n_u + j} \tag{14}$$

$$\theta_{2j} = \delta_{n_g + n_u + j} \tag{15}$$

Writing up KCL at the sending and receiving buses of the UPFC and doing some math one can get the following equations:

$$i = 1, ..., n_u$$

$$\begin{aligned} V_{1d_i} = & -\sum_{j=n_g+1}^{n_g+2n_u} \sum_{k=1}^{n_g} Z_{i+n_g,j} Y_{jk} E_k \sin(\Psi_{i+n_g,j} + \Phi_{jk} + \delta_k) \\ & + \sum_{j=1}^{n_u} Z_{i+n_g,j+n_g} \left[i_{d_{1j}} \cos(\Psi_{i+n_g,j+n_g}) - i_{q_{1j}} \sin(\Psi_{i+n_g,j+n_g}) \right] \\ & + \sum_{j=1}^{n_u} Z_{i+n_g,j+n_g} \left[-i_{d_{2j}} \cos(\Psi_{i+n_g,j+n_g}) + i_{q_{2j}} \sin(\Psi_{i+n_g,j+n_g}) \right] \\ & + \sum_{j=1}^{n_u} Z_{i+n_g,j+n_g+n_u} \left[i_{d_{2j}} \cos(\Psi_{i+n_g,j+n_g+n_u}) - i_{q_{2j}} \sin(\Psi_{i+n_g,j+n_g+n_u}) \right] \end{aligned} \tag{16}$$

$$\begin{aligned} V_{1q_i} = & -\sum_{j=n_g+1}^{n_g+2n_u} \sum_{k=1}^{n_g} Z_{i+n_g,j} Y_{jk} E_k \sin(\Psi_{i+n_g,j} + \Phi_{jk} + \delta_k) \\ & + \sum_{j=1}^{n_u} Z_{i+n_g,j+n_g} \left[i_{d_{1j}} \sin(\Psi_{i+n_g,j+n_g}) + i_{q_{1j}} \cos(\Psi_{i+n_g,j+n_g}) \right] \\ & + \sum_{j=1}^{n_u} Z_{i+n_g,j+n_g} \left[-i_{d_{2j}} \sin(\Psi_{i+n_g,j+n_g}) - i_{q_{2j}} \cos(\Psi_{i+n_g,j+n_g}) \right] \\ & + \sum_{j=1}^{n_u} Z_{i+n_g,j+n_g+n_u} \left[i_{d_{2j}} \sin(\Psi_{i+n_g,j+n_g+n_u}) + i_{q_{2j}} \cos(\Psi_{i+n_g,j+n_g+n_u}) \right] \end{aligned} \tag{17}$$

$$
\begin{aligned}
V_{2d_i} = & -\sum_{j=n_g+1}^{n_g+2n_u}\sum_{k=1}^{n_g} Z_{i+n_g+n_u,j} Y_{jk} E_k \sin(\Psi_{i+n_g+n_u,j} + \Phi_{jk} + \delta_k) \\
& + \sum_{j=1}^{n_u} Z_{i+n_g+n_u,j+n_g} \left[i_{d_{1j}} \cos(\Psi_{i+n_g+n_u,j+n_g}) - i_{q_{1j}} \sin(\Psi_{i+n_g+n_u,j+n_g}) \right] \\
& + \sum_{j=1}^{n_u} Z_{i+n_g+n_u,j+n_g} \left[-i_{d_{2j}} \cos(\Psi_{i+n_g+n_u,j+n_g}) + i_{q_{2j}} \sin(\Psi_{i+n_g+n_u,j+n_g}) \right] \\
& + \sum_{j=1}^{n_u} Z_{i+n_g+n_u,j+n_g+n_u} \left[i_{d_{2j}} \cos(\Psi_{i+n_g+n_u,j+n_g+n_u}) - i_{q_{2j}} \sin(\Psi_{i+n_g+n_u,j+n_g+n_u}) \right]
\end{aligned}
\tag{18}
$$

$$
\begin{aligned}
V_{2q_i} = & -\sum_{j=n_g+1}^{n_g+2n_u}\sum_{k=1}^{n_g} Z_{i+n_g+n_u,j} Y_{jk} E_k \sin(\Psi_{i+n_g+n_u,j} + \Phi_{jk} + \delta_k) \\
& + \sum_{j=1}^{n_u} Z_{i+n_g+n_u,j+n_g} \left[i_{d_{1j}} \sin(\Psi_{i+n_g+n_u,j+n_g}) + i_{q_{1j}} \cos(\Psi_{i+n_g+n_u,j+n_g}) \right] \\
& + \sum_{j=1}^{n_u} Z_{i+n_g+n_u,j+n_g} \left[-i_{d_{2j}} \sin(\Psi_{i+n_g+n_u,j+n_g}) - i_{q_{2j}} \cos(\Psi_{i+n_g+n_u,j+n_g}) \right] \\
& + \sum_{j=1}^{n_u} Z_{i+n_g+n_u,j+n_g+n_u} \left[i_{d_{2j}} \sin(\Psi_{i+n_g+n_u,j+n_g+n_u}) + i_{q_{2j}} \cos(\Psi_{i+n_g+n_u,j+n_g+n_u}) \right]
\end{aligned}
\tag{19}
$$

where:

$$
[Z_{ij} \angle \Psi_{ij}] = [Y_{ij} \angle \Phi_{ij}]^{-1} \qquad i, j = n_g + 1, ..., n_g + 2n_u \tag{20}
$$

Equations (1) to (20) could fully describe the model used in this work for controller design.

III. ONE STAGE CONTROLLER DESIGN

Using the full state space model described in the previous section and considering the following $4n_u$ inputs:

$$
\begin{aligned}
& j = 1, ..., n_u \\
& u_{2(j-1)+1} = k_{1j} \cos(\alpha_{1j}) \\
& u_{2(j-1)+2} = k_{1j} \sin(\alpha_{1j}) \\
& u_{2(j-1)+2n_u+1} = k_{2j} \cos(\alpha_{2j}) \\
& u_{2(j-1)+2n_u+2} = k_{2j} \sin(\alpha_{2j})
\end{aligned}
\tag{21}
$$

It would be possible to get a linearized state space system of the form:

$$\dot{X} = AX + BU$$
$$X = [\delta_2, ..., \delta_{n_g}, \omega_1, ..., \omega_{n_g}, i_{d_1}, i_{q_1}, i_{d_2}, i_{q_2}, v_{dc_1}, ..., i_{d_{n_u}}, i_{q_{n_u}}, i_{d_{n_u}}, i_{q_{n_u}}, v_{dc_{n_u}}]^T \quad (22)$$
$$U = [u_1, ..., u_{4n_u}]^T$$

Where A and B are constant matrices. As it is seen in (22), the order of the system is $2n_g + 5n_u - 1$. This is because instead of the equation set (1), the following modified equation set has been used in the linearization process:

$$\dot{\delta}_j = \omega_j - \omega_1 \quad (1)'$$
$$j = 2, ..., n_g$$

The reason for the above manipulation and calculating generators' speed deviations with respect to the first generator is to get a linear system which is controllable. Using (22) and applying an optimal control scheme of the LQR format, it is possible to find an optimal K matrix to account for updated modulation amplitudes and angles from $U = -KX$ during the control process. This approach is called the one stage method because it directly calculates the controlling modulation amplitudes and angles.

IV. TWO STAGE CONTROLLER DESIGN

We write (2) as:

$$j = 1, ..., n_g$$
$$\dot{\omega}_j = (1/M_j)[P_{M_j} - E_j \sum_{k=1}^{n_g} E_k Y_{jk} \cos(\delta_j - \delta_k - \Phi_{jk})$$
$$- E_j \sum_{k=n_g+1}^{n_g+n_u} (E_k Y_{jk} \cos(\delta_j - \Phi_{jk}) r_{2(k-n_g-1)+1} + E_k Y_{jk} \sin(\delta_j - \Phi_{jk}) r_{2(k-n_g-1)+2}) \quad (2)'$$
$$- E_j \sum_{k=n_g+n_u+1}^{n_g+2n_u} (E_k Y_{jk} \cos(\delta_j - \Phi_{jk}) r_{2(k-n_g-1)+1} + E_k Y_{jk} \sin(\delta_j - \Phi_{jk}) r_{2(k-n_g-1)+2})]$$

where:

$$
\begin{aligned}
& j = 1, ..., n_u \\
& r_{2(j-1)+1} = V_{1d_j} \\
& r_{2(j-1)+2} = V_{1q_j} \\
& r_{2(j-1)+2n_u+1} = V_{2d_j} \\
& r_{2(j-1)+2n_u+2} = V_{2q_j}
\end{aligned}
\tag{23}
$$

Considering (1)' and (2)', one can get a nonlinear state space equation of the order $2n_g - 1$ with intermediate control inputs defined by (23). This state space set, which describes the first stage of the control process, is independent of the UPFC dynamics and seems to be mathematically much less complicated than the system defined in III. Linearizing this system and applying an optimal linear control based on LQR would result in optimal values of voltages at both sending and receiving buses of a UPFC at every time step of the control process. The resulting control tries to minimize speed and angle deviations of the machines. Considering UPFC voltages as intermediate inputs of the control problem would decouple them from the power network and one can independently solve the dynamical equations of a UPFC for its modulation amplitudes and angles once its bus voltages are known. This is called the second stage of the control. Fig. 4 shows a flowchart which describes this two stage control schematically.

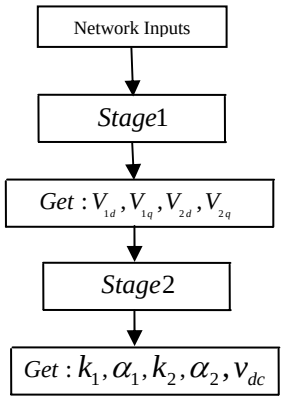

Fig. 4. Two Stage Control Design

V. EXAMPLE AND DISCUSSION

As an example, IEEE 118 bus test system has been considered [8]. This system has 20 machines, where the order of each machine is 10, containing the two-axis generator model, Type I Exciter/AVR model and turbine and governor models. The diagram of the network is shown in Fig. 5.

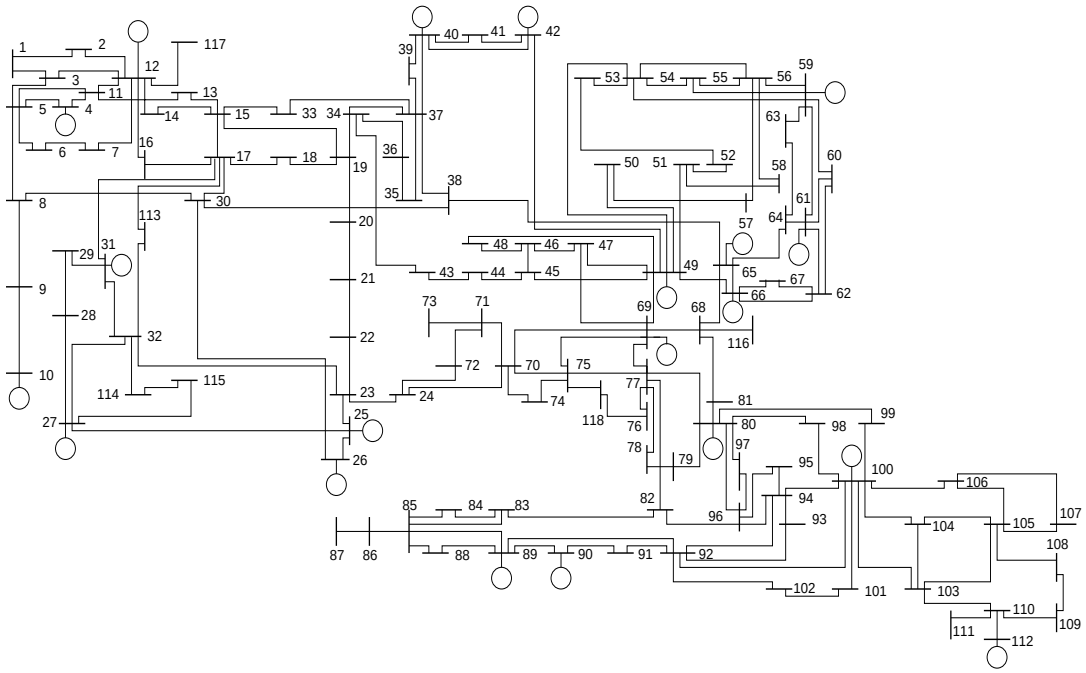

Fig. 5. IEEE 118 Bus Test System

The above system has been nonlinearly simulated using MATLAB with a fault having an admittance of 1 pu occurring on bus 43 at 0.2 s and removed at 0.4 s. Two UPFCs have been installed in the system in lines 30-26 and 64-65 respectively. They operating points of the UPFCs have been initialized using the method discussed in [9]. The characteristics of the UPFCs along with their pre-fault steady state operating points are as follows:

$-UPFC_1-$

$R_1 = 0.01 pu, L_1 = 0.15 pu$

$R_2 = 0.001 pu, L_2 = 0.015 pu$

$R_p = 500 pu$

$C = 2 pu$

$PLoss = 0.08 pu$

k_1 =0.1545, $\alpha_1 = 359.2175^\circ$

$k_2 = 0.0059, \alpha_2 = 254.9898^\circ$

$v_{dc} = 6.1098$pu

$i_{d_1} = -0.0882$pu, $i_{q_1} = 0.0031$pu

$i_{d_2} = -1.9596$pu, $i_{q_2} = 1.1926$pu

$-UPFC_2-$

$R_1 = 0.01 pu, L_1 = 0.10 pu$

$R_2 = 0.001 pu, L_2 = 0.010 pu$

$R_p = 500 pu$

$C = 2 pu$

$PLoss = 0.08 pu$

k_1 =0.1582, $\alpha_1 = 359.4904^\circ$

$k_2 = 0.0018, \alpha_2 = 238.9933^\circ$

$v_{dc} = 6.1748$pu

$i_{d_1} = -0.0861$pu, $i_{q_1} = 0.0094$pu

$i_{d_2} = -1.6997$pu, $i_{q_2} = 0.8824$pu

Two controllers have been designed using the One Stage and Two Stage schemes respectively. Simulations have been compared with the case where no UPFC exists in the system and the results have been shown in the following figures. The weighting matrices for both controllers have been chosen such that the most possible damping of inter-area oscillations can be obtained. Fig. 6 shows the speed of generators. The dashed plots show the simulations with no UPFC and the thin and bold plots show the results with the One Stage and Two Stage controllers, respectively. As it is seen, speed deviations have been controlled using the Two Stage controller

effectively. Also note that for both the uncontrolled and the One Stage controller there exist low frequency components which have not been damped out completely by the end of the simulation. The results of the Two Stage controller do not show this low frequency component at all. The One Stage controller shows qualitatively compatible results with [10]. In [10], the differential-algebraic equations of the power system have been directly linearized for designing the controller. Fig. 7 shows the controlling modulation amplitudes and angles of the UPFCs during the control process. Fig. 8 depicts UPFC currents in d-q format and Fig. 9 shows UPFC ac and dc voltages.

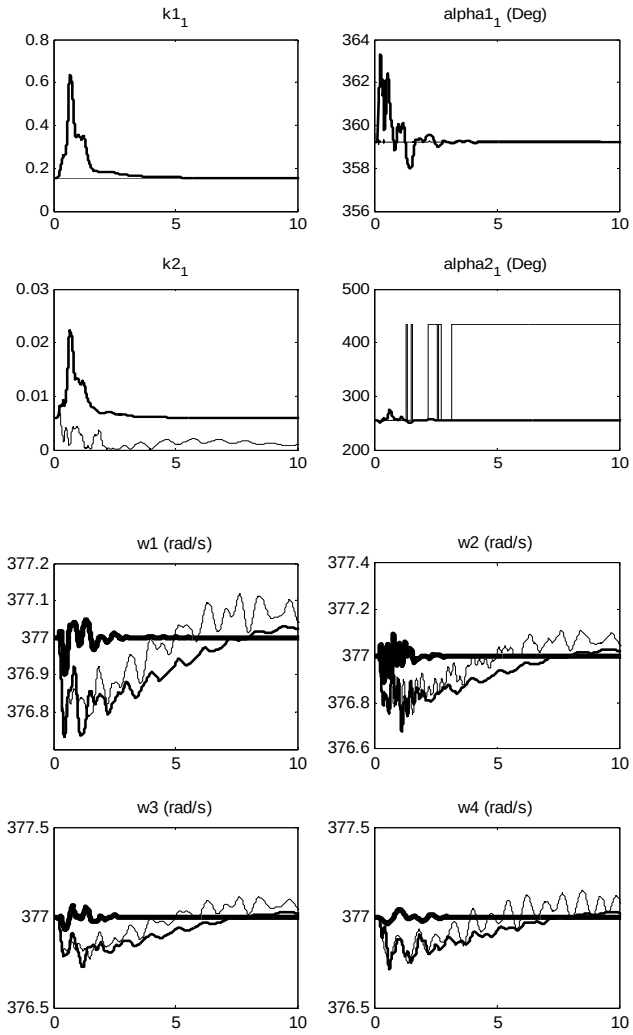

Fig. 6. Speed Deviations (No Control: thin, One Stage: bold, Two Stage: boldest)

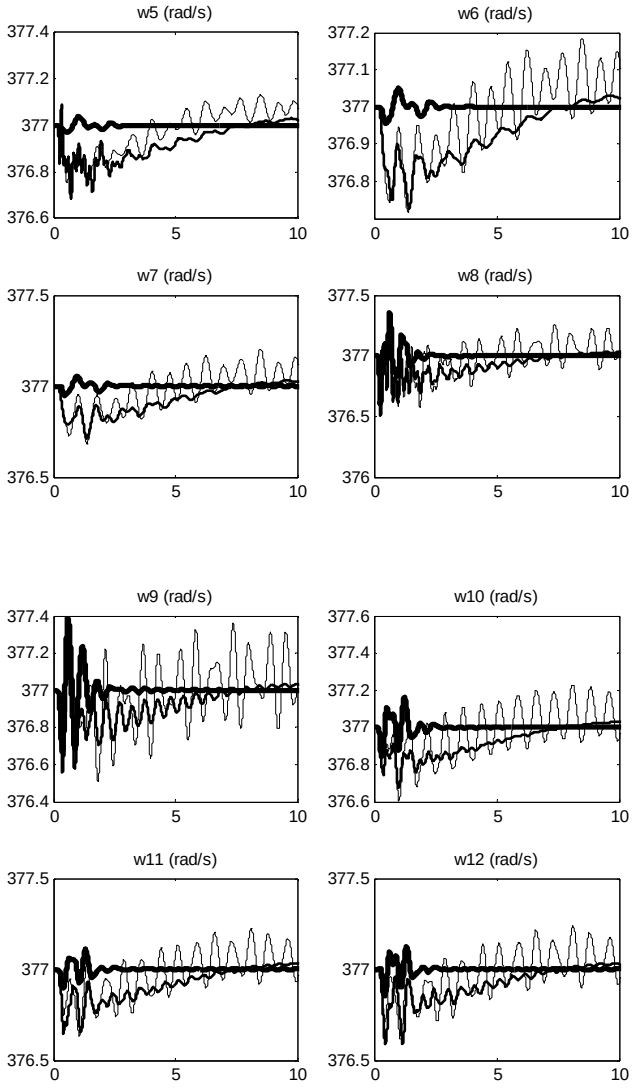

continued Fig. 6. Speed Deviations (No Control: thin, One Stage: bold, Two Stage: boldest)

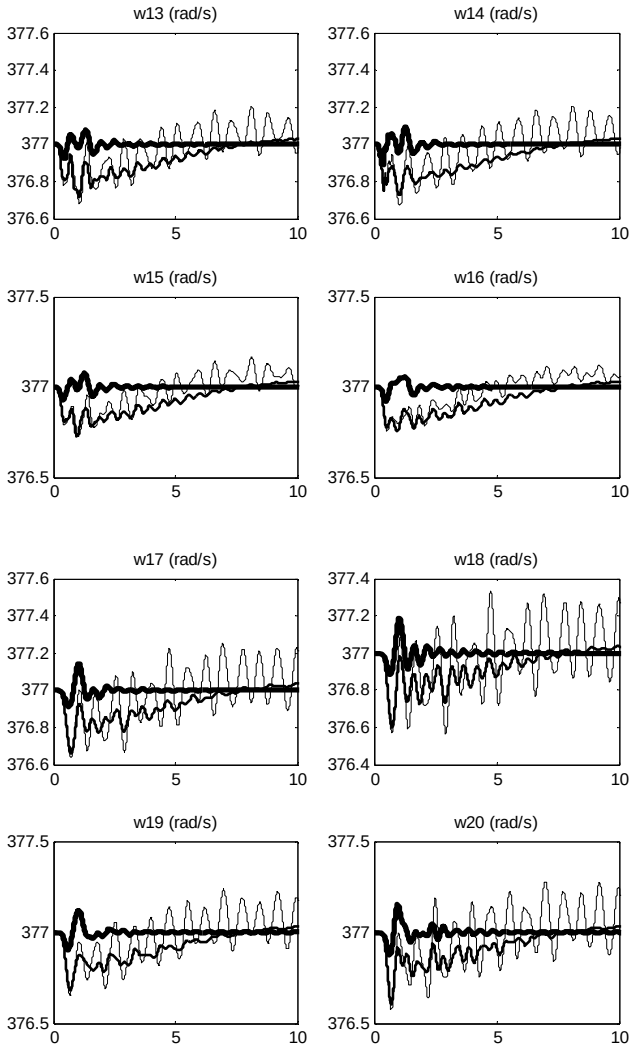

continued Fig. 6. Speed Deviations (No Control: thin, One Stage: bold, Two Stage: boldest)

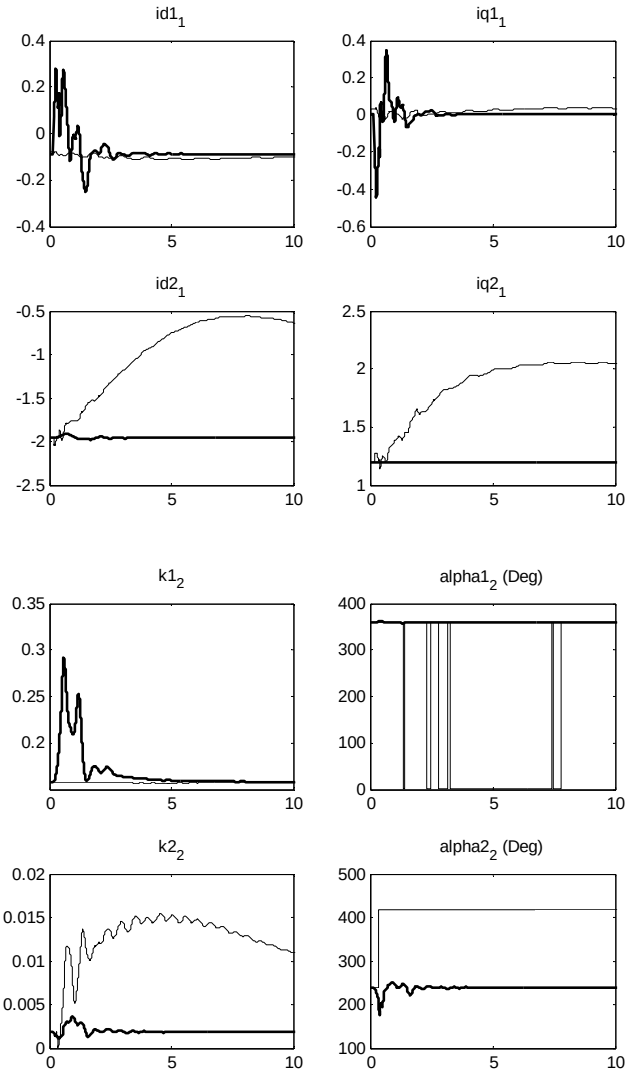

Fig. 7. Modulation Amplitudes and Angles (One Stage: thin, Two Stage: bold)

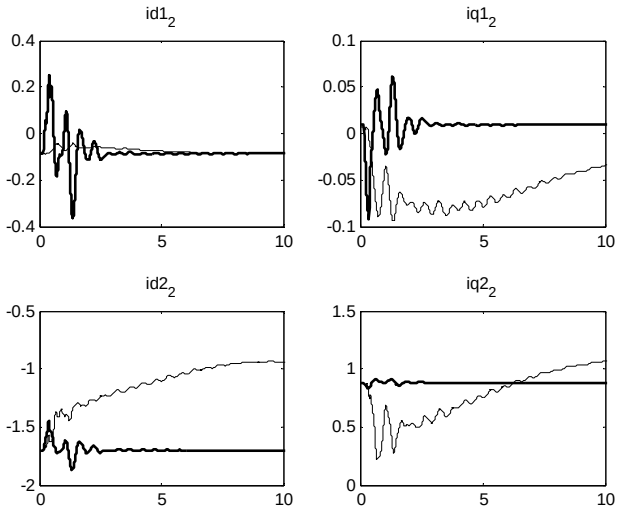

Fig. 8. UPFC Currents (One Stage: thin, Two Stage: bold)

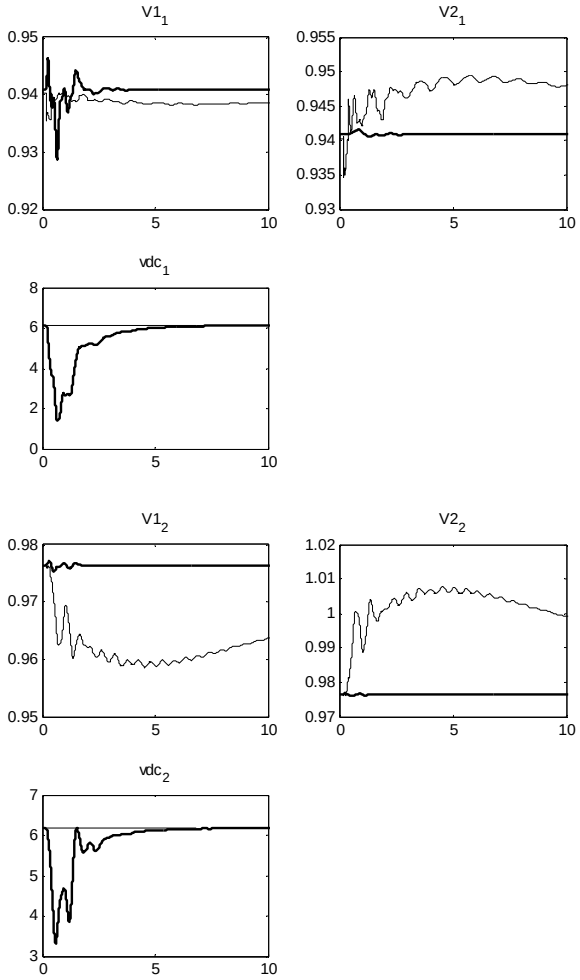

Fig. 9. UPFC ac & dc Voltages (One Stage: thin, Two Stage: bold)

As it is generally seen in the figures, the Two Stage controller shows more effective and quicker results. However, there are more severe transients for the dc voltages in the Two Stage controller. Actually, the pre-fault steady-state operating situations play an important role in the success of the Two Stage controller. As it is seen, dc voltages may come down from 6 pu to less than 2 pu during the control. This shows that in order for the Two Stage controller to do its work, the dc side should be capable of injecting enough energy into the system. Authors found out that 3 major factors effect the operation of the Two Stage controller: **(a)** C or the equivalent capacitance of the UPFC, **(b)** P_{Loss} at pre-fault steady-state which describes ac losses of the UPFC, and **(c)** R_p which describes the dc losses of the UPFC. From the above 3 factors, increase of P_{Loss} and R_p tend to increase the steady-state operating point of v_{dc}. Several simulations show that successful operation of the controller is guaranteed when the values of C, P_{Loss} and R_p are increased, or when more capacitance, more ac losses and less dc losses exist in UPFCs. This sensitivity does not hold for the One Stage controller, where the simulations were repeated with a broad range of C, P_{Loss} and R_p and the simulation results were generally successful.

VI. CONCLUSION

Two control schemes for damping inter-area oscillations using multiple UPFCs have been introduced in this paper, which are both based on the linear control theory. They are both state-feedback controllers and assume that global data of the power system is available to the controllers. The Two Stage controller shows more effective and quicker results than the One Stage controller. However, certain operating conditions must be provided for the Two Stage controller to do its job effectively. These conditions are mostly affected by UPFC dc capacitance and its ac and dc losses, where more capacitance and ac losses from one hand and less dc losses from the other hand can enhance the operation of the controller. Simulations show that a compromise between these three parameters could be gained for practical purposes.

Further work includes designing decentralized controllers which depend on only local data. Further investigation could be made on designing nonlinear controllers based on the proposed nonlinear modeling. Robustness and dependency of the designed controllers on the topology changes of the power system is also a matter of concern.

REFERENCES

[1] HaiFeng Wang, "A Unified Model for the Analysis of FACTS Devices in Damping Power System Oscillations---Part III: Unified Power Flow Controller," *IEEE Trans. Power Delivery*, vol. 15, no. 3, pp. 978-983, July 2000.

[2] Mehrdad Ghandhari, G. Andersson and Ian A. Hiskens, "Control Lyapunov Functions for Controllable Series Devices," *IEEE Trans. Power Systems*, vol. 16, no. 4, pp. 689-694, Nov. 2001.

[3] B.C. Pal, "Robust damping of interarea oscillations with unified power-flow controller," *IEE Proceedings- Generation, Transmission and Distribution*, vol. 149, pp. 733-738, Nov. 2002.

[4] S. Robak, M. Januszewski, D.D. Rasolomampionona, "Power system stability enhancement using PSS and Lyapunov-based controllers: A comparative study," *IEEE Power Tech Conference Proceedings* 2003 Bologna, vol. 3, pp. 6.

[5] N. Tambey and M.L. Kothari, "Damping of power system oscillations with unified power flow controller (UPFC)," *IEE Proceedings- Generation, Transmission and Distribution*, vol. 150, pp. 129-140, March 2003.

[6] M. Januszewski, J. Machowski and J.W. Bialek, "Application of the direct Lyapunov method to improve damping of power swings by control of UPFC," *IEE Proceedings- Generation, Transmission and Distribution*, vol. 151, pp. 252-260, March 2004.

[7] L. Dong, M.L. Crow, Z. Yang, C. Shen, L. Zhang, S. Atcitty, "A Reconfigurable FACTS System for University Laboratories," *IEEE Transactions on Power Systems*, Vol. 19, no. 1, pp. 120-128, Feb. 2004.

[8] http://www.ee.washington.edu/research/pstca/pf118/pg_tca118bus.htm

[9] M. Zarghami, M.L. Crow, "The Existence of Multiple Equilibria in the UPFC Power Injection Model," *IEEE Transactions on Power Systems*, to be published.

[10] J. Guo, "Decentralized Control and Placement of Multiple Unified Power Flow Controllers," Ph.D. dissertation, Dept. Elec. Eng., Univ. of Missouri-Rolla, 2006.

4. A Novel Approach to Inter-Area Oscillation Damping by UPFC Voltage Control

M. Zarghami, *Student Member, IEEE*, M. L. Crow, *Senior Member, IEEE*
S. Jagannathan, *Senior Member, IEEE*, and Y. Liu *Fellow, IEEE*

ABSTRACT: This paper discusses a novel approach for damping inter-area oscillations in a bulk power network using multiple unified power flow controllers (UPFC). In this paper, a new control is introduced to mitigate inter-area oscillations by directly controlling the UPFCs' sending and receiving bus voltages. The results of this controller are compared to a traditional approach that works by controlling the active and reactive power flows through the UPFCs. The proposed control provides better inter-area oscillation mitigation when applied to multiple UPFCs in the 118 bus IEEE test system.

Index Terms – UPFC, oscillation damping, power system stability

I. INTRODUCTION

In addition to steady-state power flow control, damping oscillations in a power network is one of the primary applications of a Unified Power Flow Controller (UPFC). As high voltage power electronics become less expensive, FACTS devices will become more prevalent in the bulk transmission system to control active power flow across congested corridors and ensure voltage security. An added benefit of UPFCs deployed in the transmission system is that they can also effectively control active power oscillations that can damage generators, increase line losses, and increase wear and tear on network components. Therefore developing suitable control strategies is a requirement before UPFCs can be confidently utilized in the power system.

Mitigating power oscillations can be accomplished by rapidly changing the power flow through the series part of the UPFC. By controlling the amplitude and angle of the series

injected voltage, the active and reactive power flow in the transmission line can be altered. Several authors have investigated utilizing the UPFC to damp inter-area oscillations utilizing a variety of control approaches [1]-[10]. Some of this work is based on a linear control analysis of the UPFC and power system [1]-[5], whereas other authors consider nonlinear control systems theory and Lyapunov Energy Functions [6]-[10]. Regardless of which approach the control law is based upon, the UPFC controller ultimately performs the control by commanding the appropriate modulation amplitudes (k_1, k_2) and angles (α_1, α_2) of the series and shunt voltages.

The UPFC power injection model is widely used for power system simulations (recent examples include [2]-[4]). In the power injection model, the impact of the UPFC in the network is represented by its series and shunt current injections, or similarly, its series and shunt active and reactive power injections. A common approach to incorporating the power injection model into the system is to represent the UPFC as two buses: a 'PQ' bus at the receiving end in which both active and reactive power are specified, and a 'PV' bus at the sending end in which voltage and active power are specified [11].

In this paper, a new UPFC control methodology is introduced for damping inter-area oscillations in which the sending and receiving end voltages are utilized instead of the active and reactive powers. This is based on a two-stage control scheme in which the controlling UPFC voltages are first determined and then the desired sending and receiving end conditions are imposed upon the UPFC dynamics to derive the controlling modulation amplitudes and angles. The results of the proposed controller are then compared to a traditional approach that controls the active and reactive power flows through the UPFCs. Both of these methods are based on linear control theory, however they are both validated using a full non-linear system simulation. The resulting dynamics indicate that the proposed controller provides significantly better damping in the 118 bus IEEE test system.

II. THE UPFC MODEL

The unified power flow controller, or UPFC, is the most versatile FACTS device. It consists of a combination of a shunt and series branches connected through the DC capacitor as shown in Fig. 1. The series connected inverter injects a voltage

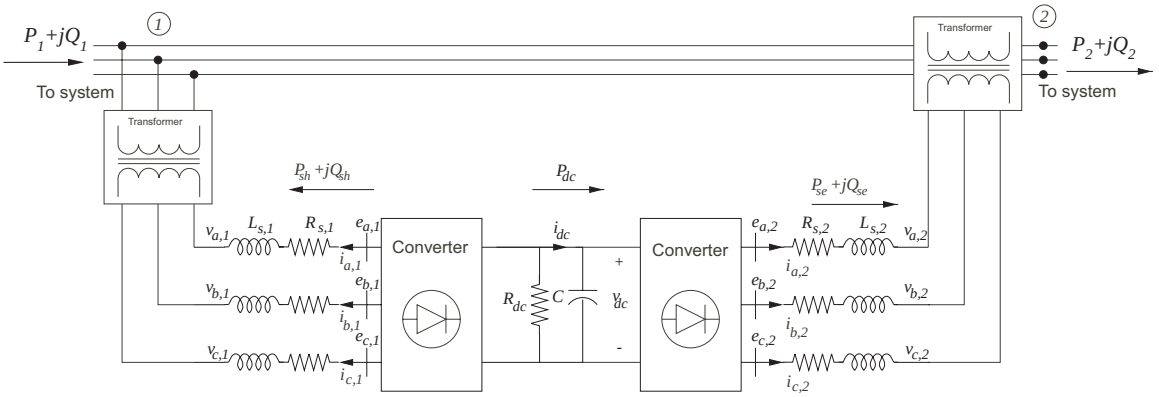

Fig. 1. Unified Power Flow Controller Diagram

with controllable magnitude and phase angle in series with the transmission line, therefore providing real and reactive power to the transmission line. The shunt-connected inverter provides the active power drawn by the series branch plus the losses and can independently provide reactive compensation to the system. The UPFC model is a combination of the STATCOM (Static Synchronous Compensator) and SSSC (Static Synchronous Series Compensator) models [12]:

$$\frac{1}{\omega_s}\frac{d}{dt}i_{d_1} = \frac{k_1 V_{dc}}{L_{s_1}}\cos(\alpha_1+\theta_1) + \frac{\omega}{\omega_s}i_{q_1} - \frac{R_{s_1}}{L_{s_1}}i_{d_1} - \frac{V_1}{L_{s_1}}\cos\theta_1 \quad (1)$$

$$\frac{1}{\omega_s}\frac{d}{dt}i_{q_1} = \frac{k_1 V_{dc}}{L_{s_1}}\sin(\alpha_1+\theta_1) - \frac{R_{s_1}}{L_{s_1}}i_{q_1} - \frac{\omega}{\omega_s}i_{d_1} - \frac{V_1}{L_{s_1}}\sin\theta_1 \quad (2)$$

$$\frac{1}{\omega_s}\frac{d}{dt}i_{d_2} = -\frac{R_{s_2}}{L_{s_2}}i_{d_2} + \frac{\omega}{\omega_s}i_{q_2} + \frac{k_2}{L_{s_2}}\cos(\alpha_2+\theta_1)V_{dc} - \frac{1}{L_{s_2}}(V_2\cos\theta_2 - V_1\cos\theta_1) \quad (3)$$

$$\frac{1}{\omega_s}\frac{d}{dt}i_{q_2} = -\frac{R_{s_2}}{L_{s_2}}i_{q_2} - \frac{\omega}{\omega_s}i_{d_2} + \frac{k_2}{L_{s_2}}\sin(\alpha_2+\theta_1)V_{dc} - \frac{1}{L_{s_2}}(V_2\sin\theta_2 - V_1\sin\theta_2) \quad (4)$$

$$\frac{C}{\omega_s}\frac{d}{dt}V_{dc} = -k_1\cos(\alpha_1+\theta_1)i_{d_1} - k_1\sin(\alpha_1+\theta_1)i_{q_1} - k_2\cos(\alpha_2+\theta_1)i_{d_2} - k_2\sin(\alpha_2+\theta_1)i_{q_2} - \frac{V_{dc}}{R_{dc}} \quad (5)$$

where the parameters are as shown in Fig. 1. The currents i_{d1} and i_{q1} are the dq components of the shunt current. The currents i_{d2} and i_{q2} are the dq components of

the series current. The voltages $V_1\angle\theta_1$ and $V_2\angle\theta_2$ are the sending end and receiving end voltage magnitudes and angles respectively. The UPFC is controlled by varying the phase angles (α_1, α_2) and magnitudes (k_1, k_2) of the converter shunt and series output voltages (e_1, e_2) respectively.

The power balance equations at bus 1 are given by:

$$0 = V_1\left((i_{d_1} - i_{d_2})\cos\theta_1 + (i_{q_1} - i_{q_2})\sin\theta_1\right) - V_1\sum_{j=1}^{n} V_j Y_{1j}\cos\left(\theta_1 - \theta_j - \phi_{1j}\right) \quad (6)$$

$$0 = V_1\left((i_{d_1} - i_{d_2})\sin\theta_1 - (i_{q_1} - i_{q_2})\cos\theta_1\right) - V_1\sum_{j=1}^{n} V_j Y_{1j}\sin\left(\theta_1 - \theta_j - \phi_{1j}\right) \quad (7)$$

and at bus 2:

$$0 = V_2\left(i_{d_2}\cos\theta_2 + i_{q_2}\sin\theta_2\right) - V_2\sum_{j=1}^{n} V_j Y_{2j}\cos\left(\theta_2 - \theta_j - \phi_{2j}\right) \quad (8)$$

$$0 = V_2\left(i_{d_2}\sin\theta_2 - i_{q_2}\cos\theta_2\right) - V_2\sum_{j=1}^{n} V_j Y_{2j}\sin\left(\theta_2 - \theta_j - \phi_{2j}\right) \quad (9)$$

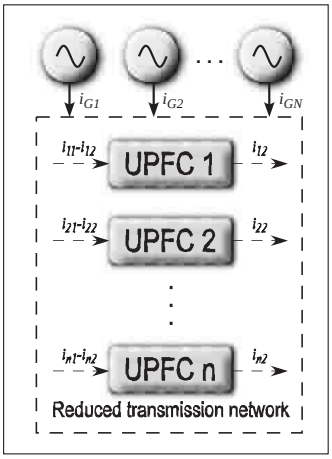

Fig. 2. Equivalent power system from the "voltage control" view

III. "VOLTAGE CONTROL" CONTROLLER DESIGN

For control development purposes, several assumptions are initially made. The two simplifying assumptions are that the system loads are modeled as constant impedance loads and can therefore be absorbed into the bus admittance matrix. Secondly, the generators are modeled as the classical "transient reactance behind constant voltage" model. Note that these assumptions are for control development only – the proposed

control is validated with the full nonlinear 10-th order power system model given in the Appendix. Using the load impedance model, the only points of current injection into the network are the generator internal buses and the UPFC sending and receiving end buses. Furthermore, Kron reduction enables the transmission network to be reduced to an admittance matrix of size $(N + 2n \times N + 2n)$ where N is the number of generator buses and n is the number of UPFCs in the system. Fig. 2 illustrates the reduced system showing the points of current injection. Each UPFC has two current injections, i_1 and i_2, at the sending and receiving ends respectively. The generator current injections are given by i_G. The classical model for the reduced network including the UPFCS is:

$$\dot{\delta}_j = \omega_j - \omega_s \tag{10}$$

$$\begin{aligned}\dot{\omega}_j = \frac{1}{M_j}\Bigg[& P_{M_j} - E_j \sum_{k=1}^{N} E_k Y_{jk} \cos\left(\delta_j - \delta_k - \phi_{jk}\right) \\ & -E_j \sum_{k=N+1}^{N+n} E_k Y_{jk} \left(\cos\left(\delta_j - \phi_{jk}\right) r_{2(k-N-1)+1} + \sin\left(\delta_j - \phi_{jk}\right) r_{2(k-N-1)+2}\right) \\ & -E_j \sum_{k=N+n+1}^{N+2n} E_k Y_{jk} \left(\cos\left(\delta_j - \phi_{jk}\right) r_{2(k-N-1)+1} + \sin\left(\delta_j - \phi_{jk}\right) r_{2(k-N-1)+2}\right) \Bigg] \\ & j = 1 \ldots, N\end{aligned} \tag{11}$$

where $E_j \angle \delta_j$ is the voltage at bus j, $Y_{jk} \angle \phi_{jk}$ is the $(j,k)th$ element of the reduced admittance matrix, $P_{m_j}, M_j,$ and ω_j are the mechanical power, inertia constant, and angular speed respectively of machine j, and ω_s is synchronous speed. The first summation represents the active power injected at each generator bus, the second summation represents the active power injected at each UPFC sending bus, and the third summation represents the active power injected at each UPFC receiving bus.

This nonlinear system has $2N$ states and $4n$ intermediate control inputs r_j defined as:

$$r_{2(j-1)+1} = V_{1dj} \tag{12}$$

$$r_{2(j-1)+2} = V_{1qj} \tag{13}$$

$$r_{2(j-1)+2n+1} = V_{2dj} \tag{14}$$

$$r_{2(j-1)+2n+2} = V_{2qj} \quad j = 1, \ldots, n \tag{15}$$

where $V_{1dj}, V_{1qj}, V_{2dj}$ and V_{2qj} are the dq components of the sending (1) and receiving (2) ends for the j-th UPFC respectively. This step describes the first stage of the two

stage control. Note that this stage is independent of the UPFC dynamics.

Linearizing this reduced system results in a linear system of the form:

$$\dot{X} = AX + BR \tag{16}$$

where R represents the vector of the UPFC dq voltages. This system can be linearized through the feedback control

$$R = -KX \tag{17}$$

where K is chosen using optimal LQR control processes to minimize speed and angle deviations in the generators. If the original system were linear, this feedback control would result in the optimal values of voltage magnitudes and angles at both the sending and receiving buses of the UPFC to damp the interarea oscillations.

The second stage of the control is to convert the control inputs R into the modulation gain and phase angles k and α for each UPFC. The first step in this stage is to find the values of currents i_{d1}, i_{q1}, i_{d2} and i_{q2} from the UPFC active and reactive power balance equations at the sending and receiving end buses given in equations (6)-(9).

If it can be assumed that the time scale difference between the UPFCs and the generator dynamics is large (i.e. $\frac{1}{\omega_s} \ll \frac{1}{M_i}$) and letting $\frac{1}{\omega_s} \approx 0$, then equations (1)-(4) can be rewritten as their algebraic counterparts:

$$0 = \frac{k_1 V_{dc}}{L_{s_1}} \cos(\alpha_1 + \theta_1) + \frac{\omega}{\omega_s} i_{q_1} - \frac{R_{s_1}}{L_{s_1}} i_{d_1} - \frac{V_1}{L_{s_1}} \cos\theta_1 \tag{18}$$

$$0 = \frac{k_1 V_{dc}}{L_{s_1}} \sin(\alpha_1 + \theta_1) - \frac{R_{s_1}}{L_{s_1}} i_{q_1} - \frac{\omega}{\omega_s} i_{d_1} - \frac{V_1}{L_{s_1}} \sin\theta_1 \tag{19}$$

$$0 = -\frac{R_{s_2}}{L_{s_2}} i_{d_2} + \frac{\omega}{\omega_s} i_{q_2} + \frac{k_2}{L_{s_2}} \cos(\alpha_2 + \theta_1) V_{dc} - \frac{1}{L_{s_2}} (V_2 \cos\theta_2 - V_1 \cos\theta_1) \tag{20}$$

$$0 = -\frac{R_{s_2}}{L_{s_2}} i_{q_2} - \frac{\omega}{\omega_s} i_{d_2} + \frac{k_2}{L_{s_2}} \sin(\alpha_2 + \theta_1) V_{dc} - \frac{1}{L_{s_2}} (V_2 \sin\theta_2 - V_1 \sin\theta_2) \tag{21}$$

Solving equations (18)-(21) together with (5) provides the values of k_1, α_1, k_2, and α_2 which are the true control inputs to the UPFC. This procedure can be repeated for each UPFC independently since the first stage of the control provides the network coupling during the determination of the input R (the sending and receiving end voltages). Fig. 3 shows a flow chart which illustrates the two stage control.

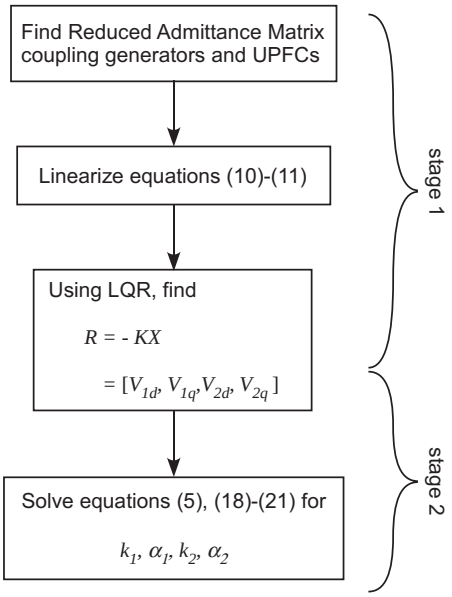

Fig. 3. Two stage control design

IV. "POWER CONTROL" CONTROLLER DESIGN

In this section, a more traditional "power control" approach is derived. It is based on the control developed in [13]. The power system equations can generally be written as

$$\dot{X} = F(X,Y) \tag{22}$$

$$0 = H(X,Y,U) \tag{23}$$

where X is the set of state variables (generator states), Y is the set of network variables (usually bus voltages and angles), and U is the set of inputs. In this control approach, the set of inputs is taken to be the set of UPFC active and reactive powers at the sending and receiving end buses. In this control approach, the UPFC is modeled as a "power injection" model [11] and the UPFC dynamics are neglected. For the purpose of control development, the changes in reactive powers are considered to be small and the UPFC losses are neglected, then equations (22)-(23) can be linearized:

$$\dot{X} = \frac{\partial F}{\partial X}\Delta X + \frac{\partial F}{\partial Y}\Delta Y \tag{24}$$

$$0 = \frac{\partial H}{\partial X}\Delta X + \frac{\partial H}{\partial Y}\Delta Y + \frac{\partial H}{\partial U}\Delta U \tag{25}$$

Solving equation (25) for ΔY in terms of ΔX and ΔU yields

$$\Delta\dot{X} = \left(\frac{\partial F}{\partial X} - \frac{\partial F}{\partial Y}\left(\frac{\partial H}{\partial Y}\right)^{-1}\frac{\partial H}{\partial X}\right)\Delta X - \left(\frac{\partial F}{\partial Y}\left(\frac{\partial H}{\partial Y}\right)^{-1}\frac{\partial H}{\partial U}\right)\Delta U \quad (26)$$

$$= A\Delta X + B\Delta U \quad (27)$$

where $\Delta U = \Delta P$ is the vector of changes to the existing active power flows through the UPFC. Once again using LQR, then

$$\Delta U = -K\Delta X \quad (28)$$

The UPFC reactive powers are calculated using a PI controller to keep the sending and receiving end voltage magnitudes at their desired levels. Once the new control values of active and reactive power are found, they are converted into the corresponding switching inputs $k_1, \alpha_1, k_2,$ and α_2 respectively.

V. THE TEST SYSTEM

The IEEE 118 bus test system has been used to compare the two different controllers. The diagram of the network is shown in Fig. 4. This system has 20 generators each modeled with the set of equations given in the Appendix. Two UPFCs have been installed in the system in lines 30-26 and 64-65 with the shunt (sending) parts on buses 30 and 64, respectively. These particular lines were chosen heuristically as being tie lines between coherent areas. Very little research has addressed the placement of UPFCs for stability improvement. Most placement algorithms consider only static line loadability or placement for conjestion reduction. However, one recent work [14] addresses the use of modal controllability indices specifically for FACTS placement for oscillation damping.

The parameters of the UPFCs are given in Table I. The per unit approach is the same as in [15] on a 100MW, 100kV system. For example, this corresponds to a Z_{base} of 100Ω.

TABLE I
UPFC PARAMETERS (IN PU)

	R_1	L_1	R_2	L_2	R_{dc}	C
UPFC1	0.01	0.15	0.001	0.015	51.0	686.0
UPFC2	0.01	0.10	0.001	0.010	51.0	686.0

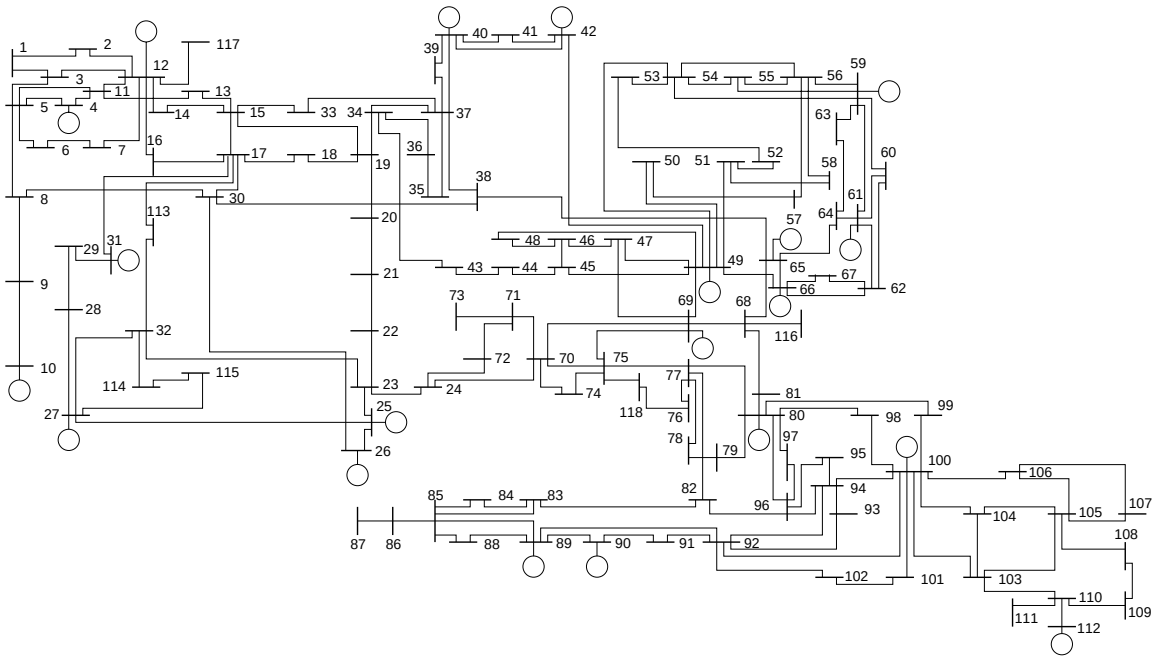

Fig. 4. IEEE 118 bus test system

VI. CONTROLLER RESULTS AND COMPARISONS

In this section the results of the “power controlled” method are compared with the “voltage controlled” approach. Although the controllers for both methods have been designed based on linear control approaches, the simulations have been performed on full nonlinear differential-algebraic systems (as given in the Appendix).

In the highlighted example, a solid symmetrical fault has been applied on bus 43 at 0.2 seconds and has been cleared in 0.4 seconds. The frequencies of a selected set of generators is shown in Fig. 5. Not all of the frequencies are shown due to space constraints, but the results are similar. The thin lines are the dynamic responses with no UPFCs, the thick lines are the “voltage control” approach and the dashed lines indicate the “power control” results respectively. As can be seen in the various traces, both the “power” and “voltage” control approaches mitigate the oscillations in comparison to the uncontrolled case. However, the “voltage” controlled case indicates much better oscillation damping and it able to hold the generator frequencies at nearly synchronous speed, whereas both uncontrolled and “power” controlled results show evidence of a very slow low frequency excursion (0.02 Hz) due to the very slow time response of the

speed-governor.

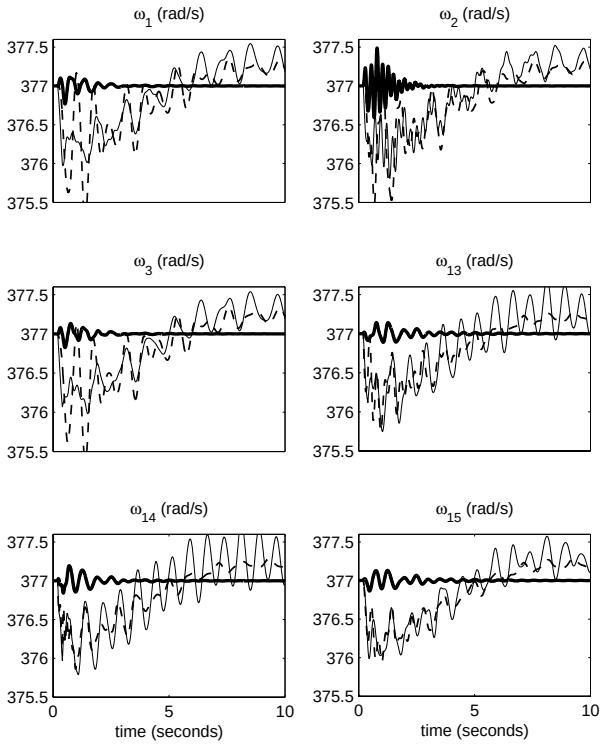

Fig. 5. Generator frequency (no control – thin line, power control – dashed line, voltage control – thick line)

Fig. 6 shows the sending and receiving end bus voltages for the two UPFCs. The time scale has been decreased for better detail. Even though V_{1d}, V_{1q}, V_{2d}, and V_{2q} are modified through the control approach, the change in the bus magnitudes $|V_d + jV_q|$ is very small and thus appears nearly constant. This is the primary design of the control approach. The power control approach yields voltages that vary during the fault, but does provide good voltage damping following the fault clearing compared to the no control case.

Fig. 7 shows the receiving end active power flows. The negative sign indicates that the active power normally flows from bus 2 to bus 1. Both the voltage and power control approaches provide significant oscillation damping. The proposed voltage control approach does result in larger transient active power excursions than the power control approach, but smaller steady-state active power excursions.

Fig. 8 shows the magnitude of the voltage injected by the series transformer. Figs. 9 and

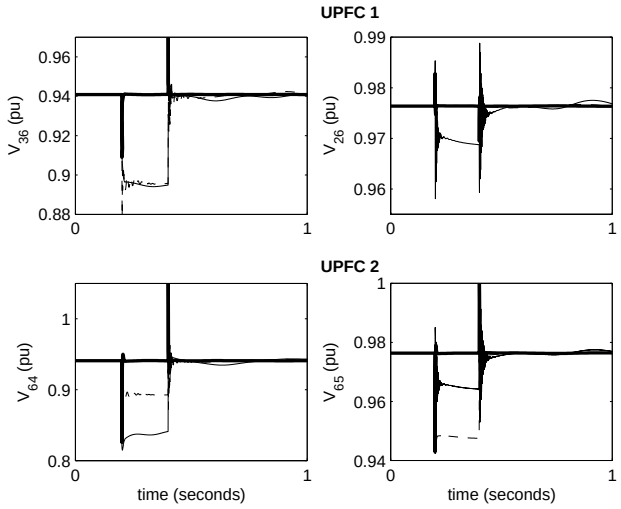

Fig. 6. UPFC voltages (no control – thin line, power control – dashed line, voltage control – thick line)

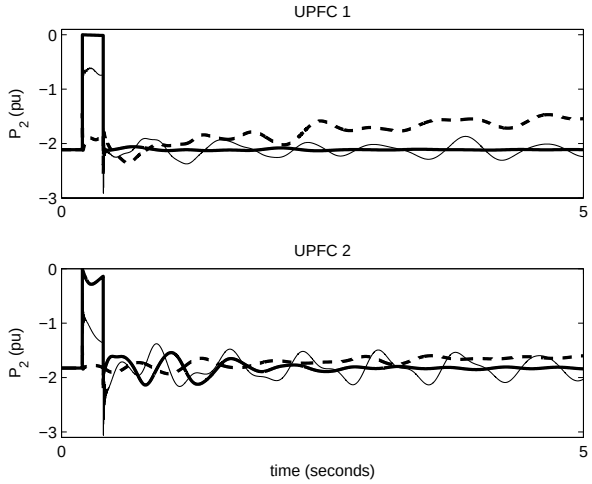

Fig. 7. UPFC receiving end power flows (no control – thin line, power control – dashed line, voltage control – thick line)

10 show the injected active and reactice powers by the series transformer respectively. Note that in all cases, the injected powers are less than 10% of the active power on the line and the injected voltage magnitude is small.

The active power injected through the shunt converter is shown in Fig. 11 and the dc link capacitor voltage is shown in Fig. 12. The primary difference between the controls

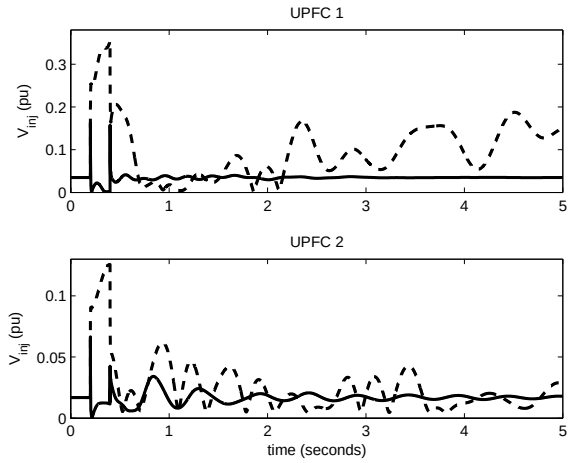

Fig. 8. UPFC injected voltage (power control – dashed line, voltage control – thick line)

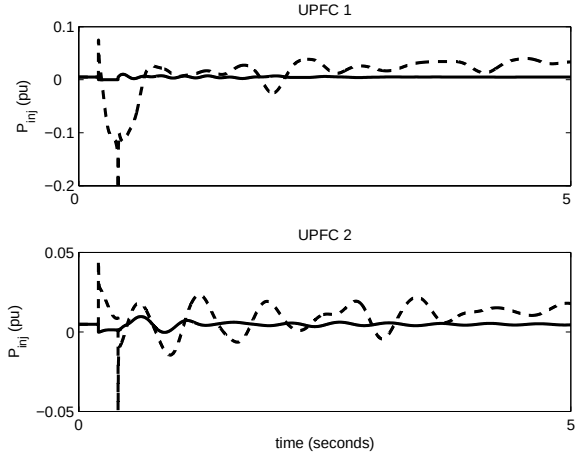

Fig. 9. UPFC injected active power (power control– dashed line, voltage control–thick line)

is that the voltage control approach more effectively utilizes the active power out of the dc link capacitor than does the power control approach to damp the interarea oscillations. After the oscillations have been damped, the active power injection returns to near zero which is the active power normally utilized by the converter to account for switching losses. Longer duration analysis shown in Fig. 13 indicates that the dc link capacitor voltage returns to nominal within 100 seconds. This is a sufficient recharge rate unless multiple contingencies occur in close succession.

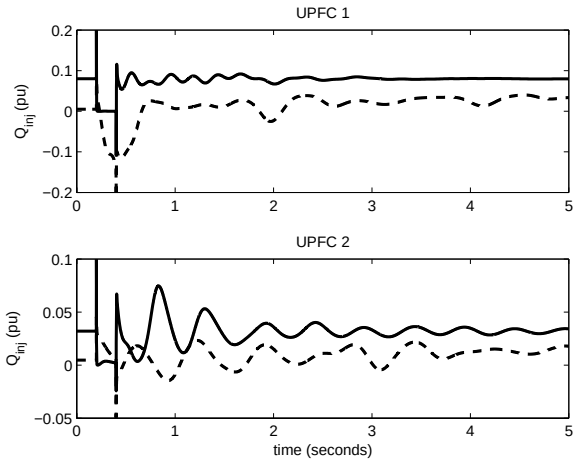

Fig. 10. UPFC injected reactive power (power control – dashed line, voltage control – thick line)

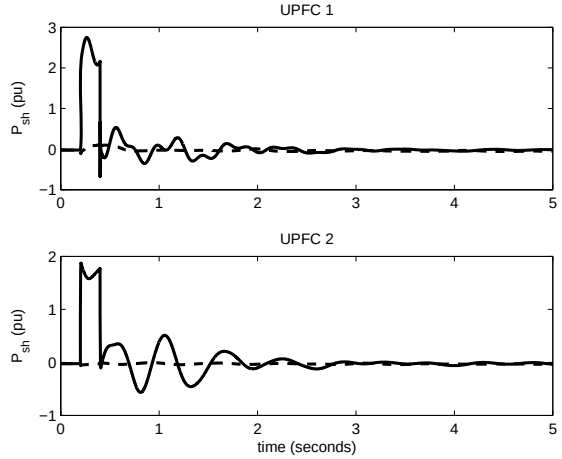

Fig. 11. UPFC shunt active power (power control – dashed line, voltage control – thick line)

In order to quantify the behavior of the controllers and compare them with the uncontrolled case, the following generator frequency and bus voltage profile indices are used:

$$I_\omega = \frac{1}{N}\sum_{i=1}^{N}\left(\frac{1}{n_s}\sum_{j=1}^{n_s}|\omega_i - \omega_s|\right) \quad (29)$$

$$I_V = \frac{1}{N_b}\sum_{i=1}^{N_b}\left(\frac{1}{n_s}\sum_{j=1}^{n_s}|V_i - V_i^\star|\right) \quad (30)$$

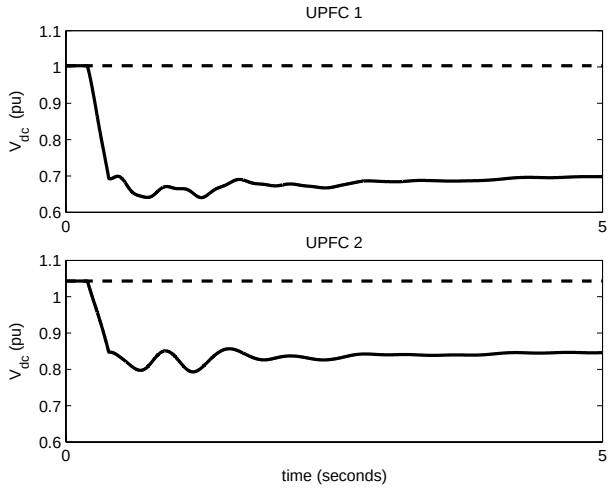

Fig. 12. UPFC dc link capacitor voltages (power control – dashed line, voltage control – thick line)

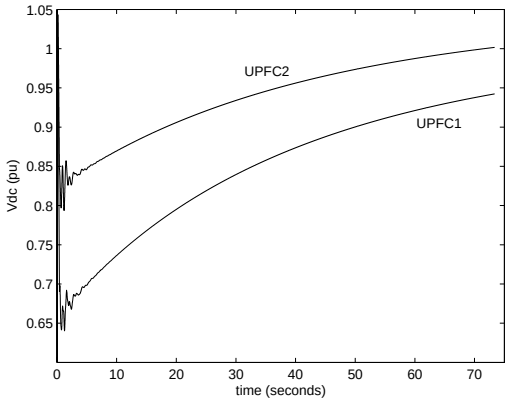

Fig. 13. UPFC dc link capacitor voltages under power control – longer duration

where N is the number of generators in the system, N_b is the number of buses, n_s is the number of samples, and $V_i^\star$ is the desired voltage magnitude at UPFC bus i. These indices provide a quantitative measure of the performance of each control approach. The lower the index, the better the performance of the control approach. Table II shows the indices for the two controlled cases and the uncontrolled case. Note that the proposed voltage control scheme provides the best performance as measured by voltage and frequency deviations.

As a further comparison, the modal content was extracted from the rotor speed

TABLE II
CONTROLLER COMPARISONS

control	I_ω	I_V
none	0.5488	0.0015
power	0.3262	0.0013
voltage	0.0113	0.0003

TABLE III
DOMINANT MODAL CONTENT

no control	power control	voltage control
-0.59 ± 24.59	-0.77 ± 23.28	-3.55 ± 23.84
-0.04 ± 9.81	-4.69 ± 10.16	-0.91 ± 10.17
0.00 ± 8.50	-0.39 ± 8.79	-0.79 ± 11.82
0.00 ± 5.75	-0.15 ± 5.70	-0.67 ± 4.97

responses using the matrix pencil method (which is a Prony-like estimation tool) [16]. The dominant modes are given in Table III for the uncontrolled, power, and voltage–controlled cases. Note that both the power– and voltage–controlled cases provide increased damping as indicated by the increased magnitude of the real part of the eigenvalue. In fact, the uncontrolled case exhibits several sustained oscillations below 1 Hz (corresponding to the $0.00 \pm j5.75$ and 0.00 ± 8.50 modes). These modes are damped considerably as indicated by both the dynamic responses and the damping coefficient.

VII. CONCLUSIONS AND FUTURE WORK

Two control schemes have been compared for damping inter-area oscillations by UPFCs. The first is a "power controlled" scheme which changes active power flows through the UPFCs for damping oscillations and the second is a novel"voltage controlled" scheme which damps oscillations by changing the sending/receiving voltage angles of the UPFCs. It is seen that the proposed "voltage controlled" scheme is much more effective in damping inter-area oscillations. One drawback however, is that the UPFC dc capacitors are discharged temporarily to inject their energy into the power system through a controlled approach. Since there is currently no specific algorithm for avoiding dc link voltage collapse in the UPFCs, further work is needed to develop a scheme for controlling dc

link voltages of UPFCs if subjected to multiple contingency faults.

Another area of future research is to design decentralized controllers or controllers that need a combination of local and selected global data. These proposed controllers were validated under the assumption that all system data was available, but in practice this assumption is not fully valid. Lastly, although these examples show that the proposed controller works under severe fault conditions, the sensitivity of the method to topology changes should also be studied.

ACKNOWLEDGMENTS

This work was supported in part by a grant from the National Science Foundation under ECCS 0701643.

APPENDIX

Two–Axis Generator Model

$$\begin{aligned}
\dot{\delta}_i &= \omega_i - \omega_s \\
M_i\dot{\omega}_i &= T_{M_i} + \frac{V_i}{x'_{d_i}}\left(E'_{d_i}\cos\left(\theta_i-\delta_i\right) + E'_{q_i}\sin\left(\theta_i-\delta_i\right)\right) \\
T'_{d0_i}\dot{E}'_{q_i} &= -\frac{x_{d_i}}{x'_{d_i}}E'_{q_i} + \frac{\left(x_{d_i}-x'_{d_i}\right)}{x'_{d_i}}V_i\cos\left(\theta_i-\delta_i\right) + E_{fd_i} \\
T'_{q0_i}\dot{E}'_{d_i} &= -\frac{x_{q_i}}{x'_{d_i}}E'_{d_i} - \frac{\left(x_{q_i}-x'_{d_i}\right)}{x'_{d_i}}V_i\sin\left(\theta_i-\delta_i\right)
\end{aligned}$$

Assumption: $x'_{q_i} = x'_{d_i}$ and $R_s = 0$

IEEE Type I Exciter/AVR Model

$$\begin{aligned}
T_{E_i}\dot{E}_{fd_i} &= -K_{E_i}E_{fd_i} - S_{E_i}\left(E_{fd_i}\right)E_{fd_i} + V_{R_i} \\
T_{A_i}\dot{V}_{R_i} &= -V_{R_i} + K_{A_i}R_{F_i} - \frac{K_{A_i}K_{F_i}}{T_{F_i}}E_{fd_i} \\
&\quad + K_{A_i}\left(V_{ref_i} - V_i\right) \quad V_{R_i}^{min} \le V_{R_i} \le V_{R_i}^{max} \\
T_{F_i}\dot{R}_{F_i} &= -R_{F_i} + \frac{K_{F_i}}{T_{F_i}}E_{fd_i}
\end{aligned}$$

Turbine Model

$$T_{RH_i}\dot{T}_{M_i} = -T_{M_i} + \left(1 - \frac{K_{HP_i}T_{RH_i}}{T_{CH_i}}\right)P_{CH_i}$$

$$+\frac{K_{HP_i}T_{RH_i}}{T_{CH_i}}P_{SV_i}$$

$$T_{CH_i}\dot{P}_{CH_i} = -P_{CH_i} + P_{SV_i}$$

Speed Governor Model

$$T_{SV_i}\dot{P}_{SV_i} = -P_{SV_i} + P_{C_i} - \frac{1}{R_i}\frac{\omega_i}{\omega_s}$$

$$0 \leq P_{SV_i} \leq P_{SV_i}^{max}$$

Power Balance Equations

Generator Buses

$$0 = \frac{V_i}{x'_{d_i}}\left(Eq'_i \sin(\delta_i - \theta_i) - Ed'_i \cos(\delta_i - \theta_i)\right)$$
$$-V_i \sum_{j=1}^{n} V_j Y_{ij} \cos(\theta_i - \theta_j - \phi_{ij})$$

$$0 = \frac{V_i}{x'_{d_i}}\left(Eq'_i \cos(\delta_i - \theta_i) + Ed'_i \sin(\delta_i - \theta_i) - V_i\right)$$
$$-V_i \sum_{j=1}^{n} V_j Y_{ij} \sin(\theta_i - \theta_j - \phi_{ij})$$

Load Buses

$$0 = P_{L_i} - V_i \sum_{j=1}^{n} V_j Y_{ij} \cos(\theta_i - \theta_j - \phi_{ij})$$

$$0 = Q_{L_i} - V_i \sum_{j=1}^{n} V_j Y_{ij} \sin(\theta_i - \theta_j - \phi_{ij})$$

REFERENCES

[1] Haifeng Wang, "A Unified Model for the Analysis of FACTS Devices in Damping Power System Oscillations—Part III: Unified Power Flow Controller," *IEEE Trans. Power Delivery*, vol. 15, no. 3, pp. 978-983, July 2000.

[2] B. C. Pal, "Robust damping of interarea oscillations with unified power-flow controller," *IEE Proc.-Gener. Transm. Distrib.*, vol. 149, no. 6. pp. 733-738, November 2002.

[3] B. Chaudhuri, B. C. Pal, A. Zolotas, I. Jaimoukha, and T. Green, "Mixed-sensitivity approach to H_∞ control of power system oscillations employing multiple FACTS devices," *IEEE Trans. on Power Systems*, vol. 18, no. 3, pp. 1149-1156, May 2004.

[4] M. M. Farsangi, Y. H. Song, and K. Y. Lee, "Choice of FACTS device control inputs for damping interarea oscillations," *IEEE Trans. on Power Systems*, vol. 19, no. 2, May 2004.

[5] N. Tambey and M.L. Kothari, "Damping of power system oscillations with unified power flow controller (UPFC)," *IEE Proceedings – Generation, Transmission and Distribution*, vol. 150, pp. 129-140, March 2003.

[6] Mehrdad Ghandhari, G. Andersson and Ian A. Hiskens, "Control Lyapunov Functions for Controllable Series Devices," *IEEE Trans. Power Systems*, vol. 16, no. 4, pp. 689-694, Nov. 2001.

[7] S. Robak, M. Januszewski, D.D. Rasolomampionona, "Power system stability enhancement using PSS and Lyapunov-based controllers: A comparative study," *IEEE 2003 Power Tech Conference Proceedings*, Bologna, vol. 3, pp. 6, 2003.

[8] Chia-Chi Chu and Hung-Chi Tsai, "Application of Lyapunov-based adaptive neural network upfc damping controllers for transient stability enhancement," *Proceedings of the 2008 IEEE Power and Energy Society General Meeting*, 20-24 July 2008.

[9] A. Bidadfar, M. Abedi, M. Karari, and Chia-Chi Chu, "Power swings damping improvement by control of UPFC and SMES based on direct Lyapunov method application," *Proceedings of the 2008 IEEE Power and Energy Society General Meeting*, 20-24 July 2008.

[10] M. Januszewski, J. Machowski and J.W. Bialek, "Application of the direct Lyapunov method to improve damping of power swings by control of UPFC," *IEE Proceedings – Generation, Transmission and Distribution*, vol. 151, pp. 252-260, March 2004.

[11] D. J. Gotham and G. T. Heydt, "Power flow control and power flow studies for systems with FACTS devices," *IEEE Trans. on Power Systems*, vol. 13, no. 1, pp. 60-65, Feb. 1998.

[12] L. Dong, M. L. Crow, Z. Yang, S. Atcitty, "A Reconfigurable FACTS System for University Laboratories," *IEEE Transactions on Power Systems*, vol. 19, no. 1, pp. 120-128, February 2004.

[13] J. Guo, “Decentralized Control and Placement of Multiple Unified Power Controllers,” Ph.D. dissertation, Dept. Electrical and Computer Engineering, Univ. of Missouri-Rolla, 2006.

[14] B. K. Kumar, S. Singh, and S. Srivastava, “Placement of FACTS controllers using modal controllability indices to damp out power system oscillations,” *IET Proceedings – Generation, Transmission and Distribution*, vol. 1, no. 2, pp. 252-260, March 2007.

[15] C. Schauder and H. Mehta, “Vector analysis and control of advanced static VAr compensators,” *IEE Proceedings C*, vol. 140, no. 4, 1993.

[16] M. L. Crow and A. Singh, “The Matrix Pencil for power system modal extraction,” *IEEE Transactions on Power Systems*, vol. 20, no. 1, pp. 501-503, February 2005.

5. Decentralized Control and Placement of Multiple UPFCs for Damping Interarea Oscillations: An LMI Approach

J. Guo, *Student Member, IEEE*, M. Zarghami, *Student Member, IEEE*,
M. L. Crow, *Senior Member, IEEE*, S. Jagannathan, *Senior Member, IEEE*

ABSTRACT: In this paper, the enhancement of interarea oscillation damping of a power network by multiple UPFCs is demonstrated. Hankel singular values and model balanced realization are utilized to reduce the large-scale power network into a reduced order model which is suitable for network control development. An LMI-based approach is used to design decentralized controllers that cooperate even though only local information is utilized. The decentralized controller performance is validated through simulation results. The results of the control approach is also used as a framework to develop a metric with which to compare the dynamic properties of various UPFC placements.

Index Terms – UPFC, oscillation damping, power system stability

I. INTRODUCTION

In bulk power transmission systems, power electronics based controllers are frequently called Flexible AC Transmission System (FACTS) devices. As the vertically integrated utility structure is phased out, transmission providers will be forced to utilize FACTS devices to address a number of potential problems such as uneven power flow through the power system, dynamic instability, interarea oscillations, and difficult voltage regulation. FACTS devices have been shown to improve dynamic stability and mitigate inter-area oscillations in the bulk power system [1]-[3].

One of the important applications of the Unified Power Flow Controller (UPFC) is to control power flow and mitigate interarea oscillations. These oscillations occur in the power system as a result of contingencies such as sudden load changes and faults. Interarea oscillations limit the amount of active power transfer on tie-lines between coherent generator groups. Additionally, these low-frequency oscillations are frequently poorly damped and may lead to stability problems and increased stress on the generator prime movers.

Most proposed controls for the FACTS are based on locally available information monitored at the sending and receiving ends of the FACTS ([4]-[6] are recent examples). More recently, researchers have started trying to develop a complete system model that incorporates both system and FACTS dynamics [7][8]. For example, in [8][9], the authors recognize the interleaved effects of observability and controllability and use input-output controllability analyses to determine the most appropriate input signals. Under certain operating conditions, an interarea mode may be controllable from one area and be observable from another; therefore local controllers may not be effective for damping that mode. In fact, local controllers may actually aggravate the interarea oscillation. It has long been hypothesized that power system controllers may interact adversely [10][11][12].

Considerable work has addressed the task of decentralized control (i.e. control based purely on local information), but there are still many open questions regarding the impact of decentralized control on controller interactions. In [2], a power system damping control design is formulated as an output disturbance rejection problem. A decentralized damping control design based on the mixed-sensitivity formulation in the linear matrix inequality framework is carried out. The disadvantage of this control design is that each device control is designed for only a single inter-area mode and frequency weights must be chosen heuristically. In [13], a TCSC control is developed to damp multiple inter-area modes, but global information is needed. In [8], a procedure for the sequential design of decentralized FACTS controllers for multi-machine power systems is presented. The focus of this design approach is to estimate the effects of other FACTS devices in the frequency domain. One loop is considered at each step, and the control is designed sequentially for each FACTS device. In this approach, for each loop to be closed, frequency characteristics are used to provide a rough estimate of the effects of closing subsequent loops. The

drawback to this approach is that the sequence of the loops may affect the design effectiveness. In [3], [14] and [15], the effects of FACTS devices on each generator's stabilizer are estimated and a global tuning procedure is developed to stabilize the system. The PSS stabilizers are selected to coordinate with the FACTS devices. However, the simultaneous design of PSS and FACTS controllers in multi-machine power system is complex and one would like to design the FACTS controllers independent of tuning the parameters of the PSS controllers. In [1], a FACTS device stabilizer damping contribution diagrams for inter-area mode is described and the effects of the FACTS devices on the damping are estimated. However, this approach does not provide any decentralized control design strategies, nor are the contribution diagrams verified by simulations. Furthermore, the control effort for each controller to attain the response is not taken into account.

The control development proposed in this paper builds on the framework established by these earlier works and endeavors to improve upon the noted limitations. Specifically, the primary contributions of this paper are:

1) the development of an approach for the decentralized control of multiple UPFCs, and
2) a method to ascertain the effectiveness of various UPFC placements on oscillation damping.

II. UPFC INTERACTIONS

In recent years, the use of the UPFC for oscillation damping has received increased attention. If multiple UPFCS (or other FACTS devices) are utilized, decentralized control must be carefully designed and implemented or the controllers may adversely interact causing loss of system stability. Consider two UPFCs placed in the IEEE 118 bus test system. Each UPFC is controlled using PI controllers utilizing local information only. Each UPFC provides good local oscillation damping when it is the *only* UPFC deployed in the system. However, when two UPFCs are deployed, they interact in unexpected ways. Figure 1 shows the dynamic response of generators 1-4 to a three-phase to ground fault with two UPFCs in the system (not all of the generator responses are shown due to space limitations). Similarly, Fig. 2 shows the active power line flows on tie-lines between areas. The two UPFCs are located geographically distant in two different areas (more details

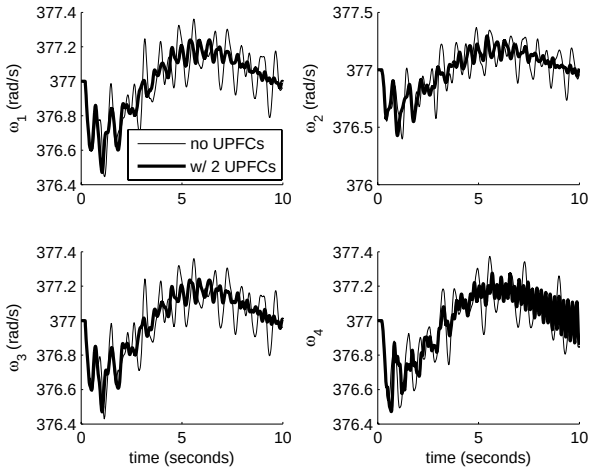

Fig. 1. UPFC interaction in the 118 bus system – generator frequencies

are provided in later sections). The thin lines show the response to the same fault with no UPFCs in the system. Note that the uncontrolled system exhibits sustained, multi-modal oscillations, but remains boundedly stable. The thick line shows the dynamic responses of the system with the two locally controlled UPFCs. Note that while the UPFCs are able to damp the oscillations at some of the generators, at other generators they cause the oscillations to worsen since both UPFCs endeavor to inject/absorb active power into the system. Because only local information is used, the UPFCs are unable to coordinate their control efforts and they start to "ring" against each other causing a resonance effect. This outcome motivates the need to develop a decentalized control approach such that the UPFCs cooperate and do not adversely affect the power system stability.

III. CONTROL DEVELOPMENT

The power system model can be generally modelled as the set of differential-algebraic equations:

$$\dot{x} = f(x, z, u) \tag{1}$$

$$0 = h(x, z, u) \tag{2}$$

where x represents the state variables of the power system including the generator dynamics and the UPFC states. The vector z represents the power system bus voltage

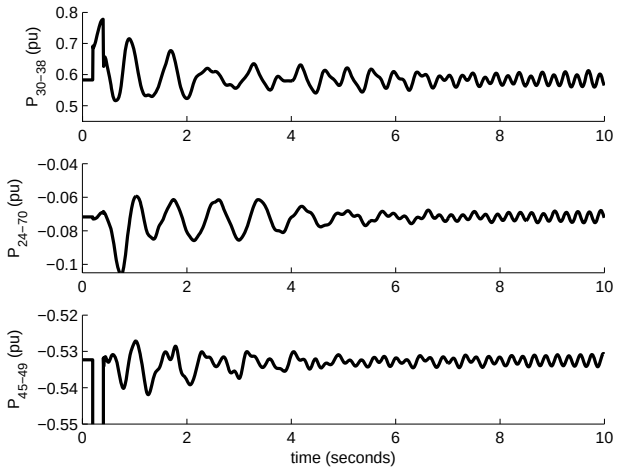

Fig. 2. UPFC interaction in the 118 bus system – active power line flows

magnitudes and angles and u is the input into the system.

For control development purposes, this system can be linearized. Although the control development will be based, in part, on the linearized system, the control effectiveness will be validated with a full nonlinear system simulation. Linearizing equations (1)-(2) yields:

$$\Delta\dot{x} = \frac{\partial f}{\partial x}\Delta x + \frac{\partial f}{\partial z}\Delta z + \frac{\partial f}{\partial u}\Delta u \tag{3}$$

$$0 = \frac{\partial h}{\partial x}\Delta x + \frac{\partial h}{\partial z}\Delta z + \frac{\partial h}{\partial u}\Delta u \tag{4}$$

Solving for Δz and substituting yields the linearized differential equation system:

$$\Delta\dot{x} = A\Delta x + B\Delta u \tag{5}$$

This linearized system can be optimally controlled using the Linear-Quadratic Regulator (LQR) approach, where

$$\Delta u = K_c\Delta x \tag{6}$$

where the matrix K_c is provides the gain that minimizes the control effort and state deviation.

While this approach typically results in very good dynamic performance, there are numerous drawbacks to implementation. First the size of the original system (equations (1)-(2)) may be too large to adequately apply the LQR method. Secondly, and possibly

more importantly, this method represents a global control; this approach assumes that *all* states x are measurable and available for use. Therefore this is not a very practical approach. Thus, the first step in developing an implementable control is to reduce the size of the system through model reduction and then to develop a decentralized control that utilizes only local information.

A. Model Reduction

The first step in designing the control is to reduce the power system model into a reduced system that still retains the dynamics of interest. The system reduction step is used to make the size of the system tractable for control development. System reduction is accomplished utilizing a linearized system model:

$$\dot{x} = Ax + Bu \tag{7}$$

$$y = Cx + Du \tag{8}$$

where y is the output vector and

$$\begin{aligned} A &= \left[\frac{\partial f}{\partial x}\right] - \left[\frac{\partial f}{\partial y}\right]\left[\frac{\partial g}{\partial y}\right]^{-1}\left[\frac{\partial g}{\partial x}\right] \\ B &= -\left[\frac{\partial f}{\partial y}\right]\left[\frac{\partial g}{\partial y}\right]^{-1} B_t \\ C &= -\left[\frac{\partial g}{\partial y}\right]^{-1}\left[\frac{\partial g}{\partial x}\right] \\ D &= -\left[\frac{\partial g}{\partial y}\right]^{-1} B_t \end{aligned}$$

The states can be partitioned as x_1 and x_2 where

$$\begin{bmatrix} \dot{x}_1 \\ \dot{x}_2 \end{bmatrix} = \begin{bmatrix} A_{11} & A_{12} \\ A_{21} & A_{22} \end{bmatrix}\begin{bmatrix} x_1 \\ x_2 \end{bmatrix} + \begin{bmatrix} B_1 \\ B_2 \end{bmatrix} u \tag{9}$$

$$y = [C_1 \quad C_2]\, x + Du \tag{10}$$

In this approach, the set of states x_1 is retained because they are more "important" than x_2. In this case, importance is determined by the amount of interarea modal information they contain.

$$A_e = \begin{bmatrix} A + \sum_{i=1}^{k} B_i K_{ci} & B_1 K_{c1} & B_2 K_{c2} & \cdots & B_k K_{ck} \\ 0 & \begin{matrix} \left[A + \sum_{j\neq 1}^{k} B_j K_{cj}\right. \\ \left. -L_{o1}\left(C_1 + \sum_{j\neq 1}^{k} D_{1j} K_{cj}\right)\right] \end{matrix} & -B_2 K_{c2} + L_{o1} D_{12} K_{c2} & \cdots & -B_k K_{ck} + L_{o1} D_{1k} K_{ck} \\ 0 & -B_1 K_{c1} + L_{o2} D_{21} K_{c1} & \begin{matrix} \left[A + \sum_{j\neq 2}^{k} B_j K_{cj}\right. \\ \left. -L_{o2}\left(C_2 + \sum_{j\neq 2}^{k} D_{2j} K_{cj}\right)\right] \end{matrix} & \cdots & -B_k K_{ck} + L_{o2} D_{2k} K_{ck} \\ \vdots & \vdots & \vdots & \vdots & \vdots \end{bmatrix} \begin{bmatrix} x_1 \\ e_1 \\ e_2 \\ \vdots \\ e_k \end{bmatrix}$$

Fig. 3. A_e matrix

By eliminating x_2, the reduced order model is given by

$$\dot{x}_1 = \left[A_{11} - A_{12}A_{22}^{-1}A_{21}\right] x_1 + \left[B_1 - A_{12}A_{22}^{-1}B_2\right] u \tag{11}$$

$$y = \left[C_1 - C_2 A_{22}^{-1} A_{21}\right] x_1 + \left[D - C_2 A_{22}^{-1} B_2\right] u \tag{12}$$

The states appropriate for elimination (those not containing relevant modal information) are chosen through the use of the Hankel norm. The Hankel norm is the root of the ratio between the future output energy resulting from any input in the past and the energy of the input, assuming that the future input is zero. The Hankel norm of a system G is defined as

$$\|G\|_H^2 = sup\left(\frac{\int_0^\infty y^T y dt}{\int_\infty^0 u^u dt}\right) \tag{13}$$

The approximation error in the reduced system is bounded by

$$2\left(\sigma_{r+1} + \ldots + \sigma_n\right) \tag{14}$$

where $\sigma_{r+1}, \ldots, \sigma_n$ are the Hankel singular values of the portion of the system that is eliminated. The Hankel singular value σ_i is defined as

$$\sigma_i = \sqrt{\lambda_i(PQ)} \tag{15}$$

where P and Q are the controllability and observability gramians respectively and λ_i is the i-th eigenvalue of PQ. By using the Hankel norm, the modes that are least involved in the energy transfer from input u to output y can be deleted while keeping the approximation error small [16].

B. Decentralized Control

For decentralized controller design, the system equations are partitioned as

$$\dot{x}_1 = \hat{A}x_1 + \sum_{i=1}^{k} B_i u_i \tag{16}$$

$$y_i = \hat{C}_1 x_1 + \sum_{j=1}^{k} D_{ij} u_j \quad i = 1, \ldots, k \tag{17}$$

where k is the number of UPFCs (and therefore areas) in the system. The matrices $\hat{A}$ and $\hat{C}_1$ are given by

$$\hat{A} = \left[A_{11} - A_{12}A_{22}^{-1}A_{21}\right]$$
$$\hat{C}_1 = \left[C_1 - C_2 A_{22}^{-1} A_{21}\right]$$

Note that only x_1 is retained in this formulation since only a subset of the states is required to sufficiently capture the system dynamics as measured by the Hankel norm. There are k inputs u_j because there are k control areas since each UPFC provides a control input into the system.

Let $\hat{x}_i$ represent the estimate of x_1 based on the local control u_i, then

$$\dot{\hat{x}}_i = A\hat{x}_i + \sum_{i=1}^{k} B_i K_{ci} \hat{x}_i + L_{oi}\left(y_i - \overline{C}_i \hat{x}_i\right) \tag{18}$$

$$u_i = K_{ci}\hat{x}_i \tag{19}$$

for $i = 1, \ldots, k$ where

$$\overline{C}_i = C_i + [D_{i1}\ D_{i2}\ \ldots\ D_{ik}] \begin{bmatrix} K_{c1} \\ K_{c2} \\ \vdots \\ K_{ck} \end{bmatrix}$$

Note that $\hat{x}_1, \hat{x}_2, \ldots, \hat{x}_k$ are all "estimates" to the reduced system state x_1 based on the control effect of the different UPFCs. Therefore a new state variable can be defined that describes the error in each of these estimates:

$$e_i = \hat{x}_i - x_1 \tag{20}$$

The closed loop system then becomes

$$\begin{bmatrix} \dot{x}_1 \\ \dot{e}_1 \\ \dot{e}_2 \\ \vdots \\ \dot{e}_k \end{bmatrix} = A_e \begin{bmatrix} x_1 \\ e_1 \\ e_2 \\ \vdots \\ e_k \end{bmatrix} \tag{21}$$

where A_e is given in Figure 3.

If P is a positive definite matrix where

$$P = \begin{bmatrix} P_0 & 0 & \dots & 0 \\ 0 & P_1 & 0 & 0 \\ \vdots & \vdots & \vdots & \vdots \\ 0 & 0 & \dots & P_k \end{bmatrix}$$

then

$$A_e^T P + P A_e < 0 \tag{22}$$

can be solved using an LMI approach if the initial feedback matrices K_{ci} are set by an LQR solution. The LMI approach to control systems is a synthesis of several robust control approaches. For certain types of problems, the LMI formulation allows the exact numerical solution of control problems that have no analytic solution [12]. To ensure asymptotic stability, k additional equations are incorporated into the LMI equations:

$$\begin{gathered} P_i \left(A + BK\right) - P_i L_{oi} \left(C_i + \left[D_{i1} \dots D_{ik}\right] K_c\right) + \\ \left(P_i \left(A + BK\right) - P_i L_{oi} \left(C_i + \left[D_{i1} \dots D_{ik}\right] K_c\right)\right)^T < 0 \end{gathered} \tag{23}$$

for $i = 1, \dots, k$. If these additional LMI equations are feasible, then the decentralized quadratic controllers exist and may be found numerically.

Note that if the resulting system is asymptotically stable, then the errors e_i will be driven to zero and the decentralized "estimated" systems will converge to the same system as time increases. Thus by design, *the UPFC controllers are forced to coordinate their actions,* even though only local line flow information is used.

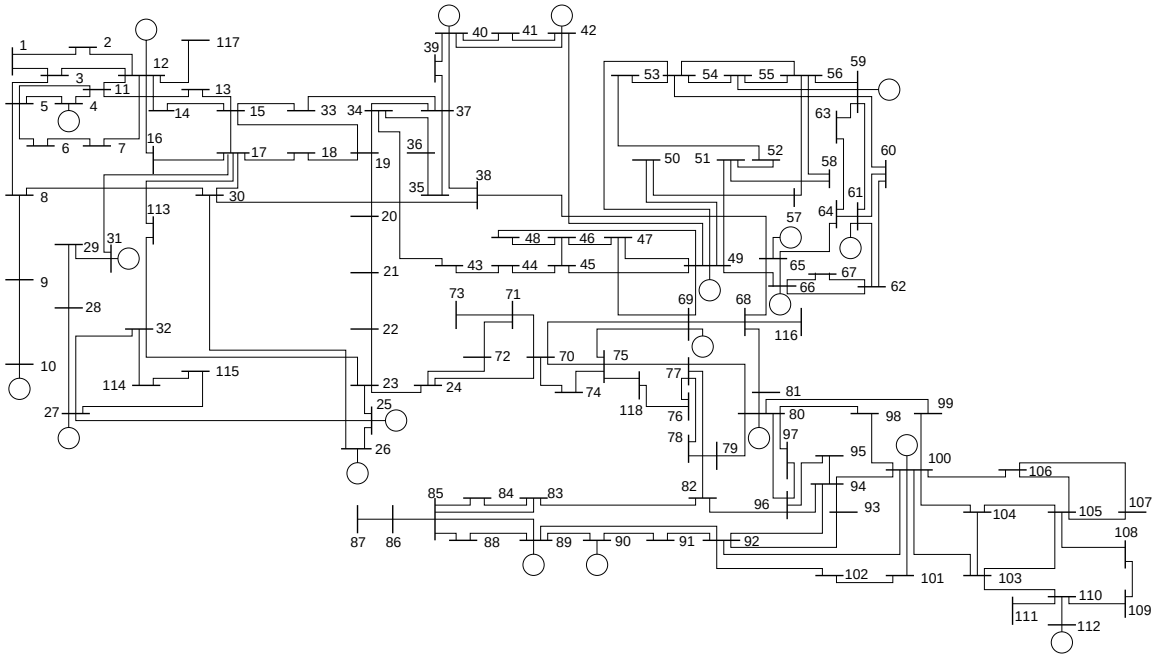

Fig. 4. IEEE 118 bus test system

IV. CONTROL VALIDATION

Figure 1 illustrated a case of two interacting UPFCs. In this section, that case will be repeated using the proposed control development with promising results. The control is validated with the IEEE 118 bus system shown in Figure 4. In this example, a three-phase-to-ground fault is placed on bus 43 at 0.2 seconds and is cleared at 0.4 seconds. The system generators are modeled as two-axis generators with a simple DC exciter, voltage regulator, and turbine/governor. The UPFC is a fifth-order model from [17]. The generator, UPFC, and network equations are given in the Appendix. One UPFC is located at bus 30 on line 26-30 and a second UPFC is located on bus 64 on line 64-65. These are geographically remote locations in two different areas of the system.

The results of the proposed control are shown in Figure 5. Once again, only local information is used as an input into the controllers and only the frequency responses of generators 1-4 are shown (due to space limitations). The proposed control rapidly damps the oscillations in rotor frequencies. This response underscores the fact that decentralized control can be effective if properly designed. The active power flows on the same lines as before under the proposed control are shown in Fig. 6. Note that with the proposed

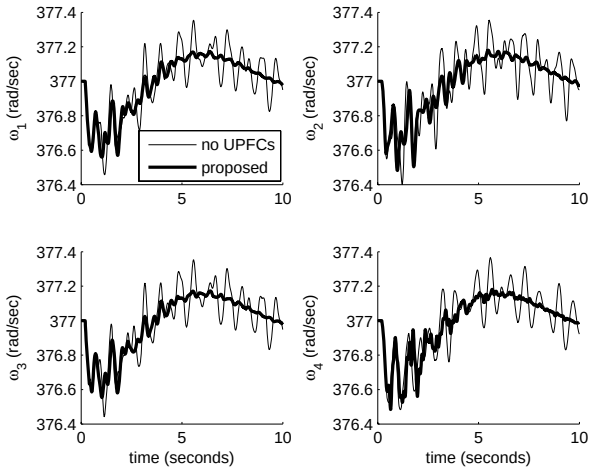

Fig. 5. Proposed control response in the IEEE 118 bus test system

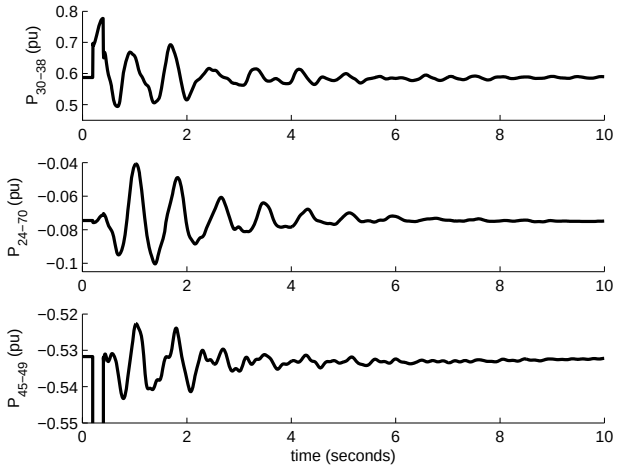

Fig. 6. Active power flow on tie lines with proposed control

control the oscillations are rapidly damped. Fig. 7 shows the series active power flow through the UPFCs. Note that variation in the active power is less than 10% of the line flow on the line.

V. UPFC PLACEMENT

Despite the fact that UPFCs can be very effective in damping power system oscillations, there is little research in the literature which addresses the role of UPFCs' placement in

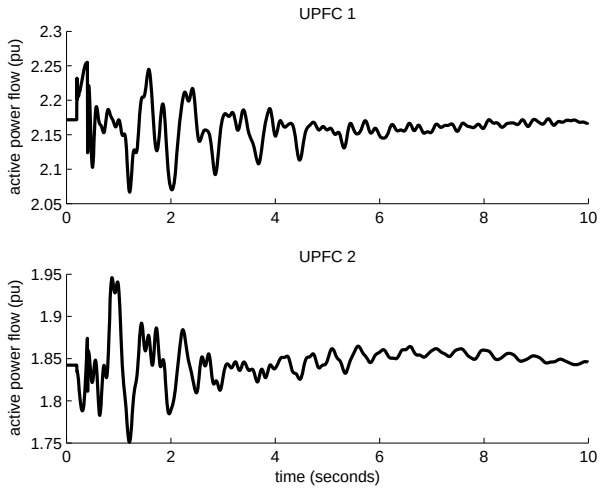

Fig. 7. UPFC series active power flow

the dynamic performance of the network. There is considerable work published on the placement of FACTS devices to improve the steady-state performance of the network, such as improving the power transfer or minimizing system losses [18]-[21]. In [22], the placement of variable impedance apparatus to improve of the stability of large scale power systems is explored, but this work does not specifically address UPFCs. Recent studies for the placement of FACTS controllers for stability improvement can be found in [23], where a fast algorithm based on controllability indices has been proposed. In this algorithm, it is assumed that UPFCs can be located simultaneously on all lines of the system. Based on this assumption, additional terms augment the original state space system and are used to determine the UPFC placements.

Because different UPFC placements can cause significant differences in the dynamic behavior of the system, placements must be chosen with care. Not only can a good placement improve the stability of the system; a poor placement can produce nondesirable behavior. In this paper, a new performance index is introduced that provides a method to compare different candidate placements in terms of the damping they can provide in the system under the same control approach.

One particular goodness measure for stability can be to use the eigenvalue of the observability gramian matrix W_0 of the linearized system. For example, consider two

TABLE I

ASSESSMENT OF CONTROL PERFORMANCE AND CONTROL EFFORT OF UPFC PLACEMENTS

	placement	
	I: 26-30, 64-65	II: 48-49, 68-69
Performance	54.44	68.19
Control Effort	70.00	127.32

linear system models that are obtained for two different UPFC placements:

$$\dot{x} = A_1 x + B_1 u \tag{24}$$

$$y = C_1 x + D_1 u \tag{25}$$

and

$$\dot{x} = A_2 x + B_2 u \tag{26}$$

$$y = C_2 x + D_2 u \tag{27}$$

where y represents the generator frequencies. The different state matrices indicate different network topologies due to different UPFC placements. A quadratic performance criterion z can be utilized to compare the controller performance such that

$$z = min \int_0^\infty \left(y^T y + u^T u \right) dt \tag{28}$$

where $\int_0^\infty y^T y dt$ gives the performance measure and $\int_0^\infty u^T u dt$ gives the required control effort for each placement. These two measurements can further be assessed by the eigenvalues of the observability gramian matrix W_0 according to linear system theory, where W_0 satisfies

$$A^T W_0 + W_0 A + C^T C = 0 \tag{29}$$

The IEEE 118 bus system is again used to test the performance of the two UPFC controllers in two different sets of placements. The two placements and their effectiveness are summarized in Table I. Both the performance and control effort assessments indicate that placement II (UPFCs placed in lines 30-26 and 64-65) is more effective than placement I (UPFCs placed in lines 48-49 and 68-69). Placement I is the placement that was used in the previous examples. These conclusions are validated in the simulation

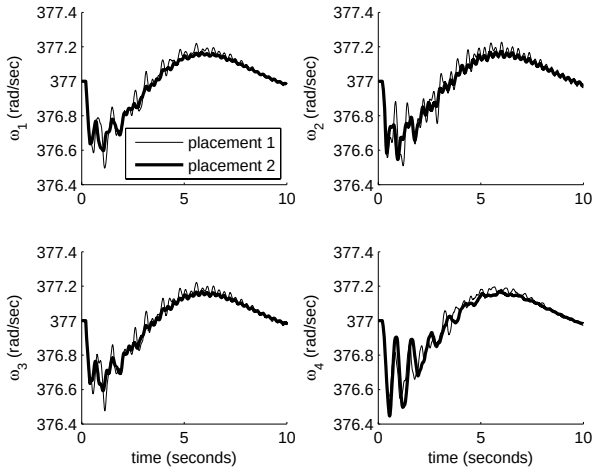

Fig. 8. Comparison of different placements

results shown in Figure 8. While it is not possible to show an exhaustive comparison of all placements in this paper, the proposed process can be used to compare the impact of placements of several potential placements.

V. CONCLUSIONS

In this paper a new method for coordinating UPFC control is proposed. The proposed control is shown to be effective even when each UPFC is operating only on local information. An additional example is given in which uncoordinated UPFC control can lead to instability. Furthermore, the proposed control is utilized as a framework in which to compare the performance of various UPFC placements. Both performance and control effort are quantified. All of the results are validated through simulations on the IEEE 118 bus test system.

APPENDIX

Two–Axis Generator Model

$$\begin{aligned} \dot{\delta}_i &= \omega_i - \omega_s \\ M_i\dot{\omega}_i &= T_{M_i} + \frac{V_i}{x'_{d_i}}\left(E'_{d_i}\cos\left(\theta_i - \delta_i\right) + E'_{q_i}\sin\left(\theta_i - \delta_i\right)\right) \end{aligned}$$

$$
\begin{aligned}
T'_{d0_i}\dot{E}'_{q_i} &= -\frac{x_{d_i}}{x'_{d_i}}E'_{q_i} + \frac{\left(x_{d_i}-x'_{d_i}\right)}{x'_{d_i}}V_i\cos\left(\theta_i-\delta_i\right) + E_{fd_i} \\
T'_{q0_i}\dot{E}'_{d_i} &= -\frac{x_{q_i}}{x'_{d_i}}E'_{d_i} - \frac{\left(x_{q_i}-x'_{d_i}\right)}{x'_{d_i}}V_i\sin\left(\theta_i-\delta_i\right)
\end{aligned}
$$

Assumption: $x'_{q_i} = x'_{d_i}$ and $R_s = 0$

IEEE Type I Exciter/AVR Model

$$
\begin{aligned}
T_{E_i}\dot{E}_{fd_i} &= -K_{E_i}E_{fd_i} - S_{E_i}\left(E_{fd_i}\right)E_{fd_i} + V_{R_i} \\
T_{A_i}\dot{V}_{R_i} &= -V_{R_i} + K_{A_i}R_{F_i} - \frac{K_{A_i}K_{F_i}}{T_{F_i}}E_{fd_i} \\
&\quad +K_{A_i}\left(V_{ref_i}-V_i\right) \quad V_{R_i}^{min} \le V_{R_i} \le V_{R_i}^{max} \\
T_{F_i}\dot{R}_{F_i} &= -R_{F_i} + \frac{K_{F_i}}{T_{F_i}}E_{fd_i}
\end{aligned}
$$

Turbine Model

$$
\begin{aligned}
T_{RH_i}\dot{T}_{M_i} &= -T_{M_i} + \left(1 - \frac{K_{HP_i}T_{RH_i}}{T_{CH_i}}\right)P_{CH_i} \\
&\quad +\frac{K_{HP_i}T_{RH_i}}{T_{CH_i}}P_{SV_i} \\
T_{CH_i}\dot{P}_{CH_i} &= -P_{CH_i} + P_{SV_i}
\end{aligned}
$$

Speed Governor Model

$$
\begin{aligned}
T_{SV_i}\dot{P}_{SV_i} &= -P_{SV_i} + P_{C_i} - \frac{1}{R_i}\frac{\omega_i}{\omega_s} \\
&\quad 0 \le P_{SV_i} \le P_{SV_i}^{max}
\end{aligned}
$$

Power Balance Equations

Generator Buses

$$
\begin{aligned}
0 &= \frac{V_i}{x'_{d_i}}\left(Eq'_i\sin\left(\delta_i-\theta_i\right) - Ed'_i\cos\left(\delta_i-\theta_i\right)\right) \\
&\quad -V_i\sum_{j=1}^{n}V_jY_{ij}\cos(\theta_i-\theta_j-\phi_{ij}) \\
0 &= \frac{V_i}{x'_{d_i}}\left(Eq'_i\cos\left(\delta_i-\theta_i\right) + Ed'_i\sin\left(\delta_i-\theta_i\right) - V_i\right) \\
&\quad -V_i\sum_{j=1}^{n}V_jY_{ij}\sin(\theta_i-\theta_j-\phi_{ij})
\end{aligned}
$$

Load Buses

$$\begin{aligned} 0 &= P_{L_i} - V_i \sum_{j=1}^{n} V_j Y_{ij} \cos(\theta_i - \theta_j - \phi_{ij}) \\ 0 &= Q_{L_i} - V_i \sum_{j=1}^{n} V_j Y_{ij} \sin(\theta_i - \theta_j - \phi_{ij}) \end{aligned}$$

UPFC

$$\frac{1}{\omega_s}\frac{d}{dt}i_{d_1} = \frac{k_1 V_{dc}}{L_{s_1}} \cos(\alpha_1 + \theta_1) + \frac{\omega}{\omega_s} i_{q_1} - \frac{R_{s_1}}{L_{s_1}} i_{d_1} - \frac{V_1}{L_{s_1}} \cos\theta_1 \tag{30}$$

$$\frac{1}{\omega_s}\frac{d}{dt}i_{q_1} = \frac{k_1 V_{dc}}{L_{s_1}} \sin(\alpha_1 + \theta_1) - \frac{R_{s_1}}{L_{s_1}} i_{q_1} - \frac{\omega}{\omega_s} i_{d_1} - \frac{V_1}{L_{s_1}} \sin\theta_1 \tag{31}$$

$$\begin{aligned} \frac{1}{\omega_s}\frac{d}{dt}i_{d_2} = &-\frac{R_{s_2}}{L_{s_2}} i_{d_2} + \frac{\omega}{\omega_s} i_{q_2} + \frac{k_2}{L_{s_2}} \cos(\alpha_2 + \theta_1) V_{dc} \\ &-\frac{1}{L_{s_2}} (V_2 \cos\theta_2 - V_1 \cos\theta_1) \end{aligned} \tag{32}$$

$$\begin{aligned} \frac{1}{\omega_s}\frac{d}{dt}i_{q_2} = &-\frac{R_{s_2}}{L_{s_2}} i_{q_2} - \frac{\omega}{\omega_s} i_{d_2} + \frac{k_2}{L_{s_2}} \sin(\alpha_2 + \theta_1) V_{dc} \\ &-\frac{1}{L_{s_2}} (V_2 \sin\theta_2 - V_1 \sin\theta_2) \end{aligned} \tag{33}$$

$$\begin{aligned} \frac{C}{\omega_s}\frac{d}{dt}V_{dc} = &-k_1 \cos(\alpha_1 + \theta_1) i_{d_1} - k_1 \sin(\alpha_1 + \theta_1) i_{q_1} \\ &-k_2 \cos(\alpha_2 + \theta_1) i_{d_2} - k_2 \sin(\alpha_2 + \theta_1) i_{q_2} - \frac{V_{dc}}{R_{dc}} \end{aligned} \tag{34}$$

Bus 1 Power Balance

$$\begin{aligned} 0 &= V_1 ((i_{d_1} - i_{d_2}) \cos\theta_1 + (i_{q_1} - i_{q_2}) \sin\theta_1) \\ &\quad -V_1 \sum_{j=1}^{n} V_j Y_{1j} \cos(\theta_1 - \theta_j - \phi_{1j}) \end{aligned} \tag{35}$$

$$\begin{aligned} 0 &= V_1 ((i_{d_1} - i_{d_2}) \sin\theta_1 - (i_{q_1} - i_{q_2}) \cos\theta_1) \\ &\quad -V_1 \sum_{j=1}^{n} V_j Y_{1j} \sin(\theta_1 - \theta_j - \phi_{1j}) \end{aligned} \tag{36}$$

Bus 2 Power Balance

$$
\begin{aligned}
0 &= V_2\left(i_{d_2}\cos\theta_2 + i_{q_2}\sin\theta_2\right) \\
&\quad -V_2\sum_{j=1}^{n} V_j Y_{2j}\cos\left(\theta_2-\theta_j-\phi_{2j}\right) \qquad (37)\\
0 &= V_2\left(i_{d_2}\sin\theta_2 - i_{q_2}\cos\theta_2\right) \\
&\quad -V_2\sum_{j=1}^{n} V_j Y_{2j}\sin\left(\theta_2-\theta_j-\phi_{2j}\right) \qquad (38)
\end{aligned}
$$

REFERENCES

[1] M. J. Gibbard, D. J. Vowles, and P. Pourbeik, "Interactions between, and effectiveness of, power system stabilizers and FACTS device stabilizers in multimachine systems," *IEEE Transactions on Power Systems*, vol. 15, no. 2, pp. 748 - 755, May 2000.

[2] B. Chaudhuri, B. C. Pal, A. C. Zolotas, I. M. Jaimoukha, and T. C. Green, "Mixed-sensitivity approach to control of power system oscillations employing multiple FACTS devices," *IEEE Transactions on Power Systems*, vol. 18, no. 3, August 2003.

[3] Cai Li-Jun and I. Erlich, "Simultaneous coordinated tuning of PSS and FACTS damping controllers in large power systems," *IEEE Transactions on Power Systems*, vol. 20, no. 1, pp. 294 -300, February 2005.

[4] N. Tambey and M. L. Kothari, "Damping of power system oscillations with unified power flow controller (UPFC)," *IEE Proc.-Gener. Transm. Distrib.*, vol. 150, no. 2. pp. 129-140, March 2003.

[5] S. Kannan, S. Jayaram, and M. Salama, "Real and reactive power coordination for a unified power flow controller," *IEEE Trans. on Power Systems*, vol. 19, no. 3, pp. 1454-1461, August 2004.

[6] E. Gholipour and S. Saadate, "Improving of transient stability of power systems using UPFC," *IEEE Trans. on Power Delivery*, vol. 20, no. 2, pp. 1677-1682, April 2005.

[7] H. Wang, "A Unified model for the analysis of FACTS devices in damping power system oscillations - part III: Unified power flow controller," *IEEE Trans. on Power Delivery*, vol. 15, no. 3, pp. 978-983, July 2000.

[8] M. M. Farsangi, Y. H. Song, X. F. Wang, and M. Tan, “Sequential design of decentralised control for FACTS devices in large power systems,” *IEE Proceedings-Generation, Transmission and Distribution*, vol. 150, no. 2, pp. 162-168, March 2003.

[9] Y. Zhang and A. Bose, “Design of wide-area damping controllers for interarea oscillations,” *IEEE Transactions on Power Systems*, vol. 23, no. 3, August 2008.

[10] K. Clark, B. Fardanesh, R. Adapa, “Thyristor controlled series compensation application study-control interaction considerations,” *IEEE Transactions on Power Delivery*, vol. 10, no. 2, April 1995.

[11] H. F. Wang, M. Jazaeri, A. T. Johns, “Investigation into the dynamic interactions of multiple multifunctional Unified Power Flow Controllers,” *IEEE Power Engineering Review*, July 2000.

[12] K. Mekki, N. HadjSaid, R. Feuillet, D. Georges, “Design of damping controllers using linear matrix inequalities techniques and distant signals to reduce control interactions,” *IEEE 2001 Power Industry Computer Applications Conference*, 2001.

[13] B. Chaudhuri, and B. C. Pal, “Robust damping of multiple swing modes employing global stabilizing signals with a TCSC,” *IEEE Transactions on Power Systems*, vol. 19, no. 1, pp. 499-506, February 2004.

[14] Lei Xianzhang, E. N. Lerch, and D. Povh, “Optimization and coordination of damping controls for improving system dynamic performance,” *IEEE Transactions on Power Systems*, vol 16, no. 3, pp. 473 - 480, August 2001.

[15] P. Pourbeik, and M. J. Gibbard, “Simultaneous coordination of power system stabilizers and FACTS device stabilizers in a multimachine power system for enhancing dynamic performance,” *IEEE Trans, on Power Systems*, vol. 13, no. 2, May 1998.

[16] M. Gree and D.J.N. Limebeer, Linear Robust Control, Upper Saddle River, NJ: Prentice-Hall, 1995.

[17] L. Dong, M. L. Crow, Z. Yang, C. Shen, L. Zhang, S. Atcitty, “A reconfigurable FACTS system for university laboratories,” *IEEE Transactions on Power Systems*, Vol. 19, No. 1, pp. 120-128, February 2004.

[18] P. Preedavichit and S. C. Srivastava, “Optimal reactive power dispatch considering FACTS devices,” *Electr. Power Syst. Res.*, vol. 46, pp. 251-257, 1998.

[19] Y. Lu and A. Abur, “Improving system static security via optimal placement of thyristor controlled series capacitors (TCSC),” *Proceedings of the 2001 IEEE Power Eng. Society Winter Meeting*, pp. 516-521, 2001.

[20] S. Gerbex, R. Cherkaoui and A. J. Germond, “Optimal location of multi-type FACTS devices in a power system by means of genetic algorithm,” *IEEE Transaction on Power Systems*, vol. 16, pp. 537-544, 2001.

[21] Y. Xiao, Y. H. Song, C. C. Liu, and Y. Z. Sun, “Available transfer capability enhancement using FACTS devices,” *IEEE Transactions on Power Systems*, vol. 18, pp. 305-312, 2003.

[22] H. Okamoto, A. Kuriata, and Y. Sekine, “A method for identification of effective locations of variable impedance apparatus on enhancement of steady state stability in large scale power systems,” *IEEE Transactions on Power Systems*, vol. 10, no. 3, pp. 1401-1407, 1995.

[23] B. Kalyan Kumar, S.N. Singh and S.C. Srivastava, “Placement of FACTS controllers using modal controllability indices to damp out power system oscillations,” *IET Gener. Transm. Distrib.*, vol. 1, no. 2, pp. 209-217, 2007.

6. Damping Inter-Area Oscillations by UPFCs Based on Selected Global Measurements

Mahyar Zarghami, *Student Member, IEEE,* Mariesa. L. Crow, *Senior Member, IEEE,*
S. Jagannathan, *Senior Member, IEEE,* Yilu Liu, *Fellow, IEEE*

ABSTRACT: This paper introduces a method of using local data and a selected set of the global data for controlling inter-area oscillations of the power network using Unified Power Flow Controllers. This novel algorithm utilizes reduced order observers for estimating the missing data the purpose of control when all the data is unavailable through frequency measurements in a Wide Area Control approach. The paper will also address the problem of time-delay in data acquisition through examples.

Index Terms: UPFC, Inter-Area Oscillation, PMU, Wide Area Control, Reduced Order Observer

I. INTRODUCTION

Damping inter-area oscillations in a power network is one of the important applications of a Unified Power Flow Controller (UPFC) [1]-[6]. These oscillations can occur in a system as a result of a number of contingencies including sudden load changes or power system faults. Fig. 1 shows a schematic diagram of a UPFC, which is a series-shunt flexible AC Transmission (FACTS) device. Controlling power oscillations can be done by rapidly changing the power flow via the series part of the UPFC, which in turn can impact the power flow through the entire network. The needed electrical power to do this action is channeled from the UPFC's shunt part. Namely, the series part is controlled by the modulation gain and phase angle (k_2, α_2) of the injected voltage vector and the shunt part is controlled by modulation gain and phase angle (k_1, α_1) of the internal voltage of the shunt converter.

As explained earlier, damping inter-area oscillations demands the dynamic change of active power flow through the network. To rapidly damp interarea oscillations requires knowledge of the many modes that are inherent in oscillatory behavior. Frequency responses are rich in modal content and have been shown to be excellent inputs in controller design. In previous work [7], the

authors have shown that using global frequency data as input to the UPFC controller provides effective inter-area oscillation damping. Although the introduction of frequency measurements (such as from FNET [12]) has made wide area control of the power networks feasible, it is still not reasonable to expect that the full set of frequency measurements is available for controller use. Therefore most UPFC controls still rely heavily on locally available measurements. This is why decentralized control schemes for damping inter-area oscillations must be developed. However, decentralized control schemes that depend primarily on local information can be significantly improved by the addition of select global frequency information.

This paper introduces an approach which shows that it is possible to damp out power network oscillations using only a limited set of measurements. The work is based on the two stage type of controller introduced in [7], which instead of using a whole set of global state feedback data, uses a subset of the global data plus an estimated set of data to run the controller. Simulations on the IEEE 14 bus test system show that the scheme is satisfactory.

In the following sections, the two stage controller will be reviewed. Then the method for designing a reduced order estimator based on the available feedback data will be provided. Next, simulation examples and their comparison with full state feedback controllers will be provided. In the end, the effect of time delay in global data acquisition will be shown and further work will be proposed.

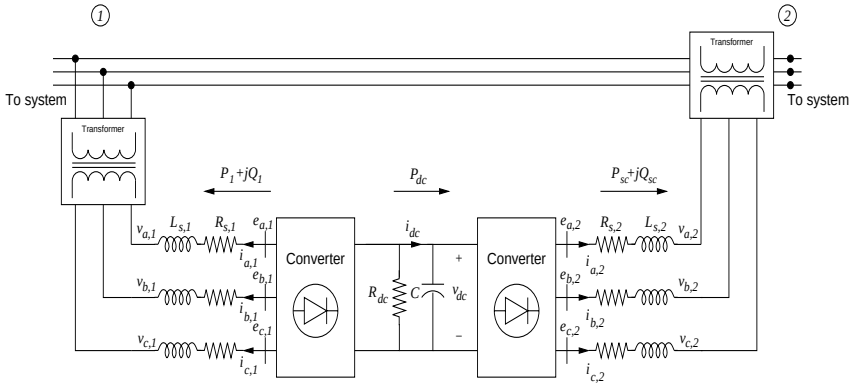

Fig. 1. Unified Power Flow Controller Diagram

II. TWO STAGE CONTROLLER

In this section, the two stage controller design is summarized from [7].

Using a power injection model for the UPFC schematically shown in Fig. 2, the dynamical equations for the UPFC can be written as [8]:

$$\frac{1}{\omega_S}\dot{i}_{d_{1j}} = -\frac{R_{1j}}{L_{1j}} i_{d_{1j}} + i_{q_{1j}} + \frac{k_{1j}}{L_{1j}} \cos(\theta_{1j} + \alpha_{1j}) v_{dc_j} - \frac{V_{1d_j}}{L_{1j}} \tag{1}$$

$$\frac{1}{\omega_S}\dot{i}_{q_{1j}} = -\frac{R_{1j}}{L_{1j}} i_{q_{1j}} - i_{d_{1j}} + \frac{k_{1j}}{L_{1j}} \sin(\theta_{1j} + \alpha_{1j}) v_{dc_j} - \frac{V_{1q_j}}{L_{1j}} \tag{2}$$

$$\frac{1}{\omega_S}\dot{i}_{d_{2j}} = -\frac{R_{2j}}{L_{2j}} i_{d_{2j}} + i_{q_{2j}} + \frac{k_{2j}}{L_{2j}} \cos(\theta_{1j} + \alpha_{2j}) v_{dc_j} - \frac{V_{2d_j}}{L_{2j}} + \frac{V_{1d_j}}{L_{2j}} \tag{3}$$

$$\frac{1}{\omega_S}\dot{i}_{q_{2j}} = -\frac{R_{2j}}{L_{2j}} i_{q_{2j}} - i_{d_{2j}} + \frac{k_{2j}}{L_{2j}} \sin(\theta_{1j} + \alpha_{2j}) v_{dc_j} - \frac{V_{2q_j}}{L_{2j}} + \frac{V_{1q_j}}{L_{2j}} \tag{4}$$

$$\begin{aligned} \frac{C}{\omega_S}\dot{v}_{dc_j} &= -k_{1j} \cos(\theta_{1j} + \alpha_{1j}) i_{d_{1j}} - k_{1j} \sin(\theta_{1j} + \alpha_{1j}) i_{q_{1j}} \\ &-k_{2j} \cos(\theta_{1j} + \alpha_{2j}) i_{d_{2j}} - k_{2j} \sin(\theta_{1j} + \alpha_{2j}) i_{q_{2j}} - \frac{v_{dc_j}}{R_{p_j}} \end{aligned} \tag{5}$$

$$V_{1d_j} = V_{1j} \cos\theta_{1j} \tag{6}$$

$$V_{1q_j} = V_{1j} \sin\theta_{1j} \tag{7}$$

$$V_{2d_j} = V_{2j} \cos\theta_{2j} \tag{8}$$

$$V_{2q_j} = V_{2j} \sin\theta_{2j} \tag{9}$$

where:

n_u : Number of UPFCs

$j = 1, ..., n_u$

$i_{1,j} = i_{d_{1j}} + j i_{q_{1j}}$: Shunt injection current in UPFC j (pu)

$i_{2,j} = i_{d_{2j}} + j i_{q_{2j}}$: Series injection current in UPFC j (pu)

R_{1j} : Equivalent shunt resistance of UPFC j (pu)

L_{1j} : Equivalent shunt inductance of UPFC j (pu)

R_{2j} : Equivalent series resistance of UPFC j (pu)

L_{2j} : Equivalent series inductance of UPFC *j* (pu)

v_{dc_j} : DC bus voltage in UPFC *j* (pu)

C_j : Equivalent capacitance of UPFC *j* (pu)

R_{p_j} : Equivalent dc resistance in UPFC j (pu)

k_{1j}, α_{1j} : Modulation amplitude and angle of the shunt part of UPFC *j*

k_{2j}, α_{2j} : Modulation amplitude and angle of the series part of UPFC *j*

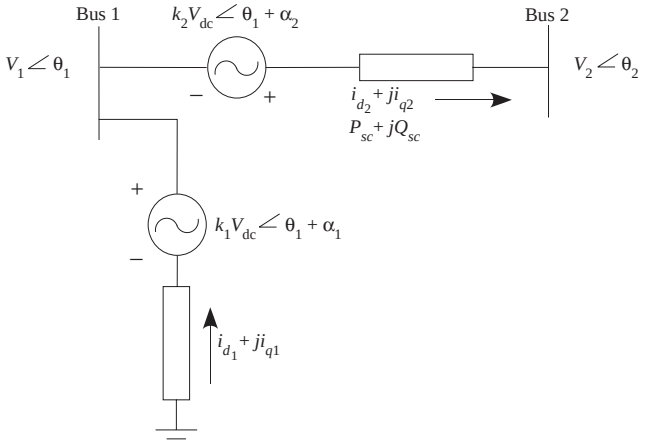

Fig. 2. Power Injection Model for UPFC

To derive the two stage controller, the loads in the system are initially converted to constant impedance. Further, the generators are modeled as the classical "transient reactance behind constant voltage." Note that these assumptions are made only to develop the UPFC control – the proposed two stage control will be validated on a system with constant power loads and with fully modeled (10^{th} order) generators with voltage regulators. With the constant impedance assumption, it is possible to find a reduced admittance matrix of order $n_g + 2n_u$, where n_g internal machine buses are connected to $2n_u$ UPFC buses as shown in Fig. 3. The dashed lines in the figure show that in the reduced order network, virtually all the buses are connected to each other.

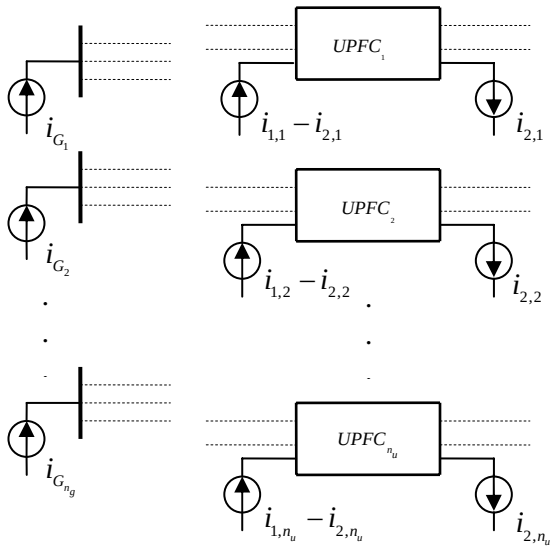

Fig. 3. Equivalent Power System from the Controller's View

Using the above, the resulted state space system for the power network would be of the following format:

$$\dot{\delta}_j = \omega_j - \omega_1 \qquad j = 2,\ldots,n_g \tag{10}$$

and for

$$j = 1,\ldots,n_g$$

$$\begin{aligned}\dot{\omega}_j = (1/M_j)[P_{M_j} - E_j \sum_{k=1}^{n_g} E_k Y_{jk} \cos(\delta_j - \delta_k - \Phi_{jk}) \\ - E_j \sum_{k=n_g+1}^{n_g+n_u} (E_k Y_{jk} \cos(\delta_j - \Phi_{jk}) r_{2(k-n_g-1)+1} + E_k Y_{jk} \sin(\delta_j - \Phi_{jk}) r_{2(k-n_g-1)+2}) \\ - E_j \sum_{k=n_g+n_u+1}^{n_g+2n_u} (E_k Y_{jk} \cos(\delta_j - \Phi_{jk}) r_{2(k-n_g-1)+1} + E_k Y_{jk} \sin(\delta_j - \Phi_{jk}) r_{2(k-n_g-1)+2})]\end{aligned} \tag{11}$$

where:

$j = 1, \ldots, n_g$

ω_j : Speed of machine j (rad/s)

M_j : Inertia at machine j (pu) $\quad j = 1, ..., n_g$

P_{M_j} : Mechanical input at machine j (pu) $\quad j = 1, ..., n_g$

δ_i : Angle at bus i (Radians) $\quad i = 1, ..., n_g + 2n_u$

E_i : Bus magnitude at bus i (pu) $\quad i = 1, ..., n_g + 2n_u$

$Y_{jk} \angle \Phi_{jk}$: Admittance matrix of the equivalent reduced system for $j, k = 1, ..., n_g + 2n_u$

This nonlinear state space system is of the order $2n_g - 1$ with intermediate control inputs r_i defined as:

$$\begin{aligned} r_{2(j-1)+1} &= V_{1dj} \qquad j = 1, \ldots, n_u \\ r_{2(j-1)+2} &= V_{1qj} \\ r_{2(j-1)+2n_u+1} &= V_{2dj} \\ r_{2(j-1)+2n_u+2} &= V_{2qj} \end{aligned} \tag{12}$$

The above state space set, describes the first stage of the control process. Note that this first stage is independent of the UPFC dynamics of equations (1)-(5). Linearizing this system results in a linear time invariant system of the form:

$$\dot{X} = AX + BR \tag{13}$$

Linear feedback control is given by:

$$R = -KX \tag{14}$$

where K is chosen using optimal LQR control processes to minimize speed and angle deviations in the generators.

If the system were linear, the above control results in optimal values of voltages at both sending and receiving buses of the UPFC. The second control stage is to convert the control inputs R into modulation gain and phase angles k and α for each UPFC. The first step in the

second control stage is to find the values of $i_{d_1}, i_{q_1}, i_{d_2}, i_{q_2}$ from the following four active and reactive power balance equations at the sending and receiving buses of the UPFC:

$$P_{1j} = V_{1dj}\left(i_{d1j} - i_{d2j}\right) + V_{1qj}\left(i_{q1j} - i_{q2j}\right) \tag{15}$$

$$Q_{1j} = V_{1qj}\left(i_{d1j} - i_{d2j}\right) - V_{1dj}\left(i_{q1j} - i_{q2j}\right) \tag{16}$$

$$P_{2j} = V_{2dj} i_{d2j} + V_{2qj} i_{q2j} \tag{17}$$

$$Q_{2j} = V_{2qj} i_{d2j} - V_{2dj} i_{q2j} \tag{18}$$

where:

P_{1j} : Active Power from j^{th} UPFCs sending end bus

Q_{1j} : Reactive Power from j^{th} UPFCs sending end bus

P_{2j} : Active Power from j^{th} UPFCs receiving end bus

Q_{2j} : Reactive Power from j^{th} UPFCs receiving end bus

The calculation made above is based on the fact that the UPFC's dynamics are much faster than the machines' dynamics so that $i_{d_1}, i_{q_1}, i_{d_2}, i_{q_2}$ can be taken to be algebraic quantities. With this assumption, converting (1) to (4) to algebraic equations results in:

$$0 = -\frac{R_{1j}}{L_{1j}} i_{d_{1j}} + i_{q_{1j}} + \frac{k_{1j}}{L_{1j}} \cos(\theta_{1j} + \alpha_{1j}) v_{dc_j} - \frac{V_{1d_j}}{L_{1j}} \tag{19}$$

$$0 = -\frac{R_{1j}}{L_{1j}} i_{q_{1j}} - i_{d_{1j}} + \frac{k_{1j}}{L_{1j}} \sin(\theta_{1j} + \alpha_{1j}) v_{dc_j} - \frac{V_{1q_j}}{L_{1j}} \tag{20}$$

$$0 = -\frac{R_{2j}}{L_{2j}} i_{d_{2j}} + i_{q_{2j}} + \frac{k_{2j}}{L_{2j}} \cos(\theta_{1j} + \alpha_{2j}) v_{dc_j} - \frac{V_{2d_j}}{L_{2j}} + \frac{V_{1d_j}}{L_{2j}} \tag{21}$$

$$0 = -\frac{R_{2j}}{L_{2j}} i_{q_{2j}} - i_{d_{2j}} + \frac{k_{2j}}{L_{2j}} \sin(\theta_{1j} + \alpha_{2j}) v_{dc_j} - \frac{V_{2q_j}}{L_{2j}} + \frac{V_{1q_j}}{L_{2j}} \tag{22}$$

Solving the differential-algebraic equation set of (19) to (22) and (5) will result in the values of $k_1, \alpha_1, k_2, \alpha_2, v_{dc}$. It should be noted that in a network having multiple UPFCs, this procedure can be done independently for each of them, since the first stage control provides the

network coupling in the determination of the input *R* which are the *dq* sending and receiving voltages. Fig. 4 shows a flowchart which describes the two stage control.

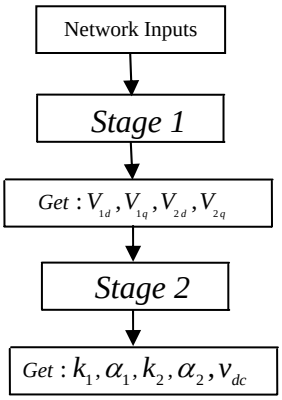

Fig. 4. Two Stage Control Design

III. REDUCED ORDER ESTIMATOR DESIGN

The control scheme explained in section II is best implemented if all the feedback data (machines' speeds and angles) are available to the controller. However, in a wide-area network spread over long distances this assumption may not be feasible. The idea behind a reduced order observer is to estimate the unavailable feedback data using the available data. Dividing the states into a directly available set of X_1 and observable set of X_2, equation (3) can be rewritten [9]:

$$\begin{bmatrix} \dot{X}_1 \\ \dot{X}_2 \end{bmatrix} = \begin{bmatrix} A_{11} & A_{12} \\ A_{21} & A_{22} \end{bmatrix} \begin{bmatrix} X_1 \\ X_2 \end{bmatrix} + \begin{bmatrix} B_1 \\ B_2 \end{bmatrix} U \tag{23}$$

The directly available set of X_1 can be verified through:

$$Y = C_1 X_1 \tag{24}$$

where C_1 is a square and nonsingular matrix. The estimated set of $\hat{X}_2$ is of the form:

$$\hat{X}_2 = LY + Z \tag{25}$$

Considering the dynamics of *Z* to be of the form:

$$\dot{Z} = FZ + GY + HU \tag{26}$$

The estimation error can be written as:

$$e_2 = X_2 - \hat{X}_2 \tag{27}$$

Therefore, the dynamics of the error is given by:

$$\dot{e}_2 = (A_{21} - LC_1A_{11} + FLC_1 - GC_1)X_1 + (A_{22} - LC_1A_{12} - F)X_2 + (B_2 - LC_1B_1 - H)U + Fe_2 \tag{28}$$

Setting the coefficients of X_1, X_2 and U to be zero in equation (28) results in:

$$\dot{e}_2 = Fe_2 \tag{29}$$

$$H = B_2 - LC_1B_1 \tag{30}$$

$$F = A_{22} - LC_1A_{12} \tag{31}$$

$$G = A_{21}C_1^{-1} - LC_1A_{11}C_1^{-1} + FL \tag{32}$$

Defining L to be the observer gain, L can be chosen such that F is negative definite. This guarantees the estimator to be stable and accurate.

Based on the designed estimator, the applied control takes the form of:

$$U = -[K_1, K_2]\begin{bmatrix} X_1 \\ \hat{X}_2 \end{bmatrix} \tag{33}$$

IV. EXAMPLE AND DISCUSSION

The IEEE 14 bus test system [10] has been used to validate the reduced order estimator and the proposed two stage control process in the control of inter-area oscillations. This system has 5 machines and can be roughly considered to have two areas, where machines 1, 2 and 3 form one area and machines 4 and 5 form the other area. The generators are modeled with 10^{th} order models containing the two-axis generator model, Type I Exciter/AVR model and turbine and governor models. The diagram of the network is shown in Fig. 5.

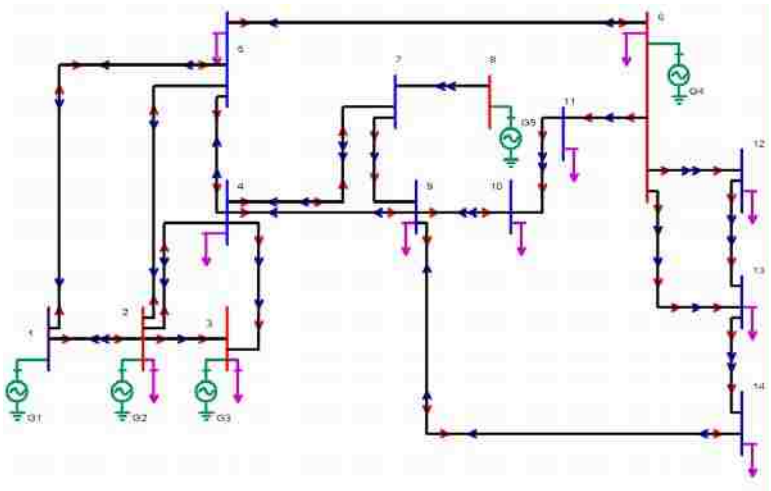

Fig. 5. IEEE 14 Bus Test System

The full differential-algebraic system has been simulated using MATLAB with a high impedance fault of 1 pu applied on bus 10 at 0.2 s and removed at 0.4 s. One UPFC has been installed in the system on the line between buses 5 and 6 with the shunt (sending) part of the UPFC on bus 5. The operating point of the UPFC has been initialized using the method discussed in [11]. The characteristics of the UPFC along with its pre-fault steady state operating points are as follows:

$R_1 = 0.01 pu, L_1 = 0.15 pu$

$R_2 = 0.001 pu, L_2 = 0.015 pu$

$R_p = 200 pu$

$C = 5 pu$

$PLoss = 0.2 pu$

k_1=0.1654, $\alpha_1 = 358.3661^{\circ}$

$k_2 = 0.0015, \alpha_2 = 98.4359^{\circ}$

$v_{dc} = 6.3147$pu

$i_{d_1} = -0.2036$pu, $i_{q_1} = -0.0401$pu

$i_{d_2} = 0.4369$pu, $i_{q_2} = 0.0442$pu

Table I provides the detail of six different cases that were simulated. The first case is the base case in which there is no UPFC control. In Case II, the proposed two-stage control is

utilized with full state feedback. Cases III and IV provide a comparison between scenarios in which different global signals are available (frequencies only according to FNET) and the remaining frequencies and all angles are estimated. The final two cases (V and VI) illustrate the impact of time delay on the global signal feedback.

Fig. 6 shows the simulation results for the speeds of machines 2, 4 and 5 (from top to bottom, respectively), for case I (thin) and II (bold). The figure shows that the proposed two stage control using the entire machine's data as feedback to the controller can effectively damp out inter-area oscillations uniformly in a short time.

TABLE I

Simulation Cases According to the Feedback and Estimated States

	Feedback States	Feedback States' Delay (ms)	Estimated States
Case I (No Control)	---	0	---
Case II (All Feedback Available)	$\omega_1, \omega_2, \omega_3, \omega_4, \omega_5$ $\delta_2, \delta_3, \delta_4, \delta_5$	0	---
Case III	ω_2, ω_5	0	$\omega_1, \omega_3, \omega_4$ $\delta_2, \delta_3, \delta_4, \delta_5$
Case IV	ω_2, ω_4	0	$\omega_1, \omega_3, \omega_5$ $\delta_2, \delta_3, \delta_4, \delta_5$
Case V	ω_2, ω_4	5<t<15	$\omega_1, \omega_3, \omega_5$ $\delta_2, \delta_3, \delta_4, \delta_5$
Case VI	ω_2, ω_4	5<t<20	$\omega_1, \omega_3, \omega_5$ $\delta_2, \delta_3, \delta_4, \delta_5$

Fig. 7 shows a comparison between cases II (bold), III (thin) and IV (boldest). Note that although in cases III and IV the same number of feedback states is available, the overall performance of case IV shows better performance. This shows that selecting the proper feedback

states can play an important role in the performance of the controller. On the other hand, although in case IV, we get good speed deviations' damping for machines 2 and 4, but for machine 5 this is not happening.

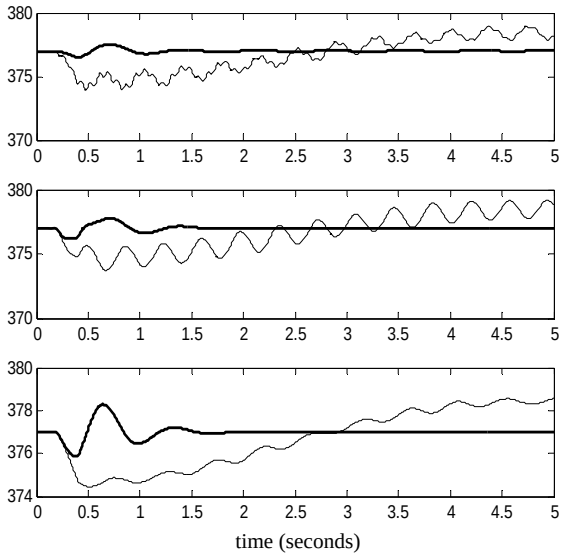

Fig. 6. Machine speeds $\omega_2, \omega_4, \omega_5$ (rad/s) (thin: case I, bold: case II)

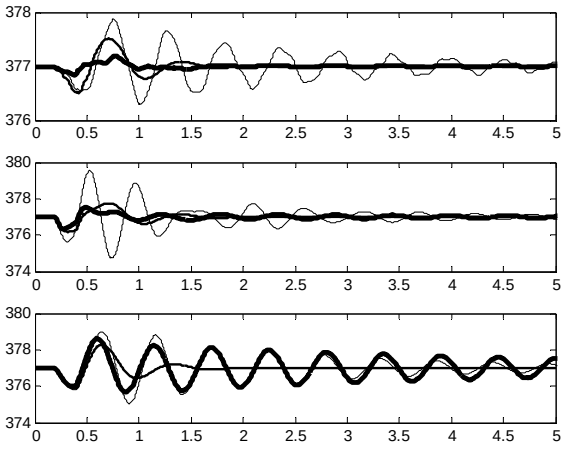

Fig. 7. Machine speeds $\omega_2, \omega_4, \omega_5$ (rad/s) (bold: Case II, thin: Case III, boldest: Case IV)

To verify how time delays from the available states in a wide-area controlled system impact the performance of a controller, cases V and VI introduce a randomly varying time delay into each of the globally available signals. In Case V, the time delay varies randomly between 5 and

15 ms. In Case VI, the time delay varies randomly between 5 and 20 ms.

Fig. 8 compares Cases IV and V, which both have the same observer design. The only difference is in the amount of time delay in the global signal feedback. The comparison shows that there is a slight degradation in performance caused by the signal delay, the controller and estimator still perform well and suitably control the system.

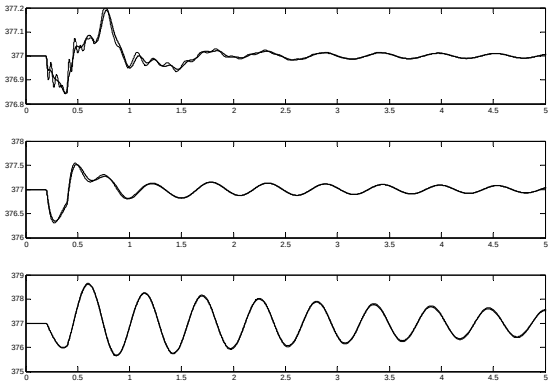

Fig. 8. Machine speeds $\omega_2, \omega_4, \omega_5$ (rad/s) (thin: Case V, bold: Case IV)

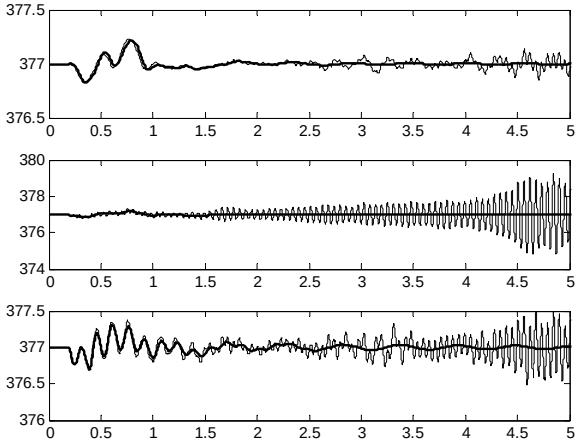

Fig. 9. Machine speeds $\omega_1, \omega_2, \omega_3$ (rad/s) (thin: case VI, bold: case IV)

Fig. 9 shows the comparison of Case IV and Case VI in which the random delays can be up to 20ms. This difference has a significant impact on the ability of the UPFC to damp the system oscillations. In fact, the UPFC actually destabilizes the system by causing undamped high

frequency oscillations. At this time, the authors are investigating whether the estimator or the control is affected by the time delay causing the instability.

V. CONCLUSIONS AND FURTHER WORK

This work shows that using a selected group of measurements in a wide-area controlled network can provide suitable inter-area oscillation damping performance provided the remaining states are estimated through properly designed observers. In a multi-area system, the selected measurements must be chosen from all the major areas of the system to guarantee the controller's successful performance. However, the choice of measurements within an area and the optimal number and type of measurements is still an open question.

Further work is needed to verify the number and type of the optimized measurements in a power network in a more organized scheme based on the control theory. Validity of the proposed approach should be tested in larger networks with more areas and oscillatory modes. Moreover, it is possible that local measurements used as auxiliary outputs of controller's linearized state space would contribute to the control process and reduce the number of needed global measurements.

REFERENCES

[1] HaiFeng Wang, "A Unified Model for the Analysis of FACTS Devices in Damping Power System Oscillations---Part III: Unified Power Flow Controller," *IEEE Trans. Power Delivery*, vol. 15, no. 3, pp. 978-983, July 2000.

[2] Mehrdad Ghandhari, G. Andersson and Ian A. Hiskens, "Control Lyapunov Functions for Controllable Series Devices," *IEEE Trans. Power Systems*, vol. 16, no. 4, pp. 689-694, Nov. 2001.

[3] B.C. Pal, "Robust damping of interarea oscillations with unified power-flow controller," *IEE Proceedings- Generation, Transmission and Distribution*, vol. 149, pp. 733-738, Nov. 2002.

[4] S. Robak, M. Januszewski, D.D. Rasolomampionona, "Power system stability enhancement using PSS and Lyapunov-based controllers: A comparative study," *IEEE Power Tech Conference Proceedings* 2003 Bologna, vol. 3, pp. 6.

[5] N. Tambey and M.L. Kothari, "Damping of power system oscillations with unified power flow controller (UPFC)," *IEE Proceedings- Generation, Transmission and Distribution*, vol. 150, pp. 129-140, March 2003.

[6] M. Januszewski, J. Machowski and J.W. Bialek, "Application of the direct Lyapunov method to improve damping of power swings by control of UPFC," *IEE Proceedings- Generation, Transmission and Distribution*, vol. 151, pp. 252-260, March 2004.

[7] M. Zarghami, M. Crow, "Discussion on Effective Control of Inter-Area Oscillations by UPFCs," *39'th North American Power Symposium, New Mexico State University*, Sep.-Oct. 2007.

[8] L. Dong, M.L. Crow, Z. Yang, C. Shen, L. Zhang, S. Atcitty, "A Reconfigurable FACTS System for University Laboratories," *IEEE Transactions on Power Systems*, Vol. 19, no. 1, pp. 120-128, Feb. 2004.

[9] Notes of the course ME 4811 by Prof. Fotis A. Papoulias, http://web.nps.navy.mil/~me/blackboard/me4811/docs/notes3.pdf

[10] http://www.ee.washington.edu/research/pstca/pf14/pg_tca14bus.htm

[11] M. Zarghami, M.L. Crow, "The Existence of Multiple Equilibria in the UPFC Power Injection Model," *IEEE Transactions on Power Systems*, vol. 22, no. 4, pp. 2280-2282, Nov. 2007.

[12] Zhian Zhong; Chunchun Xu; B. J. Billian, Li Zhang; S. J. Tsai, R. W. Conners, V. A. Centeno, A. G. Phadke, and Yilu Liu, "Power system frequency monitoring network (FNET) implementation," *IEEE Transactions on Power Systems*, November 2005, vol. 20, no. 4, pp. 1914-1921.

7. Damping Inter-Area Oscillations in Power Systems by STATCOMs

Mahyar Zarghami, *Student Member, IEEE*, Mariesa. L. Crow, *Senior Member, IEEE*

ABSTRACT: Shunt FACTS devices such as STATCOMs are best known for their impact on reactive power flow in power networks. This is usually done by local reactive compensation which also regulates voltage magnitude of the bus to which the shunt FACTS device is connected. On the other hand, these devices are less known for their effect on active power flow. This paper discusses a novel approach for damping inter-area oscillations in a large power network using multiple STATCOMs. In the paper, it will be shown that these oscillations can be controlled by changing STATCOMs' bus voltage angles, hence regulating active power flow through the network. Feasibility of the new approach is also discussed.

Index Terms: STATCOM, Inter-Area Oscillation

I. INTRODUCTION

FACTS devices have so far been used to solve numerous dynamic and steady-state problems in power systems by controlling voltage, impedance and power through the networks. One way to categorize these devices is to divide them into shunt, series and series-shunt devices. While shunt devices are usually used for applications such as reactive power compensation and voltage control, series devices are mostly applied in active power flow changes and damping power oscillations in the network. It is obvious that series-shunt devices such as UPFCs have characteristics of both shunt and series devices. Applications for STATCOMs, SSSCs and UPFCs as shunt, series and series-shunt devices can be found in [1]-[8].

A STATCOM, which is a shunt device, has not been well known for damping power system oscillations. These oscillations can occur in a system because of contingencies such as sudden load changes or power system faults. They usually exist between groups of generators which are located at the sides of tie-lines in a power system. Controlling oscillations can be done by rapidly changing active power flows through these lines. So far, UPFCs have been mostly found in the literature as proper devices for damping these types of oscillations.

In this paper, STATCOMs have been used in a multi-area power network for controlling

inter-area oscillations. The idea behind this type of control is to control voltage angles at the buses to which STATCOMs are connected. In the sections to come, first the model used for STATCOM has been introduced. Then the control method will be discussed. The method is tested by simulations on IEEE 118 bus system and feasibility of the control will also be addressed.

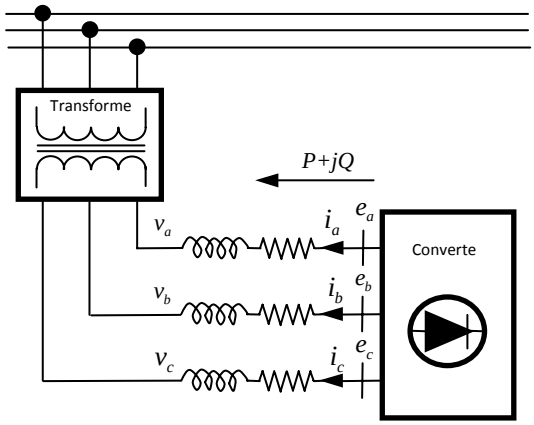

Fig. 1. STATCOM Diagram

II. STATCOM MODEL

A STATCOM consists of a shunt branch connected through a dc capacitor as shown in Fig. 1. This branch can inject reactive and active powers through its dc capacitor, hence changing both its ac bus magnitude and angle. The state space model for STATCOM has been taken from [9]. It consists of 3 differential equations written in the dq format as follows:

$$\frac{1}{\omega_s}\dot{i}_d = -\frac{R_1}{L_1}i_d + i_q + \frac{k_1}{L_1}\cos(\theta_1+\alpha_1)v_{dc} - \frac{V_d}{L_1} \tag{1}$$

$$\frac{1}{\omega_s}\dot{i}_q = -\frac{R_1}{L_1}i_q - i_d + \frac{k_1}{L_1}\sin(\theta_1+\alpha_1)v_{dc} - \frac{V_q}{L_1} \tag{2}$$

$$\frac{C}{\omega_s}\dot{v}_{dc} = -k_1\cos(\theta_1+\alpha_1)i_d - k_1\sin(\theta_1+\alpha_1)i_q - \frac{v_{dc}}{R_p} \tag{3}$$

The power transaction in the STATCOM can be controlled by its modulation amplitude k and angle α.

III. CONTROLLER DESIGN

For control development purposes, several assumptions are initially made. The two simplifying assumptions are that the system loads are modeled as constant impedance loads and can therefore be absorbed into the bus admittance matrix. Secondly, the generators are modeled as the classical "transient reactance behind constant voltage" model. Note that these assumptions are for control development only – the proposed control is validated with the full generator model given in the Appendix. Using the load impedance model, the only points of current injection into the network are the generator internal buses and the STATCOM buses. Furthermore, using Kron reduction enables the transmission network to be reduced to an admittance matrix of size $(N+n \times N+n)$ where N is the number of generator buses and n is the number of STATCOMs in the system. Fig. 2 illustrates the reduced system showing the points of current injection. Dashed lines show that virtually all machines and STATCOMs are connected to each other.

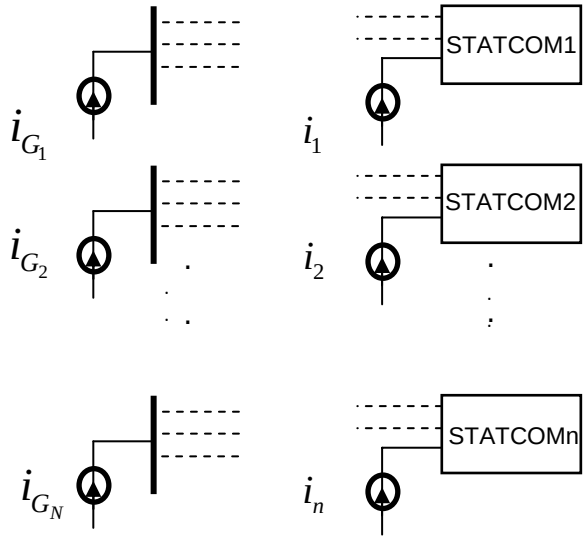

Fig. 2. Equivalent Power System from Controller's View

The classical model for the reduced network including STATCOMs is:

$$j = 1,\ldots,N$$

$$\dot{\delta}_j = \omega_j - \omega_s \tag{4}$$

$$\dot{\omega}_j = \frac{1}{M_j}[P_{M_j} - E_j \sum_{k=1}^{N} E_k Y_{jk} \cos(\delta_j - \delta_k - \phi_{jk}) \\ - E_j \sum_{k=N+1}^{N+n} E_k Y_{jk} \left(\cos(\delta_j - \phi_{jk}) r_{2(k-N-1)+1} + \sin(\delta_j - \phi_{jk}) r_{2(k-N-1)+2}\right)] \quad (5)$$

where $E_j \angle \delta_j$ is the voltage at bus *j*, $Y_{jk} \angle \phi_{jk}$ is the *(j,k)*th element of the reduced admittance matrix, P_{M_j}, M_j and ω_j are the mechanical power, inertia constant and angular speed respectively of machine *j*, and ω_s is synchronous speed. The first summation represents the active power injected at each generator bus and the second summation represents the active power injected at each STATCOM bus.

This nonlinear system has *2N* states and *2n* intermediate control inputs r_j defined as:

$$r_{2(j-1)+1} = V_{d_j} \quad (6)$$

$$r_{2(j-1)+2} = V_{q_j} \quad (7)$$

where V_{d_j} and V_{q_j} are the *dq* components of the *j*-th STATCOM respectively. This step describes the first stage of the two stage control. Note that this stage is independent of the STATCOM dynamics.

Linearizing this reduced system and assuming constant voltage magnitudes at STATCOM buses results in a linear system of the form:

$$\dot{X} = AX + BR \quad (8)$$

where *R* represents the vector of STATCOM bus angles. This system can be linearized through the feedback control:

$$R = -KX \quad (9)$$

where *K* is chosen using optimal LQR control processes to minimize speed and angle deviations in the generators. If the original system were linear, this feedback control would result in the optimal values of voltage angles at STATCOM buses to damp inter-area oscillations.

The second stage of the control is to convert the control inputs *R* into the modulation gain and angles k and α for each STATCOM. The first step in this stage is to find the values of currents i_d and i_q from the STATCOM's active and reactive power balance equations:

$$i = 1,...,n$$

$$0 = V_{d_i} i_{d_i} + V_{q_i} i_{q_i} - V_i \sum_{j=1}^{Nsys} V_j \mathrm{Y}_{ij} \cos(\theta_i - \theta_j - \Phi_{ij}) \tag{10}$$

$$0 = V_{q_i} i_{d_i} - V_{d_i} i_{q_i} - V_i \sum_{j=1}^{Nsys} V_j \mathrm{Y}_{ij} \sin(\theta_i - \theta_j - \Phi_{ij}) \tag{11}$$

where in the above $\mathrm{Y}_{ij}\angle\Phi_{ij}$ is the *(i,j)*th element of the original admittance matrix and *Nsys* is the number of system buses.

If it can be assumed that the time scale difference between the STATCOMs and the generator dynamics is large (i.e. $1/\omega_s << 1/M_i$) and letting $1/\omega_s \approx 0$, then equations (1)-(2) can be written as their algebraic counterparts:

$$0 = -\frac{R_1}{L_1} i_d + i_q + \frac{k_1}{L_1} \cos(\theta_1 + \alpha_1) v_{dc} - \frac{V_d}{L_1} \tag{12}$$

$$0 = -\frac{R_1}{L_1} i_q - i_d + \frac{k_1}{L_1} \sin(\theta_1 + \alpha_1) v_{dc} - \frac{V_q}{L_1} \tag{13}$$

Solving equations (12)-(13) together with (3) provides the values of k and α which are the true control inputs to the STATCOM. This procedure can be repeated for each STATCOM independently since the first stage of the control provides the network coupling during determination of the input R (STATCOM bus voltage angles). Fig. 3 shows a flow chart which illustrates the two stage control.

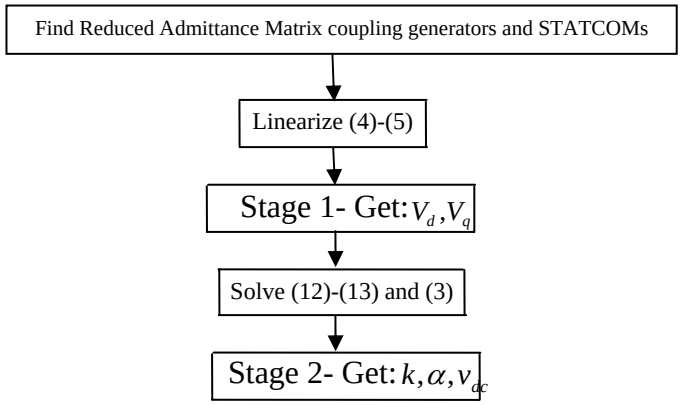

Fig. 3. Two Stage Control Design

IV. DECENTRALIZED CONTROLLER

The control method mentioned in III needs global feedback data (generator rotor speeds and angles) to be implemented. As this might not be feasible at all times, one approach is to use estimated data instead of real data for control implementation. This can be done by designing optimal local observers which altogether make a decentralized control system. In this approach, for each STATCOM, local active power flow information from connected lines is used to estimate the states of the whole control system. Optimal observers can be designed using LQR approach for the following system:

$$\dot{X} = AX + BR \tag{14}$$

$$i = 1,...,n$$

$$Y_i = C_i X + D_i R \tag{15}$$

where C_i and D_i can be evaluated after linearization of the output equations for each STATCOM. Using LQR, *n* sets of estimators would be of the following format:

$$\dot{\hat{X}}_i = A\hat{X}_i + BR_i + L_i(Y_i - \hat{Y}_i) \tag{16}$$

where L_i is the optimal observer gain. Input commands for each STATCOM will be calculated as:

$$R_i = -K\hat{X}_i \tag{17}$$

V. THE TEST SYSTEM

The IEEE 118 bus test system [10] has been used to validate the proposed controller. The diagram of the network is shown in Fig. 4. This system has 20 machines where the order of each is 10 as shown in Appendix. Three STATCOMs have been installed in the system on buses 30, 64 and 94. The parameters of the STATCOMs are similar and are shown in Table I. Steady state

operating points of STATCOMs have been chosen such that dc bus voltages would be equal to 2.0 pu.

TABLE I

STATCOM Parameters

	$R_i(pu)$	$L_i(pu)$	$R_p(pu)$	$C(pu)$
STATCOM1	0.01	0.15	100.0	100.0

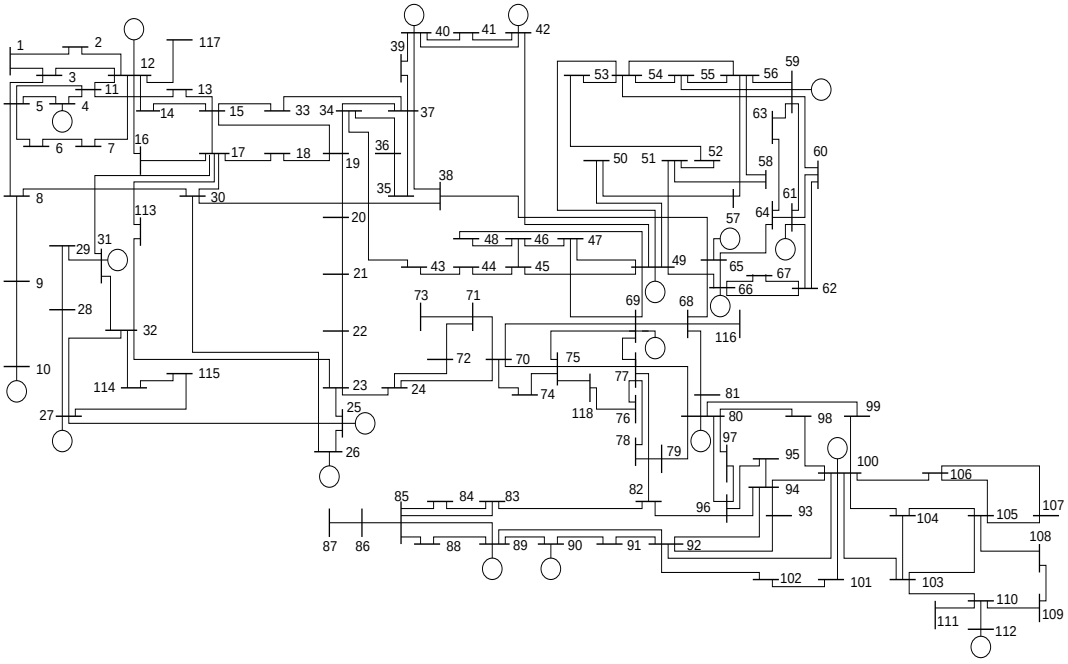

Fig. 4. IEEE 118 Bus Test System

VI. EXAMPLES AND RESULTS

In order to validate the proposed controller in IEEE 118 bus test system, a solid symmetrical fault has been applied on bus 43 of at 0 s and has been cleared at 0.2 s. Nonlinear simulations have been carried out using fully 10^{th} order machine models as shown in the Appendix. Two cases have been considered for simulations. Case I is uncontrolled and case II is decentralized controlled (when control is implemented using estimated data with local observers). Fig. 5 shows four of the machines' rotor speeds. Because of lack of space, not all generator speeds have been shown. As it is seen in this figure, the proposed control can damp out oscillations effectively. Figures 6-7 show STATCOMs' ac bus voltage magnitudes and angles

respectively. As it is seen in these figures, voltage angles are controlled in order to damp oscillations and variations of voltage magnitudes are rather small. This clearly shows that inter-area oscillations have close relationship with active power flow changes throughout the network. Fig. 8 depicts dc capacitor voltages and Fig. 9 shows injected active powers by STATCOMs. As it is seen, STATCOMs need to inject multiple orders of their nominal active powers in a short period of time and this in turn causes dc capacitors to be discharged temporarily.

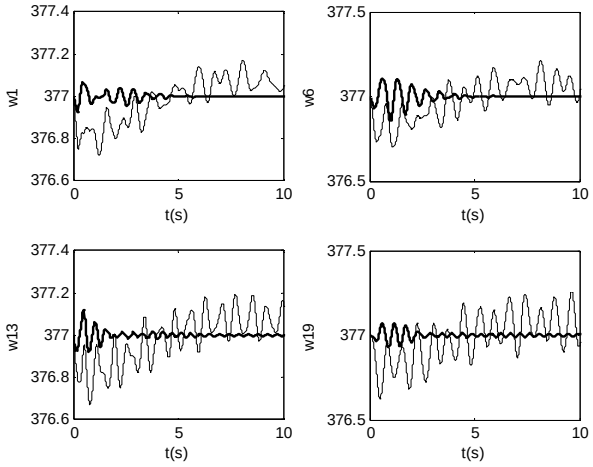

Fig. 5. Speed deviations (uncontrolled: thin, decentralized controlled: bold)

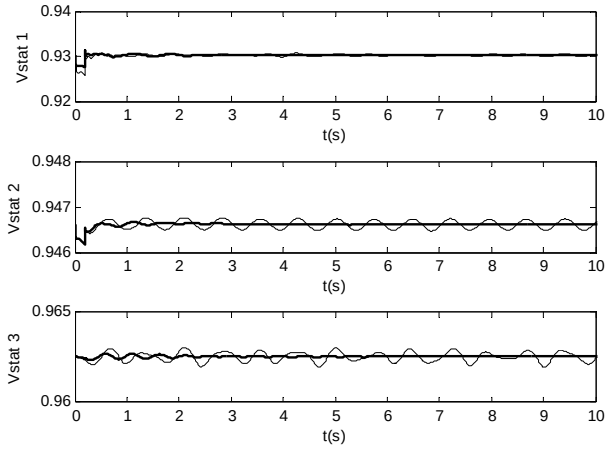

Fig. 6. STATCOM bus voltage magnitudes (uncontrolled: thin, decentralized controlled: bold)

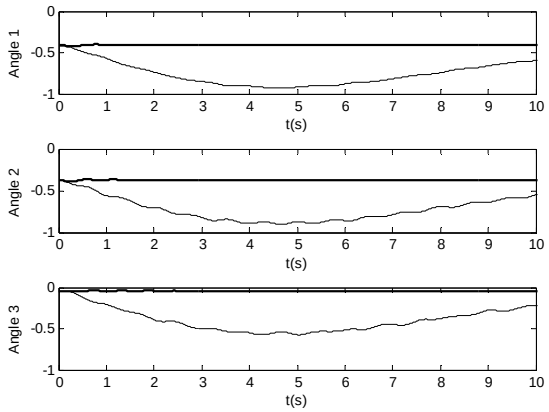

Fig. 7. STATCOM bus voltage angles (uncontrolled: thin, decentralized controlled: bold)

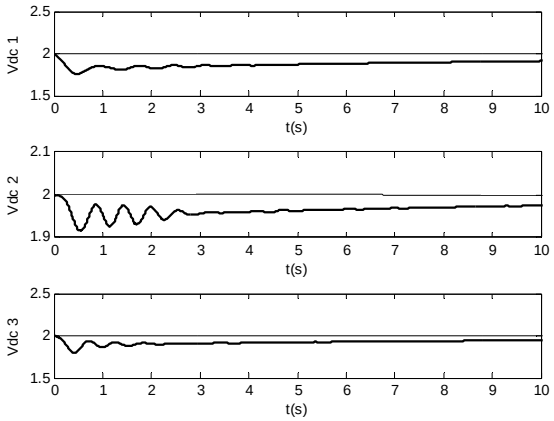

Fig. 8. STATCOM dc voltages (uncontrolled: thin, decentralized controlled: bold)

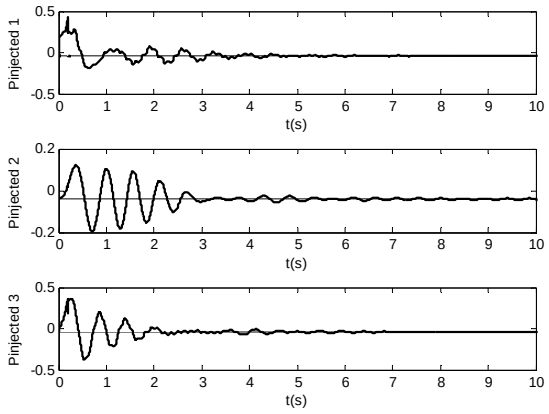

Fig. 9. STATCOM injected active powers (uncontrolled: thin, decentralized controlled: bold)

VII. CONCLUSIONS AND FURTHER WORK

A control scheme has been proposed for damping inter-area oscillations by STATCOMs which is based on changing their bus angles to control active power flow through the power network in transients. The method is showing good results in IEEE 118 bus test system. A decentralized approach has been devised for estimation of the needed feedback data through local observers which uses local active power flows as measurements. However, the method uses considerable active power flow injections from STATCOMs during transients. This might necessitate the usage of ultra capacitors as well as higher rating power electronic devices in the make of voltage source converters in STATCOMs.

Further investigation could be made on designing nonlinear controllers based on the proposed nonlinear modeling. Robustness and dependency of the designed controllers on topology changes of the power system is also a matter of concern. It is also possible to see how a bunch of FACTS devices (such as STATCOMs, UPFCs, SSSCs, etc.) existing in a network could work together to damp out inter-area oscillations.

APPENDIX

n_g : Number of generators

for $j = 1, ..., n_g$

Two Axis Generator Model

$$\dot{\delta}_j = \omega_j - \omega_S$$

$$\frac{2H_j}{\omega_s}\dot{\omega}_j = T_{Mj} + \frac{V_j}{x'_{dj}}\left(E'_{dj}\cos(\theta_j - \delta_j) + E'_{qj}\sin(\theta_j - \delta_j)\right)$$

$$T'_{d0j}\dot{E}'_{qj} = -\frac{x_{dj}}{x'_{dj}}E'_{qj} + \frac{x_{dj} - x'_{dj}}{x'_{dj}}V_j\cos(\theta_j - \delta_j) + E_{fdj}$$

$$T'_{q0j}\dot{E}'_{dj} = -\frac{x_{qj}}{x'_{dj}}E'_{dj} - \frac{(x_{qj} - x'_{dj})}{x'_{dj}}V_j\sin(\theta_j - \delta_j)$$

Assumption:

$x'_{qj} = x'_{dj}$ and $R_s = 0$

IEEE Type I Exciter/AVR Model

$$T_{Ej}\dot{E}_{fdj} = -K_{Ej}E_{fdj} + V_{Rj}$$

$$T_{Aj}\dot{V}_{Rj} = -V_{Rj} + K_{Aj}R_{Fj} - \frac{K_{Aj}K_{Fj}}{T_{Fj}}E_{fdj} + K_{Aj}(V_{refj} - V_j)$$

$$V_{Rj}^{\min} \le V_{Rj} \le V_{Rj}^{\max}$$

$$T_{Fj}\dot{R}_{Fj} = -R_{Fj} + \frac{K_{Fj}}{T_{Fj}}E_{fdj}$$

Turbine

$$T_{RHj}\dot{T}_{Mj} = -T_{Mj} + \left(1 - \frac{K_{HPj}T_{RHj}}{T_{CHj}}\right)P_{CHj} + \frac{K_{HPj}T_{RHj}}{T_{CHj}}P_{SVj}$$

$$T_{CHj}\dot{P}_{CHj} = -P_{CHj} + P_{SVj}$$

Speed Governor

$$T_{SVj}\dot{P}_{SVj} = -P_{SVj} + P_{Cj} - \frac{\omega_j}{R_j\omega_s}$$

$$0 \le P_{SVj} \le P_{SVj}^{\max}$$

REFERENCES

[1] Li Chun, Jiang Qirong, Xu Jianxin, "Investigation of voltage regulation stability of static synchronous compensator in power system," *IEEE Power Engineering Society Winter Meeting, 2000*, vol. 4, 23-27 Jan. 2000, pp. 2462-2467.

[2] Wang, H.F., "Phillips-Heffron model of power systems installed with STATCOM and applications," *IEEE Proceedings Generation, Transmission and Distribution*, vol. 146, Sept. 1999, pp 521 - 527.

[3] Ye Y., Kazerani M., Quintana V."Current-source converter based SSSC: modeling and control," *IEEE Power Engineering Society Summer Meeting, 2000.*vol. 2, 15-19 July 2001, pp. 949 - 954 vol.2.

[4] Haque, M.H., "Stability improvement by FACTS devices: a comparison between STATCOM and SSSC," *IEEE Power Engineering Society General Meeting 2005,* 12-16 June 2005, pp. 1708 - 1713 Vol. 2.

[5] Norouzi, A.H., Sharaf, A.M., "Two control schemes to enhance the dynamic performance of the STATCOM and SSSC," *IEEE Trans. On Power Delivery,* vol. 20, Jan 2005, pp. 435 – 442.

[6] Namin, M.H., "Using UPFC in order to Power flow control," *Industrial Technology, 2006. ICIT 2006. IEEE International Conference on,* 15-17 Dec. 2006, pp. 1486 – 1491.

[7] Kannan S., Jayaram S., Salama M.M.A., "Real and reactive power coordination for a unified power flow controller," *IEEE Trans. On Power Systems,*vol. 19, Aug. 2004, pp. 1454 - 1461.

[8] Zhengyu Huang, Yinxin Ni, Shen C.M., Wu F.F., Shousun Chen, Baolin Zhang, "Application of unified power flow controller in interconnected power systems-modeling, interface, control strategy, and case study," *Power Systems, IEEE Transactions on Power Systems,* vol. 15, May 2000, pp. 817 - 824.

[9] L. Dong, M.L. Crow, Z. Yang, C. Shen, L. Zhang, S. Atcitty, "A Reconfigurable FACTS System for University Laboratories," *IEEE Transactions on Power Systems*, Vol. 19, no. 1, pp. 120-128, Feb. 2004.

[10] http://www.ee.washington.edu/research/pstca/pf118/pg_tca118bus.htm

8. Nonlinear Control of FACTS Devices for Damping Inter-Area Oscillations in Wide-Area Power Systems

M. Zarghami, *Student Member, IEEE,* M. L. Crow, *Senior Member, IEEE,* and S. Jagannathan, *Senior Member, IEEE*

ABSTRACT: This paper introduces a new scheme for nonlinear control of FACTS devices for the purpose of damping inter-area oscillations in wide-area power systems. FACTS controllers consist of series, shunt or a combination of series-shunt devices which are interfaced with the bulk power system through injection buses. Controlling the angle of these buses can effectively damp low frequency interarea oscillations in the system. The proposed control method is based on finding an equivalent reduced affine nonlinear system for the network from which the dominant machines are extracted based on dynamic coherency. It is shown that if properly selected, measurements obtained from this subsystem of machines are sufficient inputs to the FACTS devices to stabilize the power system. The effectiveness of the proposed method on damping inter-area oscillations is validated on the 68 bus, 16 generator system of the New England/New York network.

Index Terms – Nonlinear Control, FACTS, Inter-Area Oscillation, PMU, Wide Area Control, Coherent Groups, Dominant Machines

I. INTRODUCTION

Flexible Alternating Current Transmission Systems (FACTS) devices can provide promising solutions to many of the stability problems that occur within the bulk power system. As high voltage power electronics become less expensive and have a wider-range of operation, FACTS devices will become more prevalent in the transmission system to control active power flow across congested corridors and ensure voltage security.

FACTS devices can be categorized into three major groups: shunt devices such as the Static Synchronous Compensator (STATCOM), series devices such as the Static Synchronous Series Compensator (SSSC) and Series-Shunt devices such as the Unified Power Flow Controller (UPFC). In addition to steady-state solutions such as power flow and voltage control, an added benefit of FACTS devices deployed in the transmission system is that they can also effectively control active power oscillations that can damage generators, increase line losses, and increase wear and tear on network components. Therefore developing suitable control strategies is a requirement before FACTS can be confidently utilized in the power system.

Several authors have investigated utilizing FACTS, especially UPFCs to damp inter-area oscillations using a variety of control approaches [1]-[10]. Interarea oscillations can occur in a system because of contingencies such as sudden load changes or faults. In [1]-[5], oscillation damping is based on a linear control approach to the UPFC and power system, whereas other authors consider nonlinear control systems theory and Lyapunov Energy Functions [6]-[10]. Typically, nonlinear approaches are more effective for large perturbations or when the power system state strays significantly from the initial operating point.

The research proposed in this paper provides a general nonlinear method for using multiple FACTS devices in a wide-area power network for the purpose of damping inter-area oscillations. In the paper, we show that any FACTS device which is capable of changing its interface bus angle(s) with the network is eligible to be part of a set of devices suitable for controlling power system oscillations. Using this method, it will be shown that even shunt FACTS devices, such as STATCOMs, which have not been traditionally considered for applications such as damping power oscillations, can also be used for this purpose. The control method is based on finding a reduced nonlinear affine state space system for the network which can be controlled by wide-area synchronized measurements of rotor frequencies. While Phasor Measurement Units based on frequency measurements (such as from FNET [11]) has made wide area control of the power networks feasible, it is still not reasonable to expect that the full set of frequency measurements is available for controller use. Therefore, we propose an approach to use a reduced set of PMUs based on the dominant machines of the system has been proposed for control action.

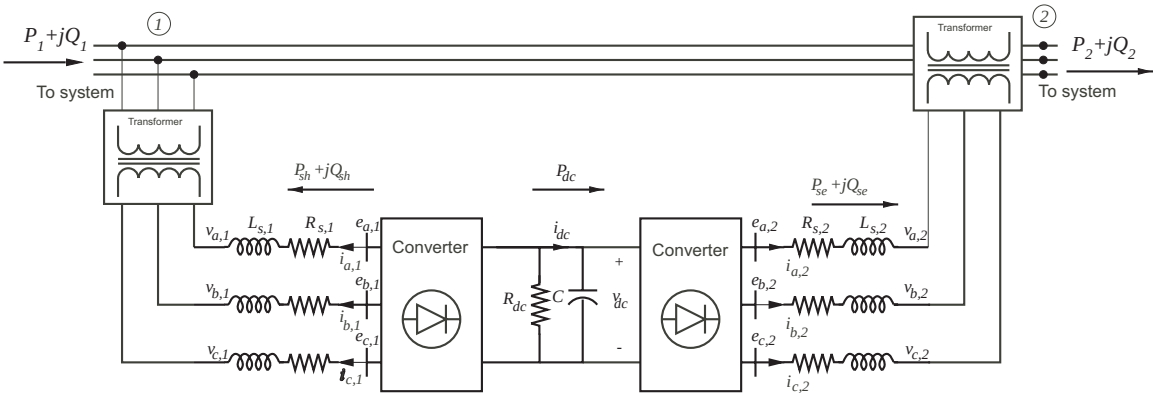

Fig. 1. Unified Power Flow Controller Diagram

II. THE UPFC MODEL

The unified power flow controller, or UPFC, is the most versatile FACTS device. It consists of a combination of a shunt and series branches connected through the DC capacitor as shown in Fig. 1. Models for STATCOM and SSSC can be easily extracted from UPFC model. The series connected inverter injects a voltage with controllable magnitude and phase angle in series with the transmission line, therefore providing real and reactive power to the transmission line. The shunt-connected inverter provides the active power drawn by the series branch plus the losses and can independently provide reactive compensation to the system. The UPFC model is a combination of the STATCOM (Static Synchronous Compensator) and SSSC (Static Synchronous Series Compensator) models [12]:

$$\frac{1}{\omega_s}\frac{d}{dt}i_{d_1} = \frac{k_1 V_{dc}}{L_{s_1}}\cos(\alpha_1+\theta_1) + \frac{\omega}{\omega_s}i_{q_1} - \frac{R_{s_1}}{L_{s_1}}i_{d_1} - \frac{V_1}{L_{s_1}}\cos\theta_1 \quad (1)$$

$$\frac{1}{\omega_s}\frac{d}{dt}i_{q_1} = \frac{k_1 V_{dc}}{L_{s_1}}\sin(\alpha_1+\theta_1) - \frac{R_{s_1}}{L_{s_1}}i_{q_1} - \frac{\omega}{\omega_s}i_{d_1} - \frac{V_1}{L_{s_1}}\sin\theta_1 \quad (2)$$

$$\frac{1}{\omega_s}\frac{d}{dt}i_{d_2} = -\frac{R_{s_2}}{L_{s_2}}i_{d_2} + \frac{\omega}{\omega_s}i_{q_2} + \frac{k_2}{L_{s_2}}\cos(\alpha_2+\theta_1)V_{dc} - \frac{1}{L_{s_2}}(V_2\cos\theta_2 - V_1\cos\theta_1) \quad (3)$$

$$\frac{1}{\omega_s}\frac{d}{dt}i_{q_2} = -\frac{R_{s_2}}{L_{s_2}}i_{q_2} - \frac{\omega}{\omega_s}i_{d_2} + \frac{k_2}{L_{s_2}}\sin(\alpha_2+\theta_1)V_{dc} - \frac{1}{L_{s_2}}(V_2\sin\theta_2 - V_1\sin\theta_2) \quad (4)$$

$$\frac{C}{\omega_s}\frac{d}{dt}V_{dc} = -k_1\cos(\alpha_1+\theta_1)i_{d_1} - k_1\sin(\alpha_1+\theta_1)i_{q_1}$$

$$-k_2 \cos(\alpha_2 + \theta_1)\, i_{d_2} - k_2 \sin(\alpha_2 + \theta_1)\, i_{q_2} - \frac{V_{dc}}{R_{dc}} \tag{5}$$

where the parameters are as shown in Fig. 1. The currents i_{d1} and i_{q1} are the dq components of the shunt current. The currents i_{d2} and i_{q2} are the dq components of the series current. The voltages $V_1\angle\theta_1$ and $V_2\angle\theta_2$ are the sending end and receiving end voltage magnitudes and angles respectively. The UPFC is controlled by varying the phase angles (α_1, α_2) and magnitudes (k_1, k_2) of the converter shunt and series output voltages (e_1, e_2) respectively.

The power balance equations at bus 1 are given by:

$$0 = V_1\left((i_{d_1} - i_{d_2})\cos\theta_1 + (i_{q_1} - i_{q_2})\sin\theta_1\right) - V_1 \sum_{j=1}^{n} V_j Y_{1j} \cos(\theta_1 - \theta_j - \phi_{1j}) \tag{6}$$

$$0 = V_1\left((i_{d_1} - i_{d_2})\sin\theta_1 - (i_{q_1} - i_{q_2})\cos\theta_1\right) - V_1 \sum_{j=1}^{n} V_j Y_{1j} \sin(\theta_1 - \theta_j - \phi_{1j}) \tag{7}$$

and at bus 2:

$$0 = V_2\left(i_{d_2}\cos\theta_2 + i_{q_2}\sin\theta_2\right) - V_2 \sum_{j=1}^{n} V_j Y_{2j} \cos(\theta_2 - \theta_j - \phi_{2j}) \tag{8}$$

$$0 = V_2\left(i_{d_2}\sin\theta_2 - i_{q_2}\cos\theta_2\right) - V_2 \sum_{j=1}^{n} V_j Y_{2j} \sin(\theta_2 - \theta_j - \phi_{2j}) \tag{9}$$

III. SYSTEM MODEL

For control development purposes, several assumptions are initially made. The two simplifying assumptions are that the system loads are modeled as constant impedance loads and can therefore be absorbed into the bus admittance matrix. Secondly, the generators are modeled as the classical "transient reactance behind constant voltage" model. Note that these assumptions are for control development only – the proposed control is validated with the full nonlinear 10-th order power system model given in the Appendix. Using the load impedance model, the only points of current injection into the network are the generator internal buses and the UPFC sending and receiving end buses. Furthermore, Kron reduction enables the transmission network to be reduced to an admittance matrix of size $(N+n \times N+n)$ where N is the number of generator buses and n is the number FACTS current injections in the system. Fig. 2 illustrates the reduced system showing the points of current injection. Each UPFC has two current injections, i_1 and i_2, at the sending and receiving ends respectively; a STATCOM has one current.

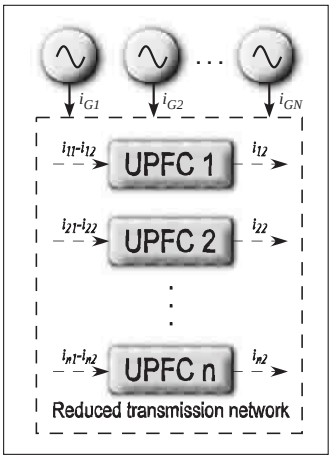

Fig. 2. Equivalent power system from the controller viewpoint

The generator current injections are given by i_G. The classical model for the reduced network including the UPFCs is:

$$\dot{\delta}_j = \omega_j - \omega_s \tag{10}$$

$$\dot{\omega}_j = \frac{1}{M_j}\left[P_{M_j} - E_j \sum_{k=1}^{N+n} E_k Y_{jk} \cos\left(\delta_j - \delta_k - \phi_{jk}\right)\right] \tag{11}$$

$$j = 1 \ldots, N$$

where $E_j \angle \delta_j$ is the voltage at bus j, $Y_{jk} \angle \phi_{jk}$ is the $(j,k)th$ element of the reduced admittance matrix, $P_{m_j}, M_j,$ and ω_j are the mechanical power, inertia constant, and angular speed respectively of machine j, and ω_s is synchronous speed. The summation represents the active power injected at each current injection point.

IV. CONTROLLER DESIGN

The controller design consists of three stages.

A. Stage I

The objective of the first design stage is to find the desired changes in mechanical powers required to stabilize the system. To obtain the amount of mechanical power required, we initially assume that the mechanical powers P_{M_j} are inputs into the system model. Note that this is *only* for controller development; we don't actually require that the generator mechanical powers change.

Under this assumption, the system model of equations (10) and (11) become

$$\dot{x} = F(x) + GU \tag{12}$$

where

$$F(X) = \begin{bmatrix} \omega_1 - \omega_s \\ -\frac{1}{M_1} E_1 \sum_{k=1}^{N+n} E_k Y_{1k} \cos\left(\delta_1 - \delta_k - \phi_{ik}\right) \\ \vdots \\ \omega_N - \omega_s \\ -\frac{1}{M_N} E_N \sum_{k=1}^{N+n} E_k Y_{1k} \cos\left(\delta_N - \delta_k - \phi_{ik}\right) \end{bmatrix} \tag{13}$$

$$G = \begin{bmatrix} 0 & 0 & \dots & 0 & 0 \\ 0 & \frac{1}{M_1} & \dots & 0 & 0 \\ \vdots & \vdots & \ddots & \vdots & \vdots \\ 0 & 0 & \dots & 0 & 0 \\ 0 & 0 & \dots & 0 & \frac{1}{M_N} \end{bmatrix} \tag{14}$$

$$U = [0\ P_{M_1}\ 0\ P_{M_2}\ \dots\ 0\ P_{M_N}] \tag{15}$$

where $x = [\delta_1\ \omega_1\ \delta_2\ \omega_2\ \dots\ \delta_N\ \omega_N]$ and

Since we only require that the system frequencies return to steady-state rapidly, a subset of equations (12) is

$$\dot{x}_2 = f\left(x_1\right) + gu \tag{16}$$

where $x_1 = [\delta_1\ \delta_2\ \dots\ \delta_N]$ and $x_2 = [\omega_1\ \omega_2\ \dots\ \omega_N]$.

$$f(x_1) = \begin{bmatrix} -\frac{1}{M_1} E_1 \sum_{k=1}^{N+n} E_k Y_{1k} \cos\left(\delta_1 - \delta_k - \phi_{ik}\right) \\ \vdots \\ -\frac{1}{M_N} E_N \sum_{k=1}^{N+n} E_k Y_{1k} \cos\left(\delta_N - \delta_k - \phi_{ik}\right) \end{bmatrix} \tag{17}$$

$$G = \begin{bmatrix} \frac{1}{M_1} & \dots & 0 \\ \vdots & \ddots & \vdots \\ 0 & \dots & \frac{1}{M_N} \end{bmatrix} \tag{18}$$

$$U = [P_{M_1}\ P_{M_2}\ \dots\ P_{M_N}] \tag{19}$$

Letting x_{1s}, x_{2s} and u_s denote the steady-state values of x_1, x_2 and u respectively, then the error in generator rotor frequencies becomes

$$e = x_2 - x_{2s} \tag{20}$$

and

$$\dot{e} = f(x_1) - f(x_{1s}) - gu_s + gu_d \tag{21}$$

Equation (21) can be stabilized with input u_d such that

$$u_d = g^{-1}\left[-f(x_1) + f(x_{1s}) + gu_s + Ke\right] \tag{22}$$

where K is a positive definite matrix and

$$\dot{e} = -Ke \tag{23}$$

Stage II

In Stage I, the required changes in the generator's mechanical powers were found that stablize the system. In this stage, these changes are translated into control signals to the FACTS devices. As noted previously, the generator mechanical powers do not actually change as a consequence of the proposed control. Using the desired active power changes, a new control signal is introduced:

$$\Delta u = u_{desired} - u_{actual} \tag{24}$$

where u_d and u_s are the desired and actual values for the generator mechanical powers. This mismatch is translated into the desired changes in the FACTS' bus voltage angles:

$$\begin{aligned} l_j \;=\; & \Delta u_j - E_j \sum_{k=N+1}^{N+n} E_k Y_{jk} \cos\left(\delta_j - \delta_k - \phi_{jk}\right) \\ & -E_j \sum_{k=N+1}^{N+n} E_k Y_{jk} \cos\left(\delta_j - \delta_k - \Delta\delta_k - \phi_{jk}\right) \\ & j = i, \ldots, N \end{aligned} \tag{25}$$

where

$$\begin{aligned} L &= \left[l_1,\ \ldots,\ l_N\right]^T \\ \overline{\Delta} &= \left[\Delta\delta_1,\ \ldots,\ \Delta\delta_n\right]^T \end{aligned}$$

The nonlinear system (25) is solved numerically for $\overline{\Delta}$. Note that if $N \neq n$, then the system of equations is not square and an exact solution to (25) is not possible. In this

case, the equations are minimized to find the best fit to $\overline{\Delta}$ which minimizes the error in (25). These values are then used to calculate the desired current injections: $i^{\star}_{d1}, i^{\star}_{q1}, i^{\star}_{d2}, i^{\star}_{q2}$.

Stage III

In this stage, the desired current injections are translated into actual control values for the FACTS devices. As before, we develop this approach for the UPFC only, noting that similar approaches can be developed for the SSSC and STATCOM. To accomplish this, a predictive control based on [13] is used. The basic methodology of predictive control is to design an asymptotically stable controller such that in an affine nonlinear system, the output $y(t)$ tracks a prescribed reference value $w(t)$ in terms of a given performance:

$$\dot{x}(t) = f(x(t)) + g(x(t))\,u(t) \tag{26}$$

$$y_i(t) = h_i(x(t)) \quad i = 1, \ldots, m \tag{27}$$

where m is the number of outputs equal to the number of inputs in $u(t)$. The receding horizon performance index is given by

$$J = \frac{1}{2}\int_0^T \left(\hat{y}(t+\tau) - \hat{w}(t+\tau)\right)^T \left(\hat{y}(t+\tau) - \hat{w}(t+\tau)\right) d\tau \tag{28}$$

where T is the predictive period. The actual control input $u(t)$ is given by the initial value of the optimal control input $\hat{u}(t+\tau)$ for $0 \leq \tau \leq T$ and $u(t+\tau) = \hat{u}(t+\tau)$ when $\tau = 0$.

The optimal predictive control law is given by:

$$u(t) = -\left(L_g l_f^{\rho-1} h(x)\right)^{-1}\left(KM_\rho + L_f^\rho h(x) - w^{[\rho]}(t)\right) \tag{29}$$

where ρ is the relative degree for the system outputs (assuming that all outputs have the same relative degree) and L is the Lie derivative defined by:

$$L_\mu \nu = \frac{\partial \nu}{\partial x}\mu \tag{30}$$

The matrix M_ρ is given by

$$M_\rho = \begin{bmatrix} h(x) - w(t) \\ L_f^1 h(x) - w^{[1]}(t) \\ \vdots \\ L_f^{\rho-1} h(x) - w^{[\rho-1]}(t) \end{bmatrix} \tag{31}$$

The matrix K is the first m rows of the matrix $\Psi_{rr}^{-1}\Psi_{\rho r}^{T}$ where

$$\Psi_{rr} = \begin{bmatrix} \psi_{(\rho+1,\rho+1)} & \cdots & \psi_{(\rho+1,\rho+r+1)} \\ \cdots & \cdots & \cdots \\ \psi_{(\rho+r+1,\rho+1)} & \cdots & \psi_{(\rho+r+1,\rho+r+1)} \end{bmatrix} \tag{32}$$

$$\Psi_{\rho r} = \begin{bmatrix} \psi_{(1,\rho+1)} & \cdots & \psi_{(1,\rho+r+1)} \\ \cdots & \cdots & \cdots \\ \psi_{(\rho,\rho+1)} & \cdots & \psi_{(\rho,\rho+r+1)} \end{bmatrix} \tag{33}$$

where

$$\psi_{i,j} = \frac{\overline{T}^{i+j-1}}{(i-1)!(j-1)!(i+j-1)!}, \quad i,j = 1,\ldots,\rho+r+1 \tag{34}$$

and

$$\overline{T} = diag\{T,\ \ldots,\ T\} \in R^{m\times m}$$

Returning to equations (1)-(5), the relative degree for all of the outputs is $\rho = 1$ and assuming the control order to be $r = 0$, then the control law for the UPFC becomes

$$u_1 = \frac{-3L_1}{\omega_s V_{dc} T}\left(i_{d1} - i_{d1}^{\star}\right) + \frac{R_1}{V_{dc}} i_{d1} - \frac{L_1}{V_{dc}} i_{q1} + \frac{V_1\cos\theta_1}{V_{dc}} + \frac{L_1}{\omega_s V_{dc}}\frac{d}{dt} i_{d1}^{\star} \tag{35}$$

$$u_2 = \frac{-3L_1}{\omega_s V_{dc} T}\left(i_{q1} - i_{q1}^{\star}\right) + \frac{R_1}{V_{dc}} i_{q1} + \frac{L_1}{V_{dc}} i_{d1} + \frac{V_1\sin\theta_1}{V_{dc}} + \frac{L_1}{\omega_s V_{dc}}\frac{d}{dt} i_{q1}^{\star} \tag{36}$$

$$u_3 = \frac{-3L_2}{\omega_s V_{dc} T}\left(i_{d2} - i_{d2}^{\star}\right) + \frac{R_2}{V_{dc}} i_{d2} - \frac{L_2}{V_{dc}} i_{q2} + \frac{V_2\cos\theta_2}{V_{dc}} - \frac{V_1\cos\theta_1}{V_{dc}} + \frac{L_2}{\omega_s V_{dc}}\frac{d}{dt} i_{d2}^{\star} \tag{37}$$

$$u_4 = \frac{-3L_2}{\omega_s V_{dc} T}\left(i_{q2} - i_{q2}^{\star}\right) + \frac{R_2}{V_{dc}} i_{q2} + \frac{L_2}{V_{dc}} i_{d2} + \frac{V_2\sin\theta_2}{V_{dc}} - \frac{V_1\sin\theta_1}{V_{dc}} + \frac{L_2}{\omega_s V_{dc}}\frac{d}{dt} i_{q2}^{\star} \tag{38}$$

These inputs are then translated into the control inputs for the UPFC:

$$k_1 = \sqrt{u_1^2 + u_2^2} \tag{39}$$

$$\alpha_1 = \tan^{-1}\frac{u_2}{u_1} \tag{40}$$

$$k_2 = \sqrt{u_3^2 + u_4^2} \tag{41}$$

$$\alpha_2 = \tan^{-1}\frac{u_4}{u_3} \tag{42}$$

The three stage control process and outcomes of each stage are summarized in Figure 3.

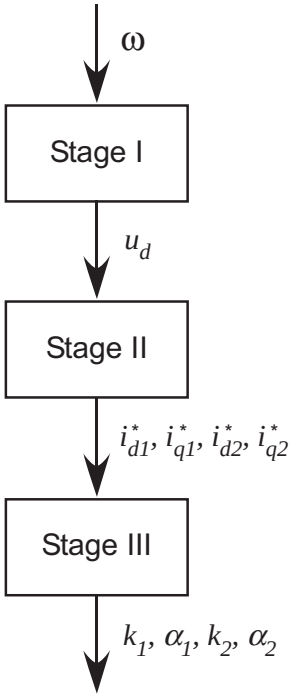

Fig. 3. The three stage control process

V. SELECTIVE FEEDBACK MEASUREMENTS BASED ON DOMINANT MACHINES

The control method discussed in the previous section requires global feedback data, such as generator rotor speeds and angles, to be implemented. Although with recent advances in Phasor Measurement Units it may be possible to provide synchronized global measurements, it is still not feasible to assume that all generator rotor speeds are simultaneously available. Therefore, it is reasonable to assume that a subset of the measurements are available for feedback and the remainder of the states must be estimated based on the available measurements. The most probable machines to obtain measurements from are those machines which are dominant within coherent groups. There are numerous methods for calculating coherent groups in the literature [14]-[17]. In [17], the coherency identification method is based on modal analysis and Gaussian elimination with full pivoting on the selected eigenvectors of the system to find the reference generators and their group members. The selected eigenvectors are chosen based on the lowest oscillatory modes of the system. Once the dominant machines are

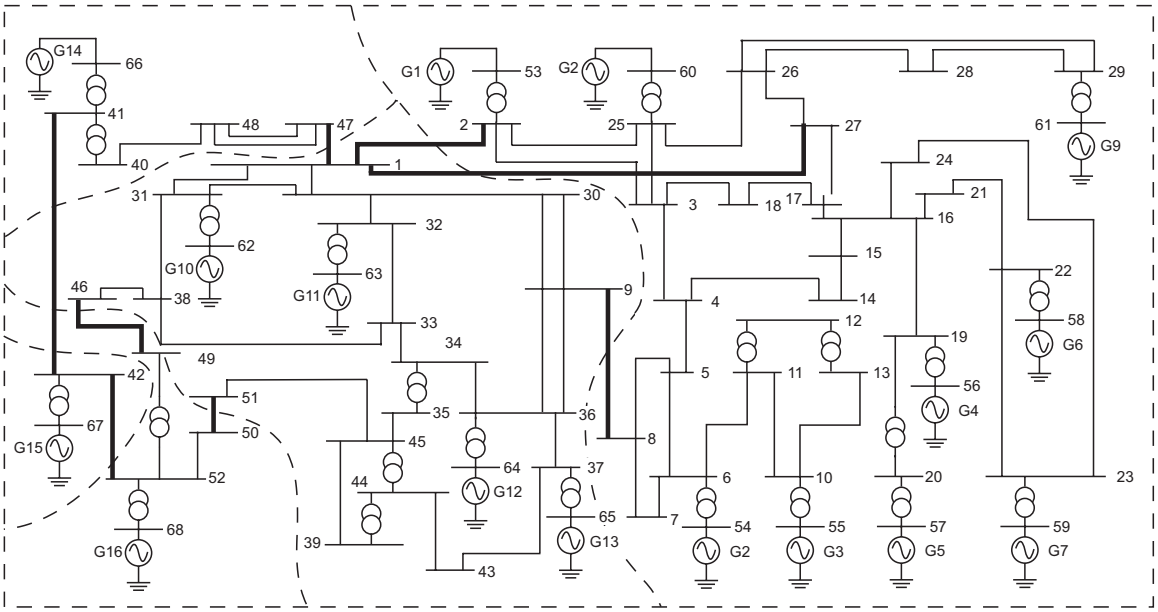

Fig. 4. 68 bus, 16 generator test system

found, a reduced order system is computed which captures the "slow" dynamics of the original system. In this process, the remaining unmeasured states of the system can be estimated based on the states which are measured via singular perturbation [18]. Let the dominant machines be ordered from 1 to Q and the rest of the machines be numbered from $Q+1$ to N, then the changes in the non-dominant machines can be approximated using a zero-th order model by:

$$\begin{bmatrix} \chi_{Q+1,Q+1} & \cdots & \chi_{Q+1,N} \\ \vdots & \ddots & \vdots \\ \chi_{N,Q+1} & \cdots & \chi_{N,N} \end{bmatrix} \begin{bmatrix} \Delta\delta_{Q+1} \\ \vdots \\ \Delta\delta_N \end{bmatrix} = \begin{bmatrix} \sum_{k=1}^{Q} \chi_{Q+1,k}\Delta\delta_k - \sum_{k=N+1}^{N+n} \chi_{Q+1,k}\Delta\delta_k \\ \vdots \\ \sum_{k=1}^{Q} \chi_{N,k}\Delta\delta_k - \sum_{k=N+1}^{N+n} \chi_{N,k}\Delta\delta_k \end{bmatrix} \tag{43}$$

where

$$\chi_{i,j} = \frac{\mu_{ij}}{\mu_{ii}} \quad i = 1, \ldots, N \text{ and } j = 1, \ldots, N+n \tag{44}$$

and

$$\mu_{ij} \;=\; -E_i E_j Y_{ij} \sin\left(\delta_i - \delta_j - \phi_{ij}\right) \quad i \neq j \tag{45}$$

$$\mu_{ii} \quad = \quad -\sum_{k\neq i}^{N+n} E_i E_k Y_{ik} \sin\left(\delta_i - \delta_k - \phi_{ik}\right) \quad i = j \tag{46}$$

Note than when only the dominant machines are selected for the control action, only the rows corresponding to the dominant machines will be used in equation (25) thereby reducing the order of the system. This is advantageous since the pseudo-inverse required to solve the set of equations is more nearly square providing better convergence.

VI. EXAMPLE AND RESULTS

Although the control has been developed using the classical generator model, the control approach will be validated using the full 10th order model which includes an exciter/AVR, turbine, and governor dynamics. The model is given in the Appendix. The proposed control is validated on the 68 bus, 16 generator New England/New York test system shown in Figure 4. The coherent groupings corresponding to the five slowest modes are indicated by the dashed lines in Fig. 4. The network data and the grouping procedure are given in [19]. The transmission tie lines are shown with bold lines. The reference generators for the five areas are G5, G13, G14, G15, and G16.

Choosing the appropriate number of FACTS devices in the network is based on the number of coherent areas. As a rule of thumb, the best number is to match the number of current injections with the number of modes. For example, five current injections can be used to control the inter-area oscillations between five areas. In the example, we have used only four current injections: one UPFC (two injections) and two STATCOMS (one injection each), to show that good results can be obtained even with few controllers if necessary.

The optimal placement of FACTS devices in a power system for oscillation damping is still an open research question. Very few authors have addressed the placement of FACTS devices for stability improvement. Most placement algorithms consider only static line loadability or placement for congestion reduction. However, one recent work addresses the use of modal controllability indices specifically for FACTS placement for oscillation damping [20]. In this paper, the UPFC is placed on line 42-41 with the shunt converter on bus 42 and the STATCOMS have been placed on buses 1 and 2. The UPFC placement was chosen to be a tie line and the STATCOMS are on centrally located buses in adjacent

coherent areas.

The parameters of the FACTS devices are given in Table I. The per unit approach is the same as in [21] on a 100 MW, 100 kV base.

TABLE I
FACTS PARAMETERS

	R_1	L_1	R_2	L_2	R_p	C
UPFC	0.01	0.15	0.001	0.015	25	1400
STATCOMs	0.01	0.10	n/a	n/a	25	1200

In the simulations, a solid three-phase fault is applied to bus 33 at 0.2 seconds and cleared at 0.3 seconds. The dynamic responses to this fault is shown in the following figures.

Case I: proposed control, all measurements available

Case II: proposed control, only dominant machine measurements available

Case III: linear control (taken from [22])

Note that in Case II, the estimation approach discussed in Section V is used to obtain approximations to the unavailable states.

Figure 5 shows a subset of the generator speeds with no FACTS devices in the system compared to Case I. Not all responses are shown for the sake of brevity. The selected generators are taken from four of the five coherent areas (generator 14 is by itself in an area and is not shown). Note that the generators go unstable as a result of the fault, but the proposed control is able to stablize the system and rapidly mitigate the oscillations.

Figure 6 shows the results of the proposed control method for Cases I (bold) and II (thin) compared against a linear control (dashed). The scale is enlarged from Figure 5 to show the detail in each case. Although it appears as if the linear case is going unstable, it actually does remain stable. The oscillations are damped over the longer simulation time. Note that in all cases, the proposed nonlinear control produces better damping than does the linear case. Recall that in Case I, all of the generator speeds are assumed to be measurable and usable for feedback, thus it is not surprising that Case I provides

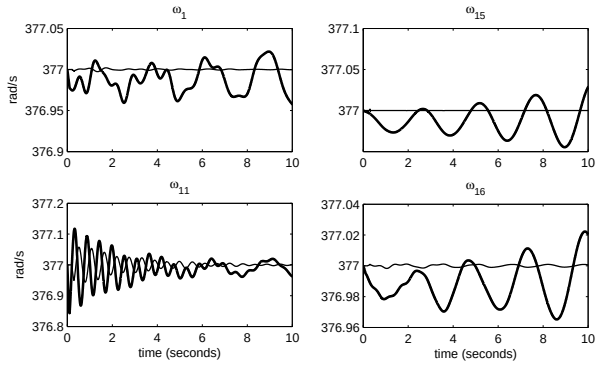

Fig. 5. Generator speeds for no FACTS devices (bold) and Case I (thin)

excellent oscillation mitigation. The important thing to note here is that the Case II results are *comparable* to the Case I results even though only five of the sixteen generators were assumed to be measurable. This indicates that not only does the proposed control provide excellent damping, the proposed estimation method also works in concert with the control very effectively.

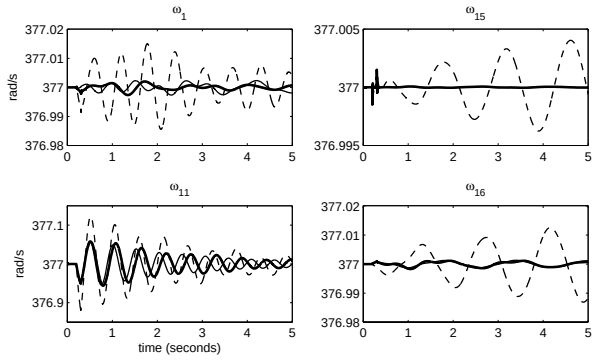

Fig. 6. Generator speeds for Case I (bold), Case II (thin), and Case III (dashed)

Figure 7 shows the active power injections of the UPFC. The series injection is shown in the top figure and the shunt injection is shown in the bottom figure. In this figure, Case II (bold) is compared to Case III (thin). These series active power injection for the proposed control is very modest; therefore the rating of the series transformer and converter do not need to be overly large. The shunt converter, however, does inject considerable active power into the system during the fault. Similar behavior is displayed by the STATCOMs as shown in Figure 8. Figure 9 shows the dc link capacitor voltages.

The UPFC and one of the STATCOMs experience a drop of approximately 5% whereas the second STATCOM experiences a slight increase in voltage. This is reasonable, since to damp oscillations, it may be necessary to inject active power in some areas and absorb active power in other areas.

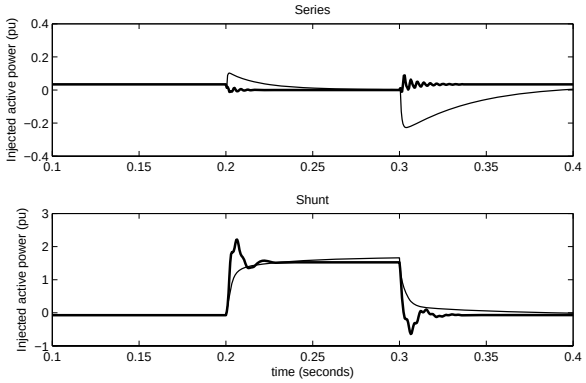

Fig. 7. UPFC injected active power: Series (top) and Shunt (bottom); Case II (bold) and Case III (thin)

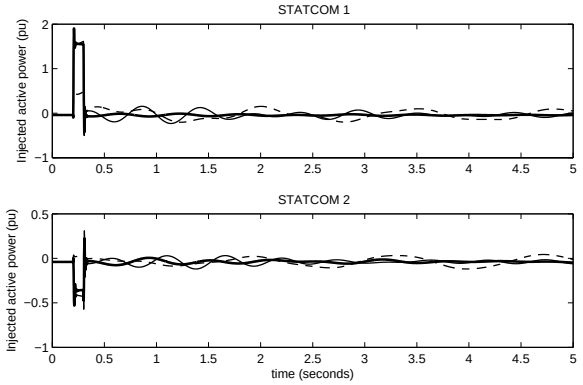

Fig. 8. STATCOM active power injection: Case I (bold), Case II (thin),Case II (dashed)

VII. CONCLUSIONS

A three stage nonlinear control scheme has been proposed for damping inter-area oscillations using multiple FACTS devices. Any FACTS device which is capable of controlling its interface bus(es) angle with the power network can be considered for this type of control. The method uses the generators' speeds as the feedback data for

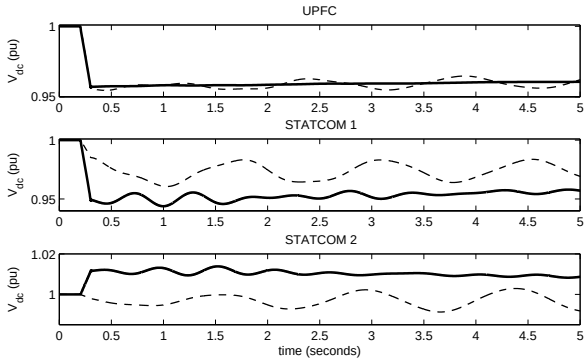

Fig. 9. FACTS Vdc Case II (bold) and Case III (dashed)

the control. Using measurements from the dominant generators and estimating the rest of the states based on equivalent reduced systems was shown to considerably reduce the number of needed global measurements for control. Based on the simulation results, the proposed method shows promising results for wide-area control of power systems. However, there are several issues which need to be considered. There is a considerable computational burden for the controller which requires fast processors for real-time performance. However, proper grouping and using the dominant machines could lower the computation time. Future work will also consider the effect of time delays and communication noise in the measured states on the control effectiveness. Sensitivity of the proposed method to system uncertainties and topology changes should also be studied.

APPENDIX

Two–Axis Generator Model

$$
\begin{aligned}
\dot{\delta}_i &= \omega_i - \omega_s \\
M_i\dot{\omega}_i &= T_{M_i} + \frac{V_i}{x'_{d_i}}\left(E'_{d_i}\cos\left(\theta_i-\delta_i\right) + E'_{q_i}\sin\left(\theta_i-\delta_i\right)\right) \\
T'_{d0_i}\dot{E}'_{q_i} &= -\frac{x_{d_i}}{x'_{d_i}}E'_{q_i} + \frac{\left(x_{d_i}-x'_{d_i}\right)}{x'_{d_i}}V_i\cos\left(\theta_i-\delta_i\right) + E_{fd_i} \\
T'_{q0_i}\dot{E}'_{d_i} &= -\frac{x_{q_i}}{x'_{d_i}}E'_{d_i} - \frac{\left(x_{q_i}-x'_{d_i}\right)}{x'_{d_i}}V_i\sin\left(\theta_i-\delta_i\right)
\end{aligned}
$$

Assumption: $x'_{q_i} = x'_{d_i}$ and $R_s = 0$

IEEE Type I Exciter/AVR Model

$$\begin{aligned} T_{E_i}\dot{E}_{fd_i} &= -K_{E_i}E_{fd_i} - S_{E_i}\left(E_{fd_i}\right)E_{fd_i} + V_{R_i} \\ T_{A_i}\dot{V}_{R_i} &= -V_{R_i} + K_{A_i}R_{F_i} - \frac{K_{A_i}K_{F_i}}{T_{F_i}}E_{fd_i} \\ &\quad + K_{A_i}\left(V_{ref_i} - V_i\right) \quad V_{R_i}^{min} \le V_{R_i} \le V_{R_i}^{max} \\ T_{F_i}\dot{R}_{F_i} &= -R_{F_i} + \frac{K_{F_i}}{T_{F_i}}E_{fd_i} \end{aligned}$$

Turbine Model

$$\begin{aligned} T_{RH_i}\dot{T}_{M_i} &= -T_{M_i} + \left(1 - \frac{K_{HP_i}T_{RH_i}}{T_{CH_i}}\right)P_{CH_i} \\ &\quad + \frac{K_{HP_i}T_{RH_i}}{T_{CH_i}}P_{SV_i} \\ T_{CH_i}\dot{P}_{CH_i} &= -P_{CH_i} + P_{SV_i} \end{aligned}$$

Speed Governor Model

$$\begin{aligned} T_{SV_i}\dot{P}_{SV_i} &= -P_{SV_i} + P_{C_i} - \frac{1}{R_i}\frac{\omega_i}{\omega_s} \\ &\quad 0 \le P_{SV_i} \le P_{SV_i}^{max} \end{aligned}$$

Power Balance Equations

Generator Buses

$$\begin{aligned} 0 &= \frac{V_i}{x'_{d_i}}\left(Eq'_i\sin\left(\delta_i - \theta_i\right) - Ed'_i\cos\left(\delta_i - \theta_i\right)\right) \\ &\quad -V_i\sum_{j=1}^{n}V_jY_{ij}\cos(\theta_i - \theta_j - \phi_{ij}) \\ 0 &= \frac{V_i}{x'_{d_i}}\left(Eq'_i\cos\left(\delta_i - \theta_i\right) + Ed'_i\sin\left(\delta_i - \theta_i\right) - V_i\right) \\ &\quad -V_i\sum_{j=1}^{n}V_jY_{ij}\sin(\theta_i - \theta_j - \phi_{ij}) \end{aligned}$$

Load Buses

$$\begin{aligned} 0 &= P_{L_i} - V_i\sum_{j=1}^{n}V_jY_{ij}\cos(\theta_i - \theta_j - \phi_{ij}) \\ 0 &= Q_{L_i} - V_i\sum_{j=1}^{n}V_jY_{ij}\sin(\theta_i - \theta_j - \phi_{ij}) \end{aligned}$$

REFERENCES

[1] HaiFeng Wang, “A Unified Model for the Analysis of FACTS Devices in Damping Power System Oscillations—Part III: Unified Power Flow Controller,” *IEEE Trans. Power Delivery*, vol. 15, no. 3, pp. 978-983, July 2000.

[2] B. C. Pal, “Robust damping of interarea oscillations with unified power flow controller,” *IEE Proc.-Gener. Transm. Distrib.*, vol. 149, no. 6. November 2002.

[3] B. Chaudhuri, B. C. Pal, A. Zolotas, I. Jaimoukha, and T. Green, “Mixed-sensitivity approach to $H\infty$ control of power system oscillations employing multiple FACTS devices,” *IEEE Trans. on Power Systems*, vol. 18, no. 3, pp. 1149-1156, May 2004.

[4] M. M. Farsangi, Y. H. Song, and K. Y. Lee, “Choice of FACTS device control inputs for damping interarea oscillations,” *IEEE Trans. on Power Systems*, vol. 19, no. 2, May 2004.

[5] N. Tambey and M.L. Kothari, “Damping of power system oscillations with unified power flow controller (UPFC),” *IEE Proceedings- Generation, Transmission and Distribution*, vol. 150, pp. 129-140, March 2003.

[6] Mehrdad Ghandhari, G. Andersson and Ian A. Hiskens, “Control Lyapunov Functions for Controllable Series Devices,” *IEEE Trans. Power Systems*, vol. 16, no. 4, pp. 689-694, Nov. 2001.

[7] S. Robak, M. Januszewski, D.D. Rasolomampionona, “Power system stability enhancement using PSS and Lyapunov-based controllers: A comparative study,” *IEEE 2003 Power Tech Conference Proceedings*, Bologna, vol. 3, pp. 6, 2003.

[8] Chia-Chi Chu and Hung-Chi Tsai, “Application of Lyapunov-based adaptive neural network upfc damping controllers for transient stability enhancement,” *Proceedings of the 2008 IEEE PES General Meeting*, July 2008.

[9] A. Bidadfar, M. Abedi, M. Karari, and Chia-Chi Chu, “Power swings damping improvement by control of UPFC and SMES based on direct Lyapunov method application,” *Proceedings of the 2008 IEEE PES General Meeting*, July 2008.

[10] M. Januszewski, J. Machowski and J.W. Bialek, “Application of the direct Lyapunov method to improve damping of power swings by control of UPFC,” *IEE Proceedings - Generation, Transmission and Distribution*, vol. 151, pp. 252-260, March 2004.

[11] Zhian Zhong, Chunchun Xu, B. J. Billian, Li Zhang, S. J. Tsai, R. W. Conners, V. A. Centeno, A. G. Phadke, and Yilu Liu, “Power system frequency monitoring network (FNET) implementation,” *IEEE Transactions on Power Systems*, November 2005, vol. 20, no. 4, pp. 1914-1921.

[12] L. Dong, M. L. Crow, Z. Yang, S. Atcitty, “A Reconfigurable FACTS System for University Laboratories,” *IEEE Trans. on Power Systems*, vol. 19, no. 1, Feb. 2004.

[13] W-H. Chen, D. J. Balance, and P.J. Gawthrop, “Optimal Control of Nonlinear Systems: A Predictive Control Approach,” *Automatica*, vol. 39, pp. 633-641, 2003.

[14] J.H. Chow, R. Galarza, P. Accari, W.W. Price, “Inertial and slow coherency aggregation algorithms for power system dynamic model reduction,” *IEEE Transactions on Power Systems*, May 1995, vol. 10, no. 2, pp. 680-685.

[15] S. Geeves, “A Modal-Coherency Technique for Deriving Dynamic Equivalents,” *IEEE Transactions on Power Systems*, Feb. 1998, vol. 3, no. 1, pp. 44-51.

[16] M. Larbi Ourari, Louis-A. Dessaint, Van-Que Do, “Dynamic Equivalent Modeling of Large Power Systems Using Structure Preservation Technique,” *IEEE Transactions on Power Systems*, Aug. 2006, vol. 21, no. 3, pp. 1284-1295.

[17] J. H. Chow, Ed., *Time-Scale Modeling of Dynamic Networks with Applications to Power Systems*, Springer-Verlag, New York, 1982.

[18] P. Sauer and M. A. Pai, *Power System Dynamics and Stability*, Prentice-Hall, 1998.

[19] G. Rogers, *Power System Oscillations*, Kluwer Academic Publishers (KAP), 2000.

[20] B. K. Kumar, S. Singh, and S. Srivastava, “Placement of FACTS controllers using modal controllability indices to damp out power system oscillations,” *IET Proceedings - Generation, Transmission, and Distribution*, vol. 1, no. 2, pp. 252-260, March 2007.

[21] C. Schauder and H. Mehta, “Vector analysis and control of advanced static VAR compensators,” *IEE Proceedings C*, vol. 140, no. 4, 1993.

[22] M. Zarghami and M. L. Crow, “Discussion of effective control of inter-area oscillations by UPFCs,” *39th North American Power Symposium*, New Mexico State University, October 2007.

9. Optimal Placement and Signal Selection for Wide-Area Controlled UPFCs for Damping Power System Oscillations

Mahyar Zarghami, *Student Member, IEEE*,
Mariesa L. Crow, *Senior Member, IEEE*

ABSTRACT: The paper discusses an optimal placement for UPFCs and an optimal method for the selection of global measurements in a wide-area controlled network for the purpose of damping power system oscillations. Both the placement and signal selection methods are optimized to damp inter-area oscillations. Optimal UPFC placement is identified by comparing different candidate placements based on the total damping they produce. Optimal selection of output measurements is based on the projection of the right eigenvectors on outputs. After the selection of the desired output measurements, observer gains are designed by LMI approaches. Test results from the IEEE 57 bus test system indicate good potential in terms of selecting UPFC placements and output signals.

Index Terms: UPFC, Power System Oscillation, UPFC Placement, Wide-Area Network, Output Signal Selection, LMI

I. INTRODUCTION

The UPFC, or Unified Power Flow Controller as shown in Fig. 1 is a series-shunt FACTS device which is capable of controlling the active and reactive power flow through the line in which it is deployed. This capability enhances the operation of the power system under steady-state conditions. However, because FACTS devices have very fast dynamics compared to generators, they can also play important roles to enhance the stability of power systems. This is usually accomplished through supplementary controls associated with these devices. Damping power system oscillations is one of the important applications of UPFCs [1]-[6]. Oscillations can occur in a system as a result of contingencies such as sudden load changes or power system faults. Traditionally power system stabilizers (PSS) have been used for damping local and inter-area oscillations, but FACTS controllers have significant potential as an alternative to PSS.

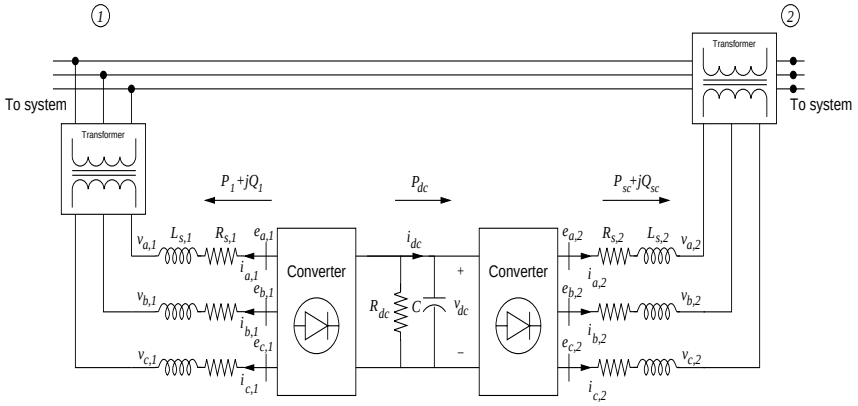

Fig. 1. Unified Power Flow Controller Diagram

Despite the fact that UPFCs can be very effective in damping power system oscillations, there is little research in the literature which addresses the role of UPFCs' placement in the dynamic performance of the network. There is considerable work published on the placement of FACTS devices to improve the steady-state performance of the network, such as improving the power transfer or minimizing system losses [7]-[10]. In [11], the placement of variable impedance apparatus to improve the stability of large scale power systems is explored, but this work does not specifically address UPFCs. Recent studies for the placement of FACTS controllers for stability improvement can be found in [12], where a fast algorithm based on controllability indices has been proposed. In this algorithm, it is assumed that UPFCs can be located simultaneously on all lines of the system. Based on this assumption, additional terms augment the original state space system and are used to determine the UPFC placements. However, previous work [13] has shown that the introduction of a UPFC into the power system changes its operating conditions from the base case, and furthermore that there can be multiple resulting operating conditions that can each affect the transient behavior of the system differently.

Because different UPFC placements can cause significant differences in the transient behavior of the system, placements must be chosen with care. Not only can a good placement improve the stability of the system; a poor placement can produce undesirable behavior. In this paper, a new performance index is introduced that provides a method to compare different candidate placements in terms of the damping they can provide in the system under the same control approach.

After the placement candidates are chosen, modal analysis based on observability indices is performed to identify the best global signals in the wide-area network for proper observer design which provides the estimated feedback data to the controller [15]. The observer design has been

performed using LMI approaches. The discussed algorithms have been validated using comprehensive nonlinear simulations using 10^{th} order generator models as given in the Appendix.

II. UPFC MODEL

The UPFC dynamic model is based on the power injection model shown in Fig. 2.

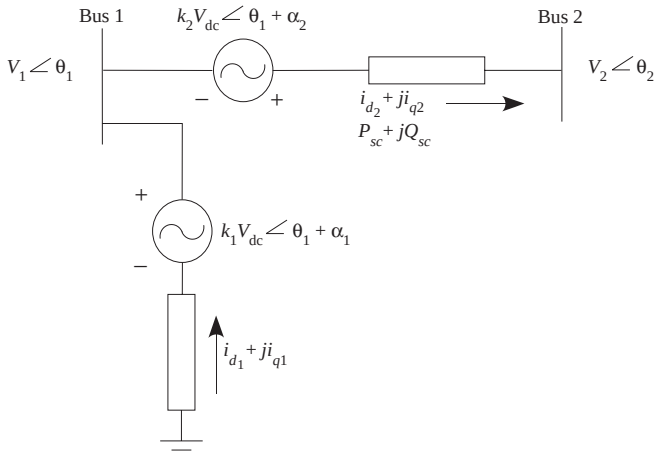

Fig. 2. Power Injection Model for UPFC

The dynamic equations for the UPFC power injection model are given as [16]:

$$\frac{1}{\omega_S}\dot{i}_{d_1} = -\frac{R_1}{L_1}i_{d_1} + i_{q_1} + \frac{k_1}{L_1}\cos(\theta_1+\alpha_1)v_{dc} - \frac{V_1\cos\theta_1}{L_1} \tag{1}$$

$$\frac{1}{\omega_S}\dot{i}_{q_1} = -\frac{R_1}{L_1}i_{q_1} - i_{d_1} + \frac{k_1}{L_1}\sin(\theta_1+\alpha_1)v_{dc} - \frac{V_1\sin\theta_1}{L_1} \tag{2}$$

$$\frac{1}{\omega_S}\dot{i}_{d_2} = -\frac{R_2}{L_2}i_{d_2} + i_{q_2} + \frac{k_2}{L_2}\cos(\theta_1+\alpha_2)v_{dc} - \frac{V_2\cos\theta_2}{L_2} + \frac{V_1\cos\theta_1}{L_2} \tag{3}$$

$$\frac{1}{\omega_S}\dot{i}_{q_2} = -\frac{R_2}{L_2}i_{q_2} - i_{d_2} + \frac{k_2}{L_2}\sin(\theta_1+\alpha_2)v_{dc} - \frac{V_2\sin\theta_2}{L_2} + \frac{V_1\sin\theta_1}{L_2} \tag{4}$$

$$\begin{aligned}\frac{C}{\omega_S}\dot{v}_{dc} = {} & -k_1\cos(\theta_1+\alpha_1)i_{d_1} - k_1\sin(\theta_1+\alpha_1)i_{q_1} \\ & -k_2\cos(\theta_1+\alpha_2)i_{d_2} - k_2\sin(\theta_1+\alpha_2)i_{q_2} - \frac{v_{dc}}{R_p}\end{aligned} \tag{5}$$

where:

$i_1 = i_{d1} + ji_{q1}$: Shunt injection current in UPFC (pu)

$i_2 = i_{d2} + ji_{q2}$: Series injection current in UPFC (pu)

R_1 : Equivalent shunt resistance in UPFC (pu)

L_1 : Equivalent shunt inductance in UPFC (pu)

R_2 : Equivalent series resistance in UPFC (pu)

L_2 : Equivalent series inductance in UPFC (pu)

v_{dc} : dc bus voltage in UPFC (pu)

C : Equivalent capacitance in UPFC (pu)

R_p : Equivalent dc resistance in UPFC (pu)

k_1, α_1 : Modulation amplitude and angle of the shunt part of UPFC

k_2, α_2 : Modulation amplitude and angle of the series part of UPFC

III. CONTROLLER DESIGN

Because the placement method depends on the controller design approach, the controller design used in this study is summarized in this section. For simplicity and moreover to remove the dynamics of the UPFC from the design (hence making the design independent of the UPFC model), the power system is reduced to the current injection points. The current injection points are the generator internal buses and the UPFC sending/receiving buses as shown in Fig. 3. The dashed lines in the figure indicate that in the reduced order network, nearly all of the current injection buses are connected to each other. The reduced admittance matrix for this simplified network is created by assuming constant admittances for the loads and absorbing them into the original admittance matrix of the power system. In addition, the generators are modeled with the classical model. This is only for model development; the controller design is validated through a full-order nonlinear simulation. The order of the reduced order system is $n_g + 2n_u$, where n_g is the number of generators and n_u is the number of UPFCs.

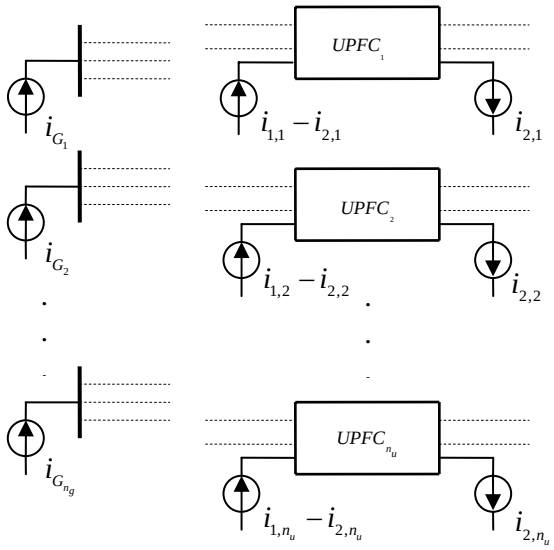

Fig. 3. Equivalent Power System from the Controller's View

The resulting state space model for the above system then becomes:

$$\dot{\delta}_j = \omega_j - \omega_s \tag{6}$$

$$\dot{\omega}_j = (1/M_j)(P_{M_j} - E_j \sum_{k=1}^{n_g+2n_u} E_k Y_{jk} \cos(\delta_j - \delta_k - \Phi_{jk})) \tag{7}$$

where:

ω_S : Synchronous speed (rad/s)

ω_j : Speed of machine j (rad/s) $\quad j = 1, ..., n_g$

M_j : Inertia at machine j (pu) $\quad j = 1, ..., n_g$

P_{M_j} : Mechanical input at machine j (pu) $\quad j = 1, ..., n_g$

δ_i : Angle at bus i (Radians) $\quad i = 1, ..., n_g + 2n_u$

E_i : Bus magnitude at bus i (pu) $\quad i = 1, ..., n_g + 2n_u$

$Y_{jk} \angle \Phi_{jk}$: Admittance matrix of the equivalent reduced system for $j, k = 1, ..., n_g + 2n_u$

Linearizing (6)-(7) results in a linear time invariant system of the form:

$$\dot{X} = AX + BR \tag{8}$$

where X is the vector of generator rotor speeds and angles and R is the vector of inputs, namely the angles of the UPFC sending/receiving buses. The state space system in (8) can be controlled using the LQR approach. This comprises the first stage of the control. The second stage is to find the modulation amplitudes and angles of the UPFCs [14].

IV. PLACEMENT FOR STABILITY IMPROVEMENT

Using the LQR approach in (8) will result in a control of the form:

$$R = -KX \tag{9}$$

Substituting (9) into (8) results in:

$$\dot{X} = (A - BK)X \tag{10}$$

Therefore for every placement, the resulting eigenvalues of *A-BK* estimate the modes of the system and their damping effect on the system. More specifically, the summation of the real parts of the eigenvalues provides an index that predicts the damping of the oscillatory modes of the system. If a specific range of oscillations (such as the inter-area modes) are of interest, then these calculations can be performed on the corresponding eigenvalues. Repeating this procedure for all placement candidates and sorting the resulting indices creates a table to show the best and worst damping candidates. Although eigenvalue calculations are repeated for every candidate placement, numerical techniques for calculating subsets of eigenvalues of large sparce matrices can be used to improve computational efficiency [17].

V. OBSERVER DESIGN

The implementation of the control method described in section III requires all rotor speeds and angles. However, in a power system spread over wide geographical areas, this requirement might not be feasible. However, with the introduction of Phasor Measurement Units (PMU) which can provide synchronized measurements from different parts of the network, the most

critical measurements for the control effectiveness can be determined based on the information they convey about the oscillatory modes of the system. This can be accomplished through the projection of the right eigenvectors of the system on the output matrix and sorting the best output measurements [15]. For a state space system of the following format:

$$\begin{aligned} \dot{X} &= AX + BR \\ Y &= CX + DR \end{aligned} \tag{11}$$

where C is the output matrix, the projection of the right eigenvector of Φ is found by:

$$C' = C\Phi \tag{12}$$

The output matrix C represents any measurement which may be available in the network. In this work, the line active power flows have been considered for measurement, since interarea oscillations have direct effect on them. Every row of the matrix C' contains the information of the corresponding line power flow from different oscillatory modes. Therefore, based on which modes are of interest, the magnitudes of the corresponding columns are summed to get an index for every power flow measurement.

Once the best output candidates are determined from (12), proper observer design can be performed for the estimation of the states. The observer structure has the following form:

$$\dot{\hat{X}} = A\hat{X} + BR + L(Y - \hat{Y}) \tag{13}$$

$$\hat{Y} = C\hat{X} + DR \tag{14}$$

where $\hat{X}$ is the vector of estimated generator rotor speeds and angles, and L is the observer gain and it can be designed using different approaches. In this work, an LMI approach has been used for designing L. The design procedure for determining L with one UPFC placement in a power system is described below. Defining the estimation error to be:

$$e = \hat{X} - X \tag{15}$$

The following state space system is created:

$$\begin{bmatrix} \dot{X} \\ \dot{e} \end{bmatrix} = A_e \begin{bmatrix} X \\ e \end{bmatrix} \tag{16}$$

where:

$$A_e = \begin{bmatrix} A - BK & -BK \\ 0 & A - LC \end{bmatrix} \tag{17}$$

By defining a positive definite matrix of the following format:

$$P = \begin{bmatrix} p_0 & 0 \\ 0 & p_1 \end{bmatrix} \tag{18}$$

then inequality $A_e^T P + P A_e < 0$ can be solved using an LMI approach if the initial feedback matrix K is set by an LQR solution. Note that if the resulting system is asymptotically stable, then the e error will be driven to zero and the "estimated" states will converge to real states as time increases. To ensure asymptotic stability, an additional inequality for the local observer is incorporated into the previous inequalities as:

$$\begin{aligned} &[p_1(A - BK) - p_1 L(C - DK)] + \ldots \\ &[p_1(A - BK) - p_1 L(C - DK)]^T < 0 \end{aligned} \tag{19}$$

VI. EXAMPLES AND RESULTS

The IEEE 57 bus test system [18] has been used to illustrate the results. This system has 7 machines that are modeled with a two-axis generator model, a type I exciter/AVR model and turbine and governor models as given in the Appendix. The full nonlinear system has been simulated using MATLAB with a solid fault occurring on bus 17 at 0.2 s and removed at 0.4 s. The UPFC parameters are given in Table I.

TABLE I
UPFC Parameters

	$R_1(pu)$	$L_1(pu)$	$R_2(pu)$	$L_2(pu)$	$R_p(pu)$	$C(pu)$
UPFC	0.01	0.15	0.001	0.015	100.00	350.0

(a) UPFC Placement

The method discussed in section IV is used to find the best placement of the UPFC. The test system has a total of 80 lines. By convection, a UPFC on line *i-j* is assumed to have the shunt converter on bus *i*. Therefore, for 80 lines, there a total of 160 possible placements for the UPFC. For every placement, the method discussed in [13] has been used to find the proper stable steady-state initial conditions of the system. Then the summation of the real parts of the eigenvalues of (10) has been used as the placement index (PI). The results of the sorted *PI*s are shown in Table II. Not all the cases have been shown because of lack of space. The shown cases have been chosen from the beginning, middle and the end of the original table.

TABLE II
UPFC Placements sorted by Placement Indices (PIs)

Case No.	From	To	PI
1	15	3	-95.0498
2	13	12	-92.7163
3	4	16	-86.3130
4	15	13	-85.2046
5	15	1	-84.9136
…			
30	10	12	-44.6083
31	10	51	-38.7585
32	55	9	-36.9371
33	55	54	-36.9285
34	29	7	-31.5083
…			
176	30	31	-1.7354
177	32	34	-1.7262
178	32	31	-1.7112
179	31	32	-1.3899
180	31	30	-1.3873

Placements 1 and 30 have been compared to show the validity of the method. Simulation results for the rotor speeds are shown in Fig. 4. In these simulations, it has been assumed that all of the state feedbacks are available. The bold, dashed and thin plots are related to Placements 1, 30 and the uncontrolled case, respectively. From the results, Placement 1 has an overall better performance.

In order to quantify the behavior of the placements, a machine speed profile index is defined as follows:

$$I_{\omega} = \frac{1}{n_g} \sum_{i=1}^{n_g} \left(\frac{1}{n_{sample}} \sum_{j=1}^{n_{sample}} \left| \omega_i - \omega_s \right| \right) \tag{20}$$

where:

I_{ω} : Speed profile index

n_g : Number of generators

n_{sample} : Number of samples in speed profile

ω_i : i'th generator speed

ω_s : Synchronous speed

The above index estimates the performance of each placement. Specifically, the lower the index is, the better the performance of the placement is expected to be. Table III shows the comparison of simulations in terms of the above defined index. As can be seen, placement 1 results in smaller values for the speed index. This means that smaller deviations of rotor speed are experienced in the simulations for this placement.

TABLE III
Comparison of the Placements Based on Speed Profile Index

	I_{ω}
Placement 1	0.0179
Placement 30	0.0417
Uncontrolled	1.2825

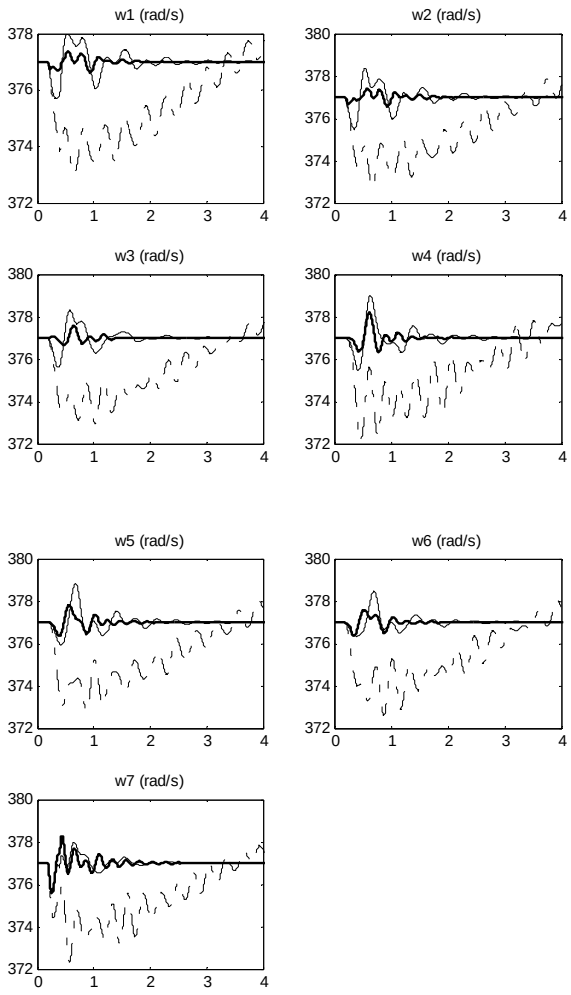

Fig. 4. Machine rotor speeds (Placement 1: bold, Placement 30: thin, uncontrolled: dashed)

(b) Observer Design

Once it is determined that Placement 1 is a good candidate in terms of its *PI*, the next step is to design an observer for the UPFC controller so that it can estimate the feedback data for the control action. This is because in most cases it is not possible for the controller to have direct access to all feedback states. Assuming that all line active power flows are possible candidates for measurement, the method discussed in section V has been applied to find the best candidates for measurement in terms of their information about the system modes. Table IV shows a selection of the best and worst candidates in terms of their observation index (*OI)*. The index *OI* is defined as the summation of the magnitudes of all columns in each row of C'.

TABLE IV

Measurement Candidates Sorted by Observation Indices (OIs)

Case No.	From	To	OI
1	1	2	2.5928
2	8	9	2.3483
…			
179	31	32	0.0107
180	32	33	0.0002

Once the best measurement candidates are found, the LMI approach can be used to design the proper observer. In this work, only the first two measurements (power flows in lines 1-2 and 8-9) have been used for designing the observer. To show how capable the observer is in estimating the states, the simulation results for generator rotor speeds are shown in Fig. 5. The bold plots show the results when all feedback data is available, while the thin plots show the results when the feedback data has been estimated, and the dashed plots show the uncontrolled case. As can be seen from the results, the controller is doing a very good job in terms of damping power system oscillations. It is also seen that as the time is increased, the observer error tends to decrease.

VII. CONCLUSIONS AND FURTHER WORK

In this paper, a method has been proposed for the placement of UPFCs for stability improvement. The method is based on a candidate comparison. The method selects the best placement candidates based on the total damping they could create on all or a range of the oscillation modes. Once the placement candidate is selected, the best output measurements are determined based on the observability indices. These measurements are used by LMI approaches to design a proper observer.

Further work is to combine placement methods to find the best candidates in terms of both static and dynamic criteria. Other work would be to study the lack of a critical output measurement on both control and estimation. $H\infty$ methods could be mixed with LMI to provide robust controllers. The sensitivity of the controllers to topology changes should also be studied.

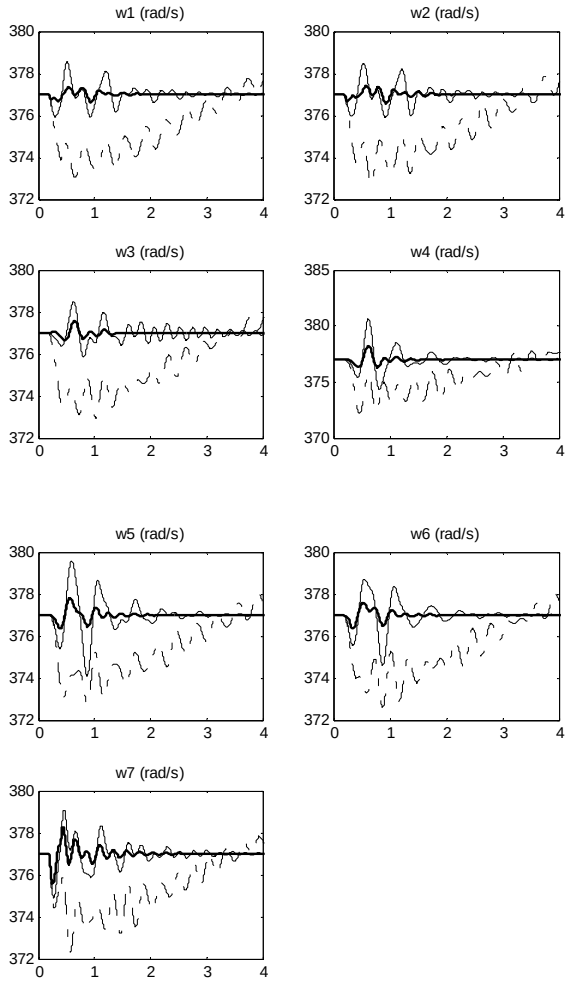

Fig. 5. Generator rotor speeds (Feedback available: bold, Feedback estimated: thin, Uncontrolled: dashed)

APPENDIX

n_g : Number of generators

for $j = 1, ..., n_g$

Two Axis Generator Model

$$\dot{\delta}_j = \omega_j - \omega_S$$

$$\frac{2H_j}{\omega_s}\dot{\omega}_j = T_{Mj} + \frac{V_j}{x'_{dj}}\left(E'_{dj}\cos(\theta_j - \delta_j) + E'_{qj}\sin(\theta_j - \delta_j)\right)$$

$$T'_{d0_j}\dot{E}'_{qj} = -\frac{x_{dj}}{x'_{dj}}E'_{qj} + \frac{x_{dj} - x'_{dj}}{x'_{dj}}V_j\cos(\theta_j - \delta_j) + E_{fdj}$$

$$T'_{q0_j}\dot{E}'_{dj} = -\frac{x_{qj}}{x'_{dj}}E'_{dj} - \frac{(x_{qj} - x'_{dj})}{x'_{dj}}V_j\sin(\theta_j - \delta_j)$$

Assumption:

$x'_{qj} = x'_{dj}$ and $R_s = 0$

IEEE Type I Exciter/AVR Model

$$T_{Ej}\dot{E}_{fdj} = -K_{Ej}E_{fdj} + V_{Rj}$$

$$T_{Aj}\dot{V}_{Rj} = -V_{Rj} + K_{Aj}R_{Fj} - \frac{K_{Aj}K_{Fj}}{T_{Fj}}E_{fdj} + K_{Aj}(V_{refj} - V_j)$$

$$V_{Rj}^{\min} \le V_{Rj} \le V_{Rj}^{\max}$$

$$T_{Fj}\dot{R}_{Fj} = -R_{Fj} + \frac{K_{Fj}}{T_{Fj}}E_{fdj}$$

Turbine

$$T_{RH_j}\dot{T}_{M_j} = -T_{M_j} + \left(1 - \frac{K_{HP_j}T_{RH_j}}{T_{CH_j}}\right)P_{CH_j} + \frac{K_{HP_j}T_{RH_j}}{T_{CH_j}}P_{SV_j}$$

$$T_{CH_j}\dot{P}_{CH_j} = -P_{CH_j} + P_{SV_j}$$

Speed Governor

$$T_{SV_j}\dot{P}_{SV_j} = -P_{SV_j} + P_{C_j} - \frac{\omega_j}{R_j\omega_s}$$

$$0 \le P_{SV_j} \le P_{SV_j}^{\max}$$

REFERENCES

[1] HaiFeng Wang, "A Unified Model for the Analysis of FACTS Devices in Damping Power System Oscillations---Part III: Unified Power Flow Controller," *IEEE Trans. Power Delivery*, vol. 15, no. 3, pp. 978-983, July 2000.

[2] Mehrdad Ghandhari, G. Andersson and Ian A. Hiskens, "Control Lyapunov Functions for Controllable Series Devices," *IEEE Trans. Power Systems*, vol. 16, no. 4, pp. 689-694, Nov. 2001.

[3] B.C. Pal, "Robust damping of interarea oscillations with unified power-flow controller," *IEE Proceedings- Generation, Transmission and Distribution*, vol. 149, pp. 733-738, Nov. 2002.

[4] S. Robak, M. Januszewski, D.D. Rasolomampionona, "Power system stability enhancement using PSS and Lyapunov-based controllers: A comparative study," *IEEE Power Tech Conference Proceedings* 2003 Bologna, vol. 3, pp. 6.

[5] N. Tambey and M.L. Kothari, "Damping of power system oscillations with unified power flow controller (UPFC)," *IEE Proceedings- Generation, Transmission and Distribution*, vol. 150, pp. 129-140, March 2003.

[6] M. Januszewski, J. Machowski and J.W. Bialek, "Application of the direct Lyapunov method to improve damping of power swings by control of UPFC," *IEE Proceedings- Generation, Transmission and Distribution*, vol. 151, pp. 252-260, March 2004.

[7] Preedavichit, P., and Srivastava, S.C., “Optrimal reactive power dispatch considering FACTS devices,” *Electr. Power Syst. Res.*, Vol. 46, pp. 251-257, 1998.

[8] Lu, Y., and Abur, A., "Improving system static security via optimal placement of thyristor controlled series capacitors (TCSC)," *IEEE Power Eng. Soc.*, Winter Meet., 2001, pp. 516-521.

[9] Gerbex, S., Cherkaoui, R., and Germond, A.J., "Optimal location of multi-type FACTS devices in a power system by means of genetic algorithm," *IEEE Trans. Power Syst.*, Vol. 16, pp. 537-544, 2001.

[10] Xiao, Y., Song, Y.H., Liu, C.C., and Sun, Y.Z., "Available transfer capability enhancement using FACTS devices," *IEEE Trans. Power Syst.*, Vol. 18, pp. 305-312, 2003.

[11] Okamoto, H., Kuriata, A., andSekine, Y., "A method for identification of effective locations of variable impedance apparatus on enhancement of steady state stability in large scale power systems," *IEEE Trans. Power Syst.*, Vol. 10, no. 3, pp. 1401-1407, 1995.

[12] B. Kalyan Kumar, S.N. Singh and S.C. Srivastava, "Placement of FACTS controllers using modal controllability indices to damp out power system oscillations," *IET Gener. Transm. Distrib.*, Vol. 1, no. 2, pp. 209-217, 2007.

[13] M. Zarghami, M.L. Crow, "The Existence of Multiple Equilibria in the UPFC Power Injection Model," *IEEE Transactions on Power Systems*, vol. 22, no. 4, pp. 2280-2282, Nov. 2007.

[14] M. Zarghami, M.L. Crow, "Discussion on effective control of inter-area oscillations by UPFCs," *39th North American Power Symposium*, pp. 623-629, Sep-Oct. 2007.

[15] A.M. A. Hamdan and A. M. Elabdalla, "Geometric measures of modal controllability and observability of power system models," *Elec. Power Syst. Res.*, vol. 15, pp. 147-155, 1988.

[16] L. Dong, M.L. Crow, Z. Yang, C. Shen, L. Zhang, S. Atcitty, "A Reconfigurable FACTS System for University Laboratories," *IEEE Transactions on Power Systems*, Vol. 19, no. 1, pp. 120-128, Feb. 2004.

[17] David S. Watkins, The Matrix Eigenvalue Problem: GR and Krylov Subspace Methods, Society for Industrial Mathematics, 2007.

[18] http://www.ee.washington.edu/research/pstca/pf118/pg_tca118bus.htm

10. Dynamic Placement and Signal Selection for UPFCs in Wide-Area Controlled Power Systems

Mahyar Zarghami, *Student Member, IEEE,* Mariesa L. Crow, *Senior Member, IEEE,* S. Jagannathan, *Senior Member*

ABSTRACT: This paper deals with the problem of damping inter-area oscillations in wide-area bulk power systems using unified power flow controllers. Dynamic placement and signal selection are two important issues when FACTS devices are deployed in the system. In the paper both problems have been investigated using a Most Dominant Branches table calculated based on modal analysis which shows the influence of active powers of the branches on inter-area modes of the system. First, dynamic placement has been explained in which the best placement candidates are selected based on their influence on inter-area modes. Next the paper deals with dynamic estimation of the states of the system based on selected global measurements. Estimation of the states is important in centralized control approaches since global feedback is not fully available. Simulations on the IEEE 118 bus test system show that the proposed approaches give valuable guidelines for dynamic placement and signal selection problems. Although the results of the discussed methods have been explored using UPFCs, applications can be extended to other series connected FACTS devices.

Index Terms: UPFC, Inter-Area Oscillation, UPFC Placement, Wide-Area Control, Signal Selection

I. INTRODUCTION

The UPFC, or Unified Power Flow Controller as shown in Fig. 1 is a series-shunt FACTS device which is capable of controlling the active and reactive power flow through the line in which it is deployed. This capability enhances the operation of the power system under steady-state conditions. However, because FACTS devices have very fast dynamics compared to generators, they can also play important roles to enhance the stability and dynamic performance of the power system. This is usually accomplished through supplementary controls associated with these devices. Damping power system oscillations is one of the important applications of

UPFCs [1]-[6]. Oscillations can occur in a system as a result of contingencies such as sudden load changes or power system faults. Traditionally power system stabilizers (PSS) have been used for damping local and inter-area oscillations, but FACTS controllers have significant potential as an alternative to PSS.

Despite the fact that UPFCs can be very effective in damping power system oscillations, there is little research in the literature which addresses the role of UPFCs' placement in the dynamic performance of the network. There is considerable work published on the placement of FACTS devices to improve the steady-state performance of the network, such as improving the power transfer or minimizing system losses [7]-[10]. In [11], the placement of variable impedance apparatus for improving the stability of large scale power systems is explored, but this work does not specifically address UPFCs. Recent studies for the placement of FACTS controllers for stability improvement can be found in [12], where a fast algorithm based on controllability indices has been proposed. In this algorithm, it is assumed that UPFCs can be located simultaneously on all lines of the system. Based on this assumption, additional terms augment the original state space system and are used to determine the UPFC placements. However, previous work [13] has shown that the introduction of each UPFC into the power system changes its operating conditions from the base case, and furthermore that there can be multiple resulting operating conditions that can each affect the transient behavior of the system differently. Because different UPFC placements can cause significant differences in the transient behavior of the system, they must be chosen with care. Not only can a good placement improve the stability of the system; a poor placement can produce undesirable behavior.

On the other hand, with the advances in Phasor Measurement Units, wide-area controllers for power systems are going to be feasible in the near future. These controllers, in contrast with decentralized controllers use the global feedback data for control implementation. However, the centralized controllers might not have direct access to all global feedbacks. This is where dynamic state estimation based on a selected set of global measurements becomes important.

In this paper, modal analysis has been used for both dynamic placement and signal selection problems. Generally speaking, dynamic behavior of a power system is dependent to numerous factors, such as the pre-fault operating status of the system, fault type, fault location and its value, etc. Because of this, a best placement candidate cannot be guaranteed for all fault scenarios. However, certain guidelines can be found for proper FACTS placements based on modal analysis on the current steady-state status of the system. As it will be shown, these guidelines can also be used for selecting the proper measurement candidates for estimation purposes in wide-area controlled systems where the feedbacks from all global states are not

available. In the sections to come, first we introduce a linear approach by modal analysis where a table of Most Dominant Branches (MDB) is calculated based on the influence of branches on inter-area modes. Then we explain the method by which we pick the best placement candidates as well as the best measurement candidates according to MDB. The discussed methods can be employed using any type of series connected FACTS device. Since UPFCs have been used in this project, a brief description of the control method used for damping oscillations using UPFCs based on previous work has been reviewed [14]. In the end simulation examples on IEEE 118 bus test system show the effectiveness of the proposed approach in determining the best placement and measurement candidates.

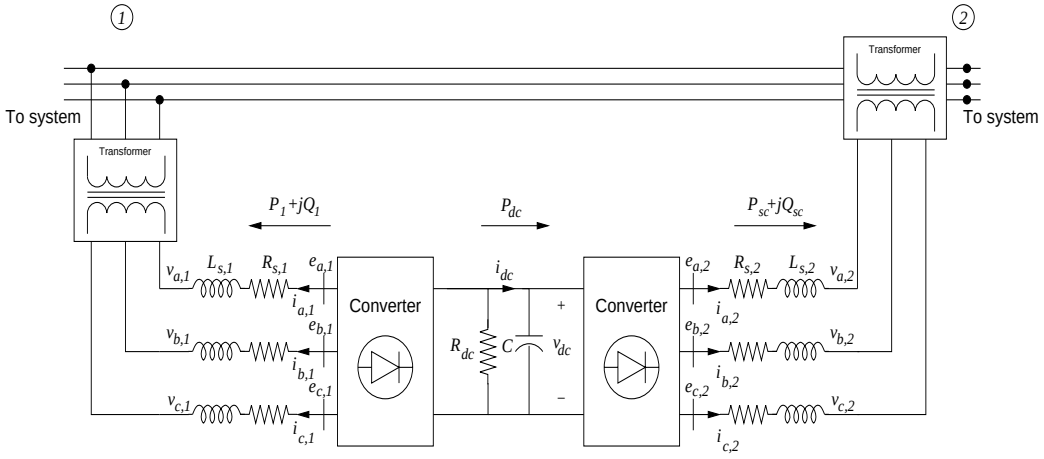

Fig. 1. Unified Power Flow Controller Diagram

II. DETERMINING THE TABLE OF MOST DOMINANT BRANCHES (MDB)

We can consider the dynamics of a power system consisting of the machines and the power network (transmission lines, power transformers, loads, etc.) to be of the following general nonlinear format:

$$\dot{X} = f(X,Y) \tag{1}$$

$$0 = g(X,Y) \tag{2}$$

In (1) and (2), $X \in R^{n\times 1}$ and $Y \in R^{m\times 1}$ represent the machine and network states (bus voltages and angles), respectively. Since the dynamics of the power network side is usually much faster than the dynamics of the machines, (2) has been approximated with algebraic equations. Note that in the differential-algebraic equation set of (1)-(2), FACTS dynamics has not been included. In other words, (1)-(2) show the situations of the system before placement of the

FACTS devices.

Linearization of (1)-(2) around its equilibrium yields in:

$$\dot{x} = \left.\frac{\partial f}{\partial X}\right|_Y x + \left.\frac{\partial f}{\partial Y}\right|_X y \tag{3}$$

$$0 = \left.\frac{\partial g}{\partial X}\right|_Y x + \left.\frac{\partial g}{\partial Y}\right|_X y \tag{4}$$

where in (3) and (4), x and y represent small changes of states X and Y around their equilibrium, respectively. Substituting from (4) into (3) one can find:

$$\dot{x} = Ax \tag{5}$$

where:

$$A = \left(\left.\frac{\partial f}{\partial X}\right|_Y\right) - \left(\left.\frac{\partial f}{\partial Y}\right|_X\right)\left(\left.\frac{\partial g}{\partial Y}\right|_X\right)^{-1}\left(\left.\frac{\partial g}{\partial X}\right|_Y\right) \tag{6}$$

$A \in R^{n\times n}$ represents the behavior of the system based on modal analysis. Finding the eigenvalues of A, one can find the oscillatory modes of the system and their frequencies.

On the other hand, since power system oscillations are occurred in a power system because of imbalances between the generation and consumption of the active power, changes of active power flows through the branches (lines and transformers) could best represent the oscillatory modes of the system. Writing active power flow equations for branches and following the linearization method discussed above we can find the following set of equations for active power flow changes:

$$p = Cx \tag{7}$$

where in (7) $p \in R^{b\times 1}$ is the vector of active power flow changes, b is the number of branches and $C \in R^{b\times n}$ is the output matrix.

In order to find the influence of active power flow changes on the oscillatory modes of the system, we find the projection of the right eigenvector of A on C as it is shown below [15]:

$$C' = |C\Phi| \tag{8}$$

where $\Phi \in R^{n\times n}$ represents the matrix of right eigenvectors. Every row of C' shows the impact of the corresponding branch power flow on different oscillatory modes. Therefore, based

on which range of mode(s) are of our interest, the elements of the corresponding columns can be summed to get an index for every power flow measurement on specific oscillatory mode(s). Usually, we are interested in damping inter-area modes. These modes can be determined by sorting the eigenvalues in terms of absolute values of their imaginary parts and finding the gap in the resulted frequencies. Modes with least values of frequencies are taken to be the inter-area modes. Once (8) is found, its rows are sorted based on their total influence on inter-area modes. The resulting table is called the Most Dominant Branches table, or simply MDB.

III. ALGORITHM FOR DYNAMIC FACTS PLACEMENT AND SIGNAL SELECTION

The following algorithm is proposed for finding the best placement candidates as well as the best power flow signals for state estimation:

1- Determine the number of UPFCs for placement.

2- Take n+1 to be the lowest modes of oscillation and determine the MDB table based on the previous section. Note that in (5), one mode would be the zero mode and it is assumed that at least the next n modes will be affected by n UPFCs.

3- For every row of MDB, also determine the individual effect of every branch on every mode.

4- Choose the best placement candidates among branches based on their total balanced influence on inter-area modes.

5- Choose the best measurement candidates among the rest of the table based on their total balanced influence on inter-area modes. The number of measurements must provide feasible solution to the observer design. Observers can be designed by numerous approaches. In this work, observers have been designed based on LMI approaches.

IV. CONTROLLER DESIGN

The controller design used in this study is summarized in this section based on [14]. For simplicity and moreover to remove the dynamics of the UPFC from the design (hence making the design independent of the UPFC model), the power system is reduced to the current injection points. The current injection points are the generator internal buses and the UPFC sending/receiving buses as shown in Fig. 2. The dashed lines in the figure indicate that in the reduced order network, nearly all of the current injection buses are connected to each other. The

reduced admittance matrix for this simplified network is created by assuming constant admittances for the loads and absorbing them into the original admittance matrix of the power system. In addition, the generators are modeled with the classical model. This is only for model development; the controller design is validated through full-order nonlinear simulations. The order of the reduced order system is $n_g + 2n_u$, where n_g is the number of generators and n_u is the number of UPFCs.

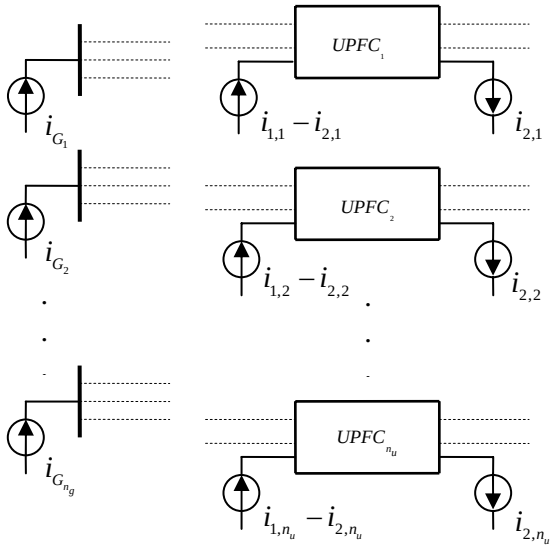

Fig. 2. Equivalent Power System from the Controller's View

The resulting state space model for the above system then becomes:

$$\dot{\delta}_j = \omega_j - \omega_s \tag{9}$$

$$\dot{\omega}_j = (1/M_j)(P_{M_j} - E_j \sum_{k=1}^{n_g+2n_u} E_k Y_{jk} \cos(\delta_j - \delta_k - \Phi_{jk})) \tag{10}$$

where:

ω_s : Synchronous speed (rad/s)

ω_j : Speed of machine j (rad/s) $\quad j = 1, ..., n_g$

M_j : Inertia at machine j (pu) $\quad j = 1, ..., n_g$

P_{M_j} : Mechanical input at machine j (pu) $\quad j = 1, ..., n_g$

δ_i : Angle at bus i (Radians) $\quad i = 1, ..., n_g + 2n_u$

E_i : Bus magnitude at bus i (pu) $\quad i = 1, ..., n_g + 2n_u$

$Y_{jk} \angle \Phi_{jk}$: Admittance matrix of the equivalent reduced system for $j, k = 1, ..., n_g + 2n_u$

Linearizing (9)-(10) results in a linear time invariant system of the form:

$$\dot{x} = Ax + Br \tag{11}$$

where x is the vector of generator rotor speeds and angles and r is the vector of inputs, namely the angles of the UPFC sending/receiving buses. The state space system in (11) can be controlled using the LQR approach where:

$$r = -Kx \tag{12}$$

This comprises the first stage of the control. The second stage is to find the modulation amplitudes and angles of the UPFCs by solving the nonlinear differential-algebraic equations resulting from the UPFC model and its interface with the power network [14].

Implementation of the control for (11) requires all rotor speeds and angles. However, in a power system spread over wide geographical areas, this requirement might not be feasible. With the introduction of Phasor Measurement Units (PMU) which can provide synchronized measurements from different parts of the network, the most critical measurements for control effectiveness can be determined based on the information they convey about the oscillatory modes of the system as explained in III. Once the best output candidates are determined, observer design can be performed for the estimation of the states. The observer structure has the following form:

$$\dot{\hat{x}} = A\hat{x} + Br + L(y - \hat{y}) \tag{13}$$

$$\hat{y} = C\hat{x} + Dr \tag{14}$$

where $\hat{x}$ is the vector of estimated generator rotor speeds and angles, and L is the observer gain and it can be designed using different approaches. In this work, an LMI approach has been used for designing L. Considering the estimation error to be:

$$e = \hat{x} - x \tag{15}$$

Matrix A_e is found such that:

$$[\dot{x}, \dot{e}]' = A_e [x, e]' \tag{16}$$

By defining a positive definite matrix of the following format:

$$P = diag(p_0, p_1, ..., p_{n_u}) \tag{17}$$

inequality $A_e^T P + P A_e < 0$ can be solved using an LMI approach if the initial feedback matrix *K* is set by an LQR solution. Note that if the resulting system is asymptotically stable, then the *e* error will be driven to zero and the "estimated" states will converge to real states as time increases. To ensure asymptotic stability, additional inequalities for the local observers are incorporated into the previous inequalities in terms of $p_1, ..., p_{n_u}$ matrices.

V. EXAMPLES AND RESULTS

The IEEE 118 bus test system [16] which is shown in Fig.3 has been used to illustrate the results. This system has 20 machines that are modeled with two-axis generator, type I exciter/AVR and turbine and governor models as given in the Appendix. The full nonlinear system has been simulated using MATLAB with a solid fault occurring on bus 43 at 0 s and removed at 0.2 s. Two UPFCs with similar parameters are to be placed in the system. The UPFC parameters are given in Table I. The state space model for UPFCs has been extracted from [17].

TABLE I

UPFC Parameters

$R_1(pu)$	$L_1(pu)$	$R_2(pu)$	$L_2(pu)$	$R_{dc}(pu)$	$C(pu)$
0.01	0.15	0.001	0.015	25.00	1400.0

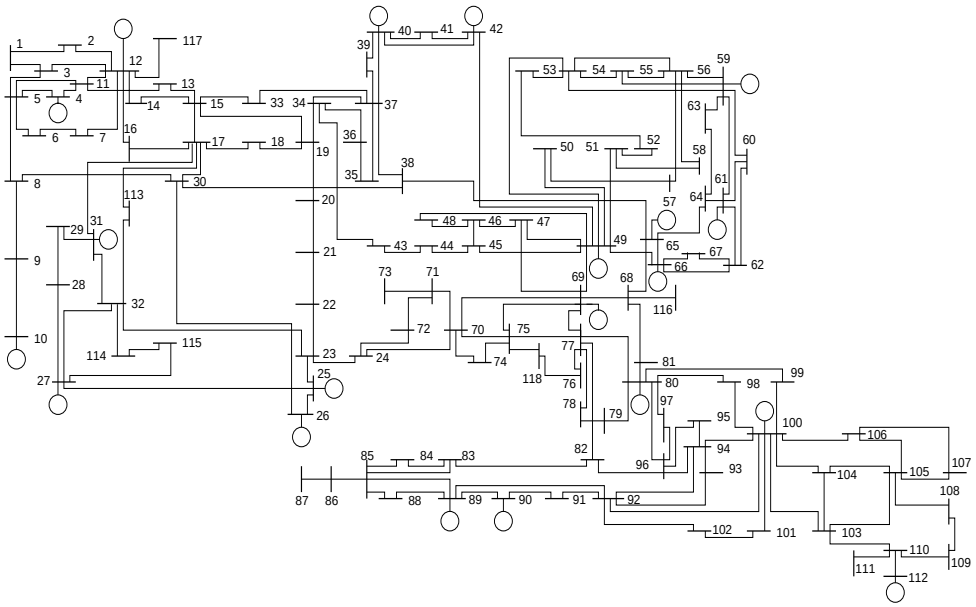

Fig. 3. IEEE 118 Bus Test System

(a) UPFC Placement

The method discussed in section III is used to find the best placement of the UPFCs. The MDB table has been created and its results for 10 upper most dominant branches are shown in Table II.

As it is seen in Table II, the influence of the branches on mode 0 is negligible. For placement, we pick the first UPFC to be located on the first dominant branch (from 68 to 65). As it is seen, the influence of this branch is more on Mode 2 with an approximate ratio of 3/2. Because of this, for the next UPFC placement, we look for a branch whose influence would be more on Mode 1. The most dominant branch which has this property is from 30 to 38 with an approximate ratio of 3/2. So this branch would be probably the best choice for placement of the second UPFC. These placements have been compared with several other placements to show the validity of our concept. One set of these placements is located on branches 5-3 and 64-63. The comparison between these two sets of placements is shown in Fig. 4 for some of the rotor speeds. In the control method, it has been assumed that all feedbacks are available. Because of lack of space, not all rotor speeds have been shown. However, the following Speed Profile Index has been defined in order to give a quantitative comparison between the placement sets:

$$I_{\omega} = \frac{1}{n_g} \sum_{i=1}^{n_g} \left(\frac{1}{n_{sample}} \sum_{j=1}^{n_{sample}} \left| \omega_i - \omega_s \right| \right) \tag{18}$$

where:

I_ω : Speed profile index

n_g : Number of generators

n_{sample} : Number of samples in speed profile

ω_i : i'th generator speed

ω_s : Synchronous speed

TABLE II

Most Dominant Branches and Their Influence on Inter-Area Modes

From	To	Mode 0 (%)	Mode 1 (%)	Mode 2 (%)	Total Weight (pu)
65	68	0.0002	39.0201	60.9797	1.1927
80	81	0.0002	43.0232	56.9766	1.0152
68	81	0.0002	43.0233	56.9764	1.0138
30	38	0.0003	60.6173	39.3824	0.8911
38	65	0.0006	69.5737	30.4258	0.7606
69	77	0.0002	43.2887	56.7112	0.4444
64	65	0.0006	9.2136	90.7858	0.4293
8	30	0.0007	70.9298	29.0696	0.4135
77	82	0.0003	42.2808	57.7189	0.4085
23	24	0.0001	74.5151	25.4848	0.4062

The above index estimates the performance of each placement set. Specifically, the lower the index is, the better the performance of the placement is expected to be. Table III shows the comparison of simulations in terms of the above defined index. As can be seen, the placement set (68-65) & (30-38) results in smaller values for the Speed Profile Index. This means that smaller deviations of rotor speeds are experienced in the simulations for this placement set.

TABLE III

Comparison of the Placements Based on Speed Profile Index

Placement	I_ω
(68-65) & (30-38)	0.0135
(5-3) & (64-63)	0.0247

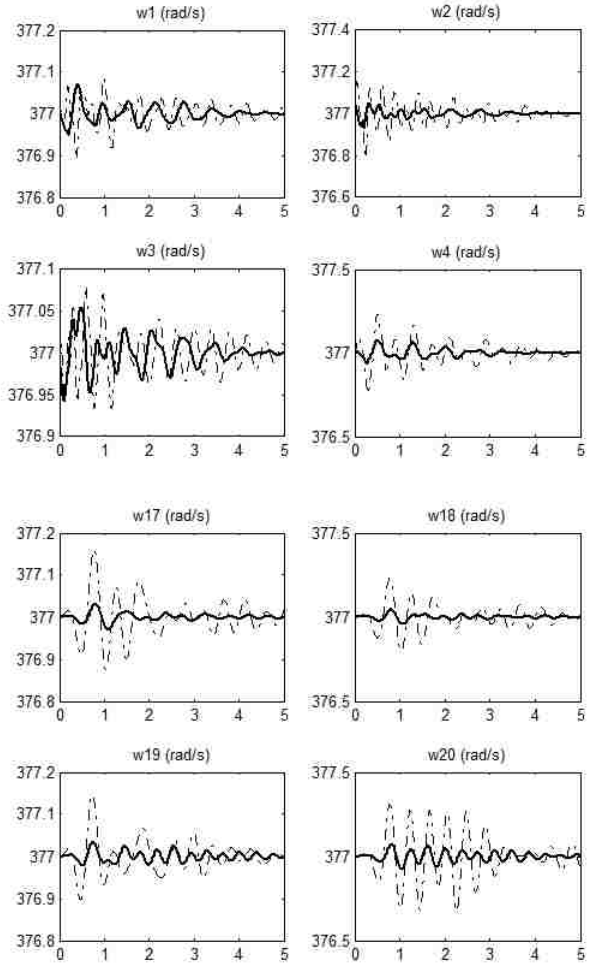

Fig. 4. Comparison of placements for rotor speeds (bold: 68-65 & 30-38, dashed: 5-3 & 64-63)

(b) Observer Design

Once it is determined that the set (68-65) & (30-38) is a good placement candidate, the next step would be to design observers for estimation of the feedback data for control action. The concept here is to use other unused dominant branches in Table II for output measurements. Since it would be desirable to have as few measurements as possible for the observer, LMI design is

repeated until feasible solution is obtained. The following 6 branches shown in Table IV are found to be the suitable output measurements. As it can be seen from Fig. 3, these outputs are a combination of local and global measurements.

TABLE IV

Output Measurements for Observer Design

From	To	Mode 0 (%)	Mode 1 (%)	Mode 2 (%)	Total Weight (pu)
80	81	0.0002	43.0232	56.9766	1.0152
38	65	0.0006	69.5737	30.4258	0.7606
69	77	0.0002	43.2887	56.7112	0.4444
64	65	0.0006	9.2136	90.7858	0.4293
8	30	0.0007	70.9298	29.0696	0.4135
77	82	0.0003	42.2808	57.7189	0.4085

Comparing Table II with Table IV, it is seen that the dominant branch 68-81 has not been selected as an output measurement. The reason is that branches 80-81 and 68-81 are in series as shown in Fig. 3 and having one of them for measurement would be enough for observer design. Dashed plots in Fig. 5 show rotor speed simulations for the case where feedbacks have been estimated. As compared to the bold plots in Fig. 5, it is seen that the observers are doing a good job in terms of estimation of the states. Fig. 6 compares the controlled case with feedback estimation with the uncontrolled case. As this figure shows, the controller has been successfully damping inter-area oscillations.

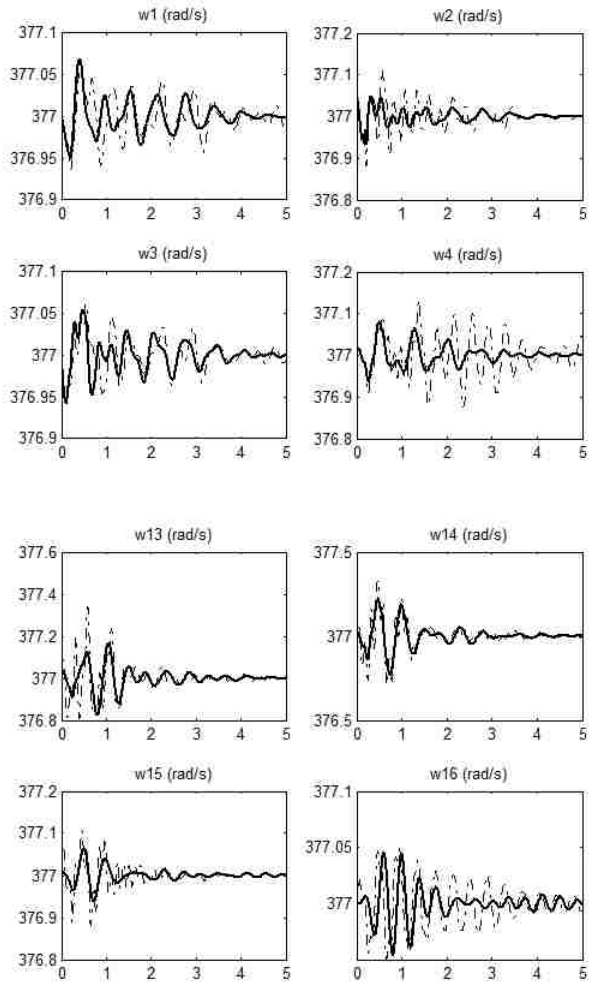

Fig. 5. Comparison of rotor speeds (bold: all feedbacks available, dashed: estimated feedbacks)

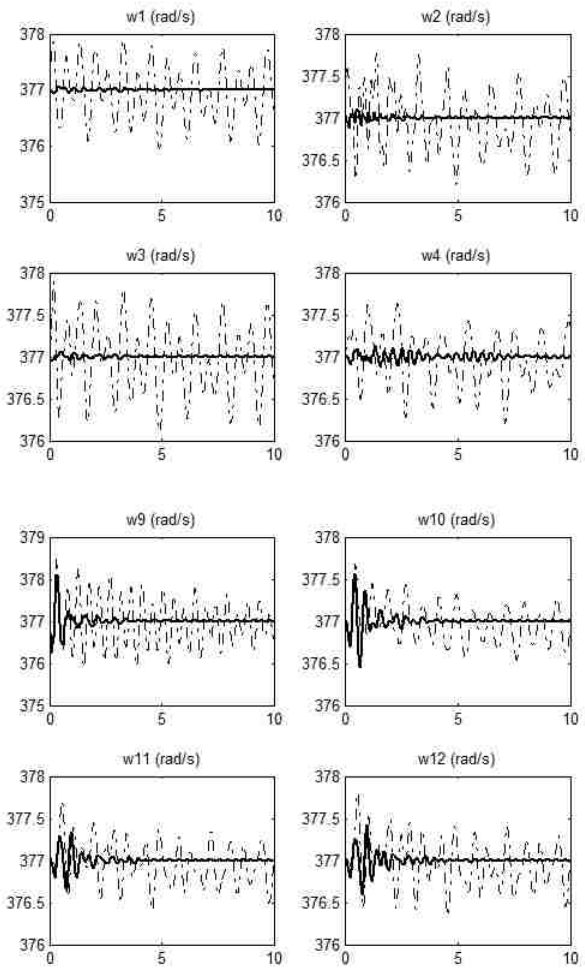

Fig. 6. Comparison of rotor speeds for controlled and uncontrolled (bold: control with estimated feedbacks, dashed: uncontrolled)

VI. CONCLUSIONS AND FURTHER WORK

In general, dynamic behavior of the power system depends on factors such as the pre-fault operating status of the system, fault type, fault location and its value. In this paper, a simple method has been proposed as a guideline for dynamic placement of UPFCs and output measurements selection for proper estimation of the states in the system. The method is based on finding the table of Most Dominant Branches in terms of their influence on inter-area modes. Simulations show successful results for both dynamic placement and signal selection. Since finding the MDB table is not dependent to UPFC dynamics, the proposed method can be extended to the placement of others series connected FACTS devices, too.

Further work would be to look for placements which are optimal from both steady-state and dynamic perspectives. Minimal measurements for state estimation should not result in unsuccessful estimation of the states when one or more of the branches are removed as a result of contingencies. This might require further investigation on finding the best optimal set of measurements.

APPENDIX

n_g : Number of generators

for $j = 1, ..., n_g$

Two Axis Generator Model

$$\dot{\delta}_j = \omega_j - \omega_S$$

$$\frac{2H_j}{\omega_s}\dot{\omega}_j = T_{Mj} + \frac{V_j}{x'_{dj}}\left(E'_{dj}\cos(\theta_j - \delta_j) + E'_{qj}\sin(\theta_j - \delta_j)\right)$$

$$T'_{d0_j}\dot{E}'_{qj} = -\frac{x_{dj}}{x'_{dj}}E'_{qj} + \frac{x_{dj} - x'_{dj}}{x'_{dj}}V_j\cos(\theta_j - \delta_j) + E_{fdj}$$

$$T'_{q0_j}\dot{E}'_{dj} = -\frac{x_{qj}}{x'_{dj}}E'_{dj} - \frac{(x_{qj} - x'_{dj})}{x'_{dj}}V_j\sin(\theta_j - \delta_j)$$

Assumption:

$x'_{qj} = x'_{dj}$ and $R_s = 0$

IEEE Type I Exciter/AVR Model

$$T_{Ej}\dot{E}_{fdj} = -K_{Ej}E_{fdj} + V_{Rj}$$

$$T_{Aj}\dot{V}_{Rj} = -V_{Rj} + K_{Aj}R_{Fj} - \frac{K_{Aj}K_{Fj}}{T_{Fj}}E_{fdj} + K_{Aj}(V_{refj} - V_j)$$

$$V_{Rj}^{\min} \le V_{Rj} \le V_{Rj}^{\max}$$

$$T_{Fj}\dot{R}_{Fj} = -R_{Fj} + \frac{K_{Fj}}{T_{Fj}}E_{fdj}$$

Turbine

$$T_{RH_j}\dot{T}_{M_j} = -T_{M_j} + \left(1 - \frac{K_{HP_j}T_{RH_j}}{T_{CH_j}}\right)P_{CH_j} + \frac{K_{HP_j}T_{RH_j}}{T_{CH_j}}P_{SV_j}$$

$$T_{CH_j}\dot{P}_{CH_j} = -P_{CH_j} + P_{SV_j}$$

Speed Governor

$$T_{SV_j}\dot{P}_{SV_j} = -P_{SV_j} + P_{C_j} - \frac{\omega_j}{R_j\omega_s}$$

$$0 \le P_{SV_j} \le P_{SV_j}^{\max}$$

REFERENCES

[1] HaiFeng Wang, "A Unified Model for the Analysis of FACTS Devices in Damping Power System Oscillations---Part III: Unified Power Flow Controller," *IEEE Trans. Power Delivery*, vol. 15, no. 3, pp. 978-983, July 2000.

[2] Mehrdad Ghandhari, G. Andersson and Ian A. Hiskens, "Control Lyapunov Functions for Controllable Series Devices," *IEEE Trans. Power Systems*, vol. 16, no. 4, pp. 689-694, Nov. 2001.

[3] B.C. Pal, "Robust damping of interarea oscillations with unified power-flow controller," *IEE Proceedings- Generation, Transmission and Distribution*, vol. 149, pp. 733-738, Nov. 2002.

[4] S. Robak, M. Januszewski, D.D. Rasolomampionona, "Power system stability enhancement using PSS and Lyapunov-based controllers: A comparative study," *IEEE Power Tech Conference Proceedings* 2003 Bologna, vol. 3, pp. 6.

[5] N. Tambey and M.L. Kothari, "Damping of power system oscillations with unified power flow controller (UPFC)," *IEE Proceedings- Generation, Transmission and Distribution*, vol. 150, pp. 129-140, March 2003.

[6] M. Januszewski, J. Machowski and J.W. Bialek, "Application of the direct Lyapunov method to improve damping of power swings by control of UPFC," *IEE Proceedings- Generation, Transmission and Distribution*, vol. 151, pp. 252-260, March 2004.

[7] Preedavichit, P., and Srivastava, S.C., "Optrimal reactive power dispatch considering FACTS devices," *Electr. Power Syst. Res.*, Vol. 46, pp. 251-257, 1998.

[8] Lu, Y., and Abur, A., "Improving system static security via optimal placement of thyristor controlled series capacitors (TCSC)," *IEEE Power Eng. Soc.*, Winter Meet., 2001, pp. 516-521.

[9] Gerbex, S., Cherkaoui, R., and Germond, A.J., "Optimal location of multi-type FACTS devices in a power system by means of genetic algorithm," *IEEE Trans. Power Syst.*, Vol. 16, pp. 537-544, 2001.

[10] Xiao, Y., Song, Y.H., Liu, C.C., and Sun, Y.Z., "Available transfer capability enhancement using FACTS devices," *IEEE Trans. Power Syst.*, Vol. 18, pp. 305-312, 2003.

[11] Okamoto, H., Kuriata, A., andSekine, Y., "A method for identification of effective locations of variable impedance apparatus on enhancement of steady state stability in large scale power systems," *IEEE Trans. Power Syst.*, Vol. 10, no. 3, pp. 1401-1407, 1995.

[12] B. Kalyan Kumar, S.N. Singh and S.C. Srivastava, "Placement of FACTS controllers using modal controllability indices to damp out power system oscillations," *IET Gener. Transm. Distrib.*, Vol. 1, no. 2, pp. 209-217, 2007.

[13] M. Zarghami, M.L. Crow, "The Existence of Multiple Equilibria in the UPFC Power Injection Model," *IEEE Transactions on Power Systems*, vol. 22, no. 4, pp. 2280-2282, Nov. 2007.

[14] M. Zarghami, M.L. Crow, "Discussion on effective control of inter-area oscillations by UPFCs," *39th North American Power Symposium*, pp. 623-629, Sep-Oct. 2007.

[15] A.M. A. Hamdan and A. M. Elabdalla, "Geometric measures of modal controllability and observability of power system models," *Elec. Power Syst. Res.*, vol. 15, pp. 147-155, 1988.

[16] http://www.ee.washington.edu/research/pstca/pf118/pg_tca118bus.htm

[17] L. Dong, M.L. Crow, Z. Yang, C. Shen, L. Zhang, S. Atcitty, "A Reconfigurable FACTS System for University Laboratories," *IEEE Transactions on Power Systems*, Vol. 19, no. 1, pp. 120-128, Feb. 2004.

2. CONCLUSIONS

In this research, several methods have been discussed for damping inter-area oscillations in multi-area power systems using multiple UPFCs. A novel effective method based on controlling UPFCs' bus voltage angles has been shown to have fast and effective results for damping oscillations. The method is extended to its nonlinear counterpart where state feedback from dominant machines of the system is needed for the control. However, enough capacitance on the dc side must exist for these methods to work successfully. Since global feedback data is not usually accessible for control implementation, decentralized and centralized wide-area methods have been proposed for dynamic feedback data estimation. Although decentralized controllers which rely only on local measurements for estimation seem more interesting, they do not always provide a feasible solution since local data does not always contain enough information about all system modes. Optimal dynamic placement of FACTS controllers has an important effect on the dynamic behavior of the system and oscillation damping. Simple methods based on modal analysis have been proposed for dynamic placement.

Further work would be to test the proposed controllers in more realistic power system models. One way to do this is through hardware in loop simulations where real laboratory scale FACTS devices are interfaced with simulated power systems. Another area of work would be to design more robust and adaptive controllers which show better results against system uncertainties and topology changes. Although through simulations it has been shown that the dc capacitor voltage would be naturally regulated in most severe single-contingency fault scenarios, control of the dc capacitor is another area of research since currently there is no specific method for capacitor voltage regulation to make sure that voltage could be maintained against multi-contingency fault scenarios. The methods proposed for dynamic placement are based on modal analysis which is inherently a linear method. Other nonlinear methods could also be investigated. One of these methods can be based on power system energy functions in which the best placement would possibly be the one maintaining the lowest level of energy in the system.

VITA

Mahyar Zarghami was born on June 1st 1971 in Tehran, Iran. He received his B.Sc. degree in Electrical Engineering from K.N. Toosi University of Technology, Iran in 1993 and his M.Sc. degree in Electrical Engineering from Sharif University of Technology, Iran in 2001. He joined the Electrical and Computer Engineering Department of the Missouri University of Science and Technology in January 2005 to get his Ph.D. degree. His research interests include Computer Methods in Power System Analysis, Power System Modeling, Power System Dynamics and FACTS devices.